Universidade de Aveiro Departamento de Química
Ano 2021

Andreia Filipa Sousa Ferreira

Chlorella vulgaris e *Porphyridium purpureum*: duas microalgas com polissacarídeos e outros compostos com potencial de valorização

Chlorella vulgaris and *Porphyridium purpureum*: two microalgae with polysaccharides and other potential valuable compounds

Universidade de Aveiro Departamento de Química
Ano 2021

Andreia Filipa Sousa Ferreira

Chlorella vulgaris e *Porphyridium purpureum*: duas microalgas com polissacarídeos e outros compostos com potencial de valorização

Chlorella vulgaris and *Porphyridium purpureum*: two microalgae with polysaccharides and other potential valuable compounds

Tese apresentada à Universidade de Aveiro para cumprimento dos requisitos necessários à obtenção do grau de Doutor em Química Sustentável, realizada sob a orientação científica da Doutora Cláudia Sofia Cordeiro Nunes, Investigadora do Departamento de Engenharia de Materiais e Cerâmica da Universidade de Aveiro, do Doutor Manuel António Coimbra Rodrigues da Silva, Professor Associado com Agregação do Departamento de Química da Universidade de Aveiro, e do Doutor Tiago José Quinteiros Lopes Henriques da Silva, Investigador Sénior do I3Bs - Instituto de Investigação em Biomateriais, Biodegradáveis e Biomiméticos da Universidade do Minho.

Este trabalho foi desenvolvido no âmbito do projeto LAQV-REQUIMTE, financiado por fundos nacionais através da FCT/MEC e quando aplicável cofinanciado pelo FEDER, no âmbito do Acordo de Parceria PT2020.

Apoio financeiro da FCT (POCH) e do FSE no âmbito do III Quadro Comunitário de Apoio (Bolsa de Doutoramento SFRH/BD/102471/2014)

Esta dissertação é dedicada aos meus pais, aos meus irmãos e ao Daniel.

o júri

presidente

Doutor Paulo Jorge de Melo Matias Faria de Vila Real
Professor Catedrático, Universidade de Aveiro

vogais

Doutor Fernando Hermínio Ferreira Milheiro Nunes
Professor Associado com Agregação, Universidade de Trás-Os-Montes e Alto Douro

Doutora Anabela Cristina da Silva Naret Moreira Raymundo
Professora Auxiliar com Agregação, Universidade de Lisboa - Instituto Superior de Agronomia

Doutora Sónia Patrícia Marques Ventura
Professora Auxiliar em Regime Laboral, Universidade de Aveiro

Doutora Cláudia Sofia Cordeiro Nunes (Orientadora)
Investigadora Doutorada, Universidade de Aveiro

Doutor Hugo Galvão Caiano Pereira
Investigador, Green Colab - Associação Oceano Verde

agradecimentos

À minha orientadora, Doutora Cláudia Nunes, em primeiro lugar, por toda a amizade, incentivo e orientação que contribuíram indubitavelmente para a concretização desta tese. Foi uma jornada de constante aprendizagem científica e pessoal, pela qual estou muito grata.

Ao meu coorientador, Professor Manuel A. Coimbra, não só por toda a orientação científica, como também pelo seu incansável incentivo e por me ajudar a tentar pensar de forma positiva ao longo deste percurso. Foi há 9 anos que entrei no seu grupo de investigação, o GlycoFoodChem, para iniciar a minha tese de mestrado e tenho muito a agradecer toda a sua confiança e oportunidades de crescimento.

Ao meu coorientador Doutor Tiago H. Silva por toda sua disponibilidade e pela sua orientação científica.

Ao Professor Manuel Vilanova e à Doutora Alexandra Correia por me terem acolhido no i3S para realizar os ensaios de atividade imunoestimuladora dos polissacarídeos das microalgas.

À ALLMICROALGAE - Natural Products, S.A. e à Necton - Companhia Portuguesa de Culturas Marinhas S.A. pelo fornecimento das microalgas e dos respetivos meios de cultura.

Aos meus colegas de laboratório, pelo companheirismo, pelo espírito de equipa e bom ambiente de trabalho.

Aos amigos da minha jornada de vida. São muitos. Não sei como agradecer todas as conversas, todas as gargalhadas, todo o apoio nos momentos mais difíceis. Fazem-me sentir de coração cheio. Obrigada.

Ao Daniel, o meu porto seguro, o meu apoio incansável. Obrigada por todos os momentos especiais que têm tornado a minha vida uma viagem muito bonita.

À minha mãe, ao meu pai, à minha irmã e ao meu irmão por toda a força, motivação e apoio incondicional.

À Fundação para a Ciência e Tecnologia (FCT) pela bolsa de doutoramento (SFRH/BD/102471/2014), e ao LAQV-REQUIMTE do Departamento de Química da Universidade de Aveiro pelas condições proporcionadas que permitiram a realização desta investigação.

palavras-chave

Microalgas, *Chlorella vulgaris*, *Porphyridium purpureum*, clorofilas, estabilidade da cor, polissacarídeos, caracterização estrutural, atividade imunoestimuladora

resumo

As microalgas eucarióticas *Chlorella vulgaris* e *Porphyridium purpureum* têm-se destacado do ponto de vista biotecnológico devido à capacidade de produzirem vários metabolitos com interesse comercial, como pigmentos e polissacarídeos, para além da proteína e dos lípidos.

A *Chlorella vulgaris* é verde devido ao seu alto teor em clorofila, sendo uma fonte valiosa deste aditivo alimentar. No entanto, uma vez que as clorofilas são compostos bastante sensíveis, podem degradar-se facilmente por vários mecanismos quando armazenadas. Assim, com o objetivo de determinar as condições mais apropriadas para a preservação de clorofilas isoladas, as clorofilas da *C. vulgaris* foram extraídas com 96% de etanol para estudar a influência da temperatura, luz, alcalinidade e atmosfera modificada na estabilidade da cor nas soluções etanólicas. Nas condições avaliadas, a perda da cor verde deveu-se principalmente à ação da luz (com um fotoperíodo de 24 h), seguida da temperatura elevada (60 °C). A perda da cor verde das soluções etanólicas com o aumento da temperatura seguiu uma cinética de 1.ª ordem, sendo mais significativa entre os 28 e os 60 °C, apresentando uma energia de ativação de 74 kJ/mol. Para temperaturas mais baixas observou-se uma resistência das clorofilas à degradação quando preservadas em etanol. A adição de NaOH e a atmosfera inerte rica em árgon não apresentaram um efeito estatisticamente positivo na preservação da cor verde. Desta forma, o extrato etanólico de *C. vulgaris* foi mais estável quando preservado no escuro à temperatura ambiente ou a temperaturas mais baixas. Os extratos etanólicos da *C. vulgaris* mostraram ser um aditivo alimentar natural adequado para corar produtos alimentares de verde. Como caso de estudo, foi corado arroz cozido frio para ser usado em sushi. Esta cor manteve-se estável durante pelo menos 3 dias de armazenamento, tanto na presença como na ausência de luz.

Para além do alto teor em clorofilas, a microalga *C. vulgaris* é rica em amido e polissacarídeos estruturais, que podem também ter elevado potencial de valorização enquanto ingredientes alimentares. Assim, de forma a testar esta hipótese, a digestibilidade do amido foi avaliada na biomassa crua e cozida de *C. vulgaris*, apresentando uma libertação de 43 e 71% de glucose, respetivamente. A baixa extratabilidade do amido obtido com água quente mostrou um impedimento devido à presença de proteína. Este impedimento de extração foi ultrapassado usando soluções aquosas de 1 M e de 4 M de KOH, permitindo obter mais 51% do total de amido da microalga. O resíduo final obtido após as extrações mostrou que apenas 16% do amido ficou por extrair.

Para além disso, as soluções de KOH também permitiram obter galactanas contendo resíduos de galactose com ligações nos carbonos 1,3, 1,6 e 1,3,6. Estas ligações também foram observadas nos polissacarídeos recuperados do meio de cultura, mostrando uma similaridade entre os polissacarídeos extracelulares e os polissacarídeos presentes na parede celular. O material polimérico extracelular revelou um efeito imunoestimulador *in vitro* em linfócitos B.

A microalga vermelha salina *Porphyridium purpureum,* também conhecida por *Porphyridium cruentum*, tem despertado interesse comercial para ser usada para alimentação de peixes em aquacultura. Esta microalga é rica em proteínas, amido florídeo e tem a capacidade de excretar elevados níveis de polissacarídeos sulfatados (sEPS) para o meio de cultura. A microalga *P. purpureum* é cultivada facilmente e pode alterar a sua taxa de crescimento e a sua composição em resposta a alterações ambientais. Neste contexto, foi avaliado o impacto da salinidade do meio de cultura (18, 32 e 50 g/L de NaCl) no crescimento celular da *P. purpureum*, assim como na composição da sua biomassa e no rendimento de produção e estrutura química dos seus polissacarídeos extracelulares. Um crescimento máximo estimado de 5.7×10^6 células/mL foi obtido no meio de cultura com uma salinidade de 32 g/L de NaCl, após 19 dias de crescimento. Apesar da composição da biomassa da microalga *P. purpureum* não mudar significativamente com o nível de salinidade do meio de cultura, o rendimento de excreção dos sEPS foi maior para a cultura com 32 g/L de NaCl (90 mg/L). Para além disso, a salinidade do meio de cultura também alterou ligeiramente o padrão de sulfatação das glucuronoglucogalactoxilanas, uma vez que os sEPS produzidos pela *P. purpureum* que cresceu com o menor nível de salinidade, tendem a ser mais sulfatados na posição *O*-3 da xilose e na posição *O*-6 da glucose, enquanto a salinidades superiores os sEPS tendem a ser mais sulfatados na posição *O*-4 da xilose e da glucose. Os sEPS produzidos com salinidades maiores também revelaram uma maior percentagem de resíduos lineares de 2-Gal, 3-Gal e 4-Gal. No entanto, em todas as amostras, os resíduos de açúcares mais representativos foram os t-Xyl, t-Xyl4S, 3-Xyl, 4-Xyl, t-Glc, 3-Glc6S, t-Gal e 2,3,4-Gal. Os sEPS mostraram um efeito imunoestimulador *in vitro* nos linfócitos B, à semelhança do efeito também demonstrado pelos polissacarídeos extracelulares da *C. vulgaris*. A produção destes sEPS pela microalga *P. purpureum* pode ser realizada a larga escala num fotobiorreator de placas planas verticais de 800 L com um bom rendimento de excreção (144 mg/L), comprovando a viabilidade destes sEPS para produção industrial e comercialização.

Em conclusão, esta tese de doutoramento aumentou o conhecimento do potencial biotecnológico dos pigmentos e polissacarídeos da *C. vulgaris* como ingredientes alimentares, com a vantagem comercial adicional de poderem ser co-extraídos. Além disso, os polissacarídeos extracelulares sulfatados da microalga *P. purpureum* revelaram um grande potencial para serem usados na aquacultura, de forma a aumentar a atividade imunoestimuladora dos peixes.

keywords

Microalgae, *Chlorella vulgaris*, *Porphyridium purpureum*, chlorophylls, color stability, polysaccharides, structural characterization, immunostimulatory activity

abstract

Chlorella vulgaris and *Porphyridium purpureum* are two eukaryotic microalgae that have been highlighted from the biotechnological point of view due to their capability of producing multiple interesting metabolites, such as pigments and polysaccharides, beyond protein and lipids.

Chlorella vulgaris is green due to the high cholorophyll content, representing a valuable source of this food aditive. However, since chlorophylls are sensitive compounds, they degrade easily by various mechanisms during storage. Aiming to find food grade suitable conditions for isolated chlorophylls preservation, *C. vulgaris* chlorophylls were extracted with 96% ethanol to study the influence of temperature, light, alkaline conditions, and modified atmosphere on the stability of the color in ethanolic solutions. Under the conditions used, the color loss was mainly due to the intense light (photoperiod 24 h), followed by the hight temperature (60 °C). The loss of green color in the ethanolic solution with temperature followed the first-order kinetic, being more significant between 28 and 60 °C, with an activation energy of 74 kJ/mol. To lower temperatures *C. vulgaris* chlorophylls showed resistance to the degradation when preserved in ethanol solutions. The addition of NaOH and the inert argon-rich atmosphere did not exhibit a statistically positive effect on the color preservation. Thus, *C. vulgaris* ethanolic extract showed to be more stable when protected from light at room temperature or bellow. *C. vulgaris* ethanolic extract showed to be a suitable natural food additive to coloring food stuffs. As case of study, the cooked cold rice was colored to be used in sushi. The color remained stable up to 3 days of storage at 4 ºC, either in the presence or absence of light.

Beyond the high content in chlorophylls, *C. vulgaris* is rich in starch and structural polysaccharides that could have also great potential to be valued as food ingredients. Therefore, to fulfill this hypothesis, starch digestibility was evaluated in raw and boiled biomass, showing 43% and 71% of glucose released, respectively. The low extraction yield of starch obtained with water (13%) allowed to infer protein hindrance. This was overcome by 1 M and 4 M KOH aqueous solutions that allowed to obtain an additional 51% of starch. The final residue left showed that only 16% of total starch remained unextracted. KOH solutions allowed also to obtain galactans composed by 1,3-, 1,6- and 1,3,6-linked galactose residues. These linkages were also observed in the polysaccharides recovered from the growth medium, showing similarity between the exopolysaccharides and those present in the cell wall. The extracellular polymeric material revealed *in vitro* immunostimulatory effect on B lymphocytes.

Porphyridium purpureum, also recognized as *Porphyridium cruentum*, is a red saline microalga that have been aroused commercial interest to be used for feeding fish in aquaculture. This microalga is rich in proteins and floridean starch, having the ability to excrete high levels of sulfated polysaccharides (sEPS) into the growth medium. *P. purpureum* is easily cultivated and could change their growth rate and composition in response to environmental variations. Thus, the impact of growth medium salinity (18, 32, and 50 g/L NaCl) on *P. purpureum* cells growth, biomass composition and on the extracellular polysaccharides production yield and chemical structure were evaluated. A maximum growth estimated as 5.7×10^6 cells/mL was obtained for 32 g/L of NaCl, after 19 days of growth. Besides biomass composition was not greatly changed, the sEPS excretion yield reflected the effect of salinity, higher for 32 g/L of NaCl (90 mg/L). The growth medium salinity slightly changed the sulfation pattern of the glucuronoglucogalactoxylan, since sEPS produced from *P. purpureum* grown at lower salinity tend to be more sulfated in *O*-3 position of xylose and *O*-6 position of glucose, while at higher salinity the sEPS tend to be more sulfated in *O*-4 position of xylose and glucose. The sEPS produced at higher salinity also revealed higher content of linear 2-Gal, 3-Gal, and 4-Gal residues. In all samples, the most representative sugar residues were constituted by t-Xyl, t-Xyl4S, 3-Xyl, 4-Xyl, t-Glc, 3-Glc6S, t-Gal, and 2,3,4-Gal. The sEPS showed immunostimulatory effect on B lymphocytes *in vitro*, similarly to the effect also demonstrated by the *C. vulgaris* extracellular polysaccharides. *P. purpureum* sEPS could be produced at large scale at an outdoor 800 L-flat panel photobioreactor with higher excretion yield (144 mg/L), revealing the potential of industrial production and commercialization of sEPS.

In conclusion, this PhD thesis significantly upgraded the knowledge about the biotechnological potential of *C. vulgaris* pigments and both starch and exopolysaccharides, as food ingredients, with the additional commercial advantage of the possibility of these metabolites' co-extraction. Moreover, *P. purpureum* sEPS revealed biotechnological potential to be used in aquaculture to enhance humoral immunoactivity of fish.

Table of content

List of figures

CHAPTER 1

CHAPTER 2

CHAPTER 3

List of tables

CHAPTER 1

CHAPTER 3

Publications and Communications

Papers in peer reviewed journals

1. **Ferreira, A. S**., Ferreira, S. S., Correia, A., Vilanova, M., Silva, T. H., Coimbra, M. A., Nunes, C., Reserve, structural and extracellular polysaccharides of *Chlorella vulgaris*: A holistic approach, *Algal Research*, 2020, 45, 101757. DOI: 10.1016/j.algal.2019.101757.
2. **Ferreira, A. S.**, Mendonça, I., Póvoa, I., Carvalho. H., Correia, A., Vilanova, M., Silva, T. H., Coimbra, M. A., Nunes, C., Impact of growth medium salinity on galactoxylan exopolysaccharides of *Porphyridium purpureum*, *Algal Research,* 2021, 59, 102439. DOI: 10.1016/j.algal.2021.102439.
3. **Ferreira, A. S.**, Cânfora, F., Pereira, L., Silva, T. H., Coimbra, M. A., Nunes, C., *Chlorella vulgaris* pigments stabilization in ethanolic solution at different storage conditions (under preparation).

Communications in scientific meetings

Oral communications

Ferreira, A.S., Oliveira, C., Novoa-Carballal, R., Nunes, C., Pashkuleva, I., Neves, N.M., Reis, R.L., Martins, A., Silva, T.H., Coimbra, M.A., The role of the fucoidan structures on their antitumor activity: the contribution of mass spectrometry, 7th Workshop Mass Spectrometry and Carbohydrates, Aveiro, Portugal, 7 March, 2018**.**

Poster communications

1. **Ferreira, A. S.**, Nunes, C., Silva, T. H., Coimbra, M. A., Physico-chemical characterization of starch from the microalgae *Chlorella vulgaris*, 12ª Reunião do Grupo dos Glúcidos (Glupor), Aveiro, Portugal, 11-13 September, 2017.
2. **Ferreira, A. S.**, Nunes, C., Silva, T. H., Coimbra, M. A., Edible microalgae *Chlorella vulgaris*: a non-conventional source of starch, Micro Biotec'17, Porto, Portugal, 7-9 December, 2017.

3. **Ferreira, A. S.**, Nunes, C., Silva, T. H., Coimbra, M. A., Polysaccharides profile of *Porphyridium cruentum* microalgae, 29th International Carbohydrate Symposium, Lisboa, Portugal, 15-19 July, 2018.

Abbreviations

μ	Specific growth rate
AA	Arachidonic acid
Ara	Arabinose
AUC	Area under the curve
ConA	Concanavalin A
Chl *a*	Chlorophyll *a*
Chl *b*	Chlorophyll *a*
DB1	100% Dimethylpolysiloxane
DW	Dry weight
EPA	Eicosapentanoic acid
EPM	Extracellular polymeric material
EPS	Extracellular polysaccharides
EtOH	Ethanol
FA	Fatty acids
FAME	Fatty acids methyl esters
FTIR	Fourier-transform infrared spectroscopy
Fuc	Fucose
Gal	Galactose
GC-FID	Gas chromatography with flame ionization detector
GC-qMS	Gas chromatography coupled to quadrupole mass spectrometry
GI	Glycemic index
Glc	Glucose
GlcN	*N*-glucosamine
HI	Hydrolysis index
LPS	Lipopolysaccharides
Man	Mannose
OD	Optical density
PB	Polymyxin B
PBR	Photobioreactor

PC	Principal component
PCA	Principal Component Analyses
Rha	Rhamnose
RPMI medium	Roswell Park Memorial Institute medium
SD	Standard deviation
SEM	Scanning Electron Microscopy
sEPS	Sulfated extracellular polysaccharides
TFA	Trifluoroacetic acid
TGA	Thermogravimetric analysis
UA	Uronic acids
Xyl	Xylose

CHAPTER 1. Introduction

1.1 An introduction to microalgae

Algae are recognized as one of the oldest life forms and include a large group of organisms from different phylogenetic groups. Algae includes macro and microalgae. Macroalgae, frequently referred to as seaweed, are macroscopic and multicellular organisms, whereas microalgae are unicellular or simple multicellular photosynthetic microscopic organisms, with cells size ranging from a few μm to about 200 μm [1,2]. Microalgae covers several life forms that are not closely related, encompassing four out of seven kingdoms: Plantae, Chromista, Protozoa, and Bacteria, including both prokaryotic and eukaryotic microorganisms [3,4]. The systemic classification of algae is traditionally based on their pigment composition and is divided into 5 main groups: green algae (*Chlorophyceae*), blue-green algae (*Cyanophyceae*), golden algae (*Chrysophyceae*), diatoms (*Bacillariophyceae*), and the named *classis nova* (*Porphyridiophyceae*) [1,5,6]. However, current systems of classification take account other criteria, such as the cytological and morphological characters, cell wall and storage products chemical nature, and phylogenetic traits [4,5,7]. Guiry and Guiry [8] considers 10 phyla: Cyanobacteria (=Cyanophyta), Euglenophyta, Heterokontophyta (=Ochrophyta), Haptophyta, Cryptophyta, Miozoa (=Dinophyceae), Cercozoa (Chlorarachniophycea), Glaucophyta, Rhodophyta, and Chlorophyta (Figure 1.1). The classifications system is constantly and rapidly under revision following the new genetic and ultrastructural evidence, and, consequently, these taxonomic organization may change as information is revealed [4,9].

The green microalga *Chlorella vulgaris* belongs to the domain Eukaryota, kingdom Plantae, phylum Chlorophyta, genus *Chlorella*, and species *Chlorella vulgaris*. The name *Chlorella* comes from the Greek word *chloros* (Χλωρός), which means green, and the Latin suffix *ella* referring to its microscopic size [10]. The red microalga *Porphyridium purpureum* belongs to domain Eukaryota, kingdom Plantae, phylum Rhodophyta, genus *Pophyridium*, and species *Porphyridium purpureum* [11].

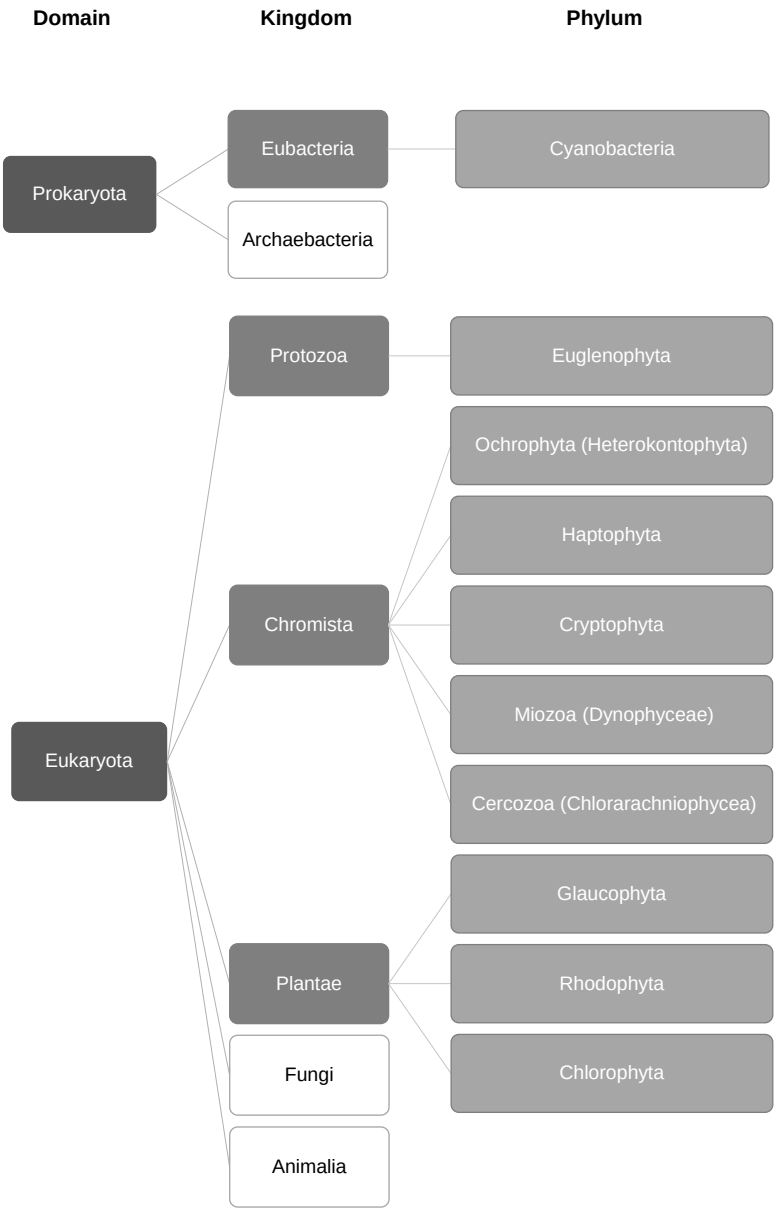

Figure 1.1 – Microalgae phyla distribution as per seven Kingdom classification according to Guiry and Guiry [8].

Microalgae can grow in freshwater, such as *C. vulgaris*, and marine environments, such as *P. purpureum*, as well as from almost every environmental condition on Earth where sunlight and water coincide, such as in soils, desert sands, rivers, lakes, snowfields, hot springs, or oceans. These microorganisms can be found either in frozen lands of Scandinavia or in hot desert soils of the Sahara. Microalgae have an ancient history that left a footprint of 3.4 billion years, thus represent an exceptionally diverse and highly specialized group of microorganisms [3,10,12,13]. The biodiversity of microalgae represents an almost untapped

resource. The estimated number of described species ranges between 40 000 to 60 000, but the number of undescribed species has been estimated as close to ten million of species spread over the globe. In comparison, only 250 000 land plant species have been recorded [6,14]. However, only a few species have been identified to be useful for commercial application, such as *Chlorella* and *Porphyridium* species [5].

Microalgae has been used by humans for a long time. It dates back thousand years to the Chinese, who used *Nostoc flagelliforme* (cyanobacteria) to survive to famine. Other microalgae species, such as the blue cyanobacteria *Arthospira* (*Spirulina*) have been also exploited as a food source by ancient civilizations such as the Aztecs in Mexico [15]. The first scientific studies on microalgae started with *Chlorella vulgaris* at the end of the 19th century [16]. However, the production of microalgal biomass really began in the early 1950's, starting first with Germany when societies after war were apprehensive at the increase of the world's population and its implication of a possibly insufficient protein supply [9,17]. The commercial large-scale culture started in the early 1960's in Japan [17]. Attention was focused on freshwater *Chlorella* species due to their high growth rate, high content of valuable compounds and resistance to variable growth conditions [18]. However, with the need of a sustainable development and to explore the vast biotechnological potential that these new sources of biomass can provide, a new wave of research and investment has been surged worldwide recently [14]. As is demonstrated in Figure 1.2, the scholarly output about microalgae from 2010 to 2020 shows the tendency of the increasing publications worldwide and in Europe, over the last decade, supporting the increasing research interest in these microorganisms.

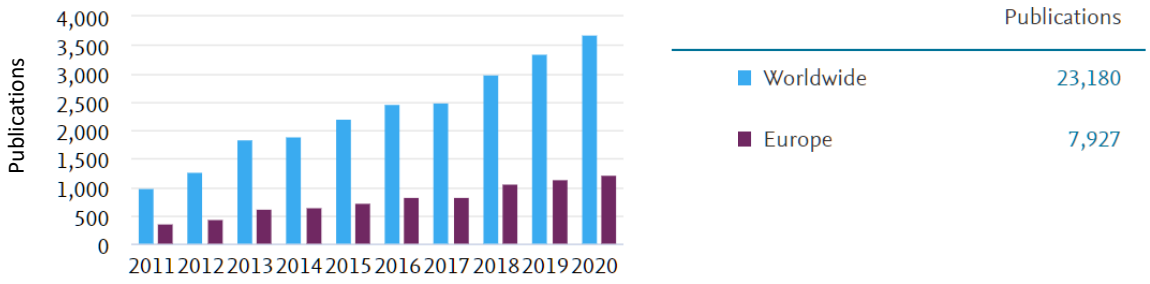

Figure 1.2 – Scholarly output (number of publications) of microalgae from 2010 to 2020 worldwide and Europe. Data source: Scopus.

There are several reasons that justifies the attention given to microalgae organisms, which are summarized in Figure 1.3. Microalgae, as a photosynthetic organism, can derive their energy from sunlight and carbon from inorganic sources, such as CO_2. Moreover, when compared to higher plants, these microorganisms show higher photosynthetic yields, with an annual photon-to-biomass conversion efficiencies of about 3% *vs.* < 1% for higher plants, no intrinsic susceptibility to seasonality, and the fact that they live in aquatic medium gives them direct access to their nutrients, which results in higher growth productivities [9,14,19]. The higher growth rates combined with the great biological diversity of microalgae and their exceptional range of adaptability allowed the production of high value compounds, such as pigments, carbohydrates, proteins, or fatty acids with high yields [14].

Microalgae can be grown on brackish water, thus they do not compete with crops for arable land and freshwater. Consequently, they do not compromise the production of food or other products from crops [20]. Since microalgae have the capacity to assimilate nutrients from most wastewaters, it also makes them a suitable alternative method for wastewater treatment [5,21,22]. Furthermore, they are able to recycle the industrial flue gases and atmospheric carbon dioxide, reducing greenhouse gases emission and improving air quality [23]. Indeed, microalgae CO_2 mitigation has been pointed as an important response to the current environmental issues due to their greater capacity to fix CO_2 compared to higher plants [24,25], being able to absorb up to 200 times more CO_2 than trees, depending on the species [3]. Microalgae produce close to 50% of all the photosynthetically worldwide produced oxygen [26].

Microalga can grow easily in reactors with high level of growth control and sterile conditions, which enables the production of valuable compounds always with similar properties. Moreover, the cultivation in reactors offers the additional possibility of adjusting and adapting culture conditions in real time, allowing growers to react instantaneously to the culture situation, increasing biomass productivity [14].

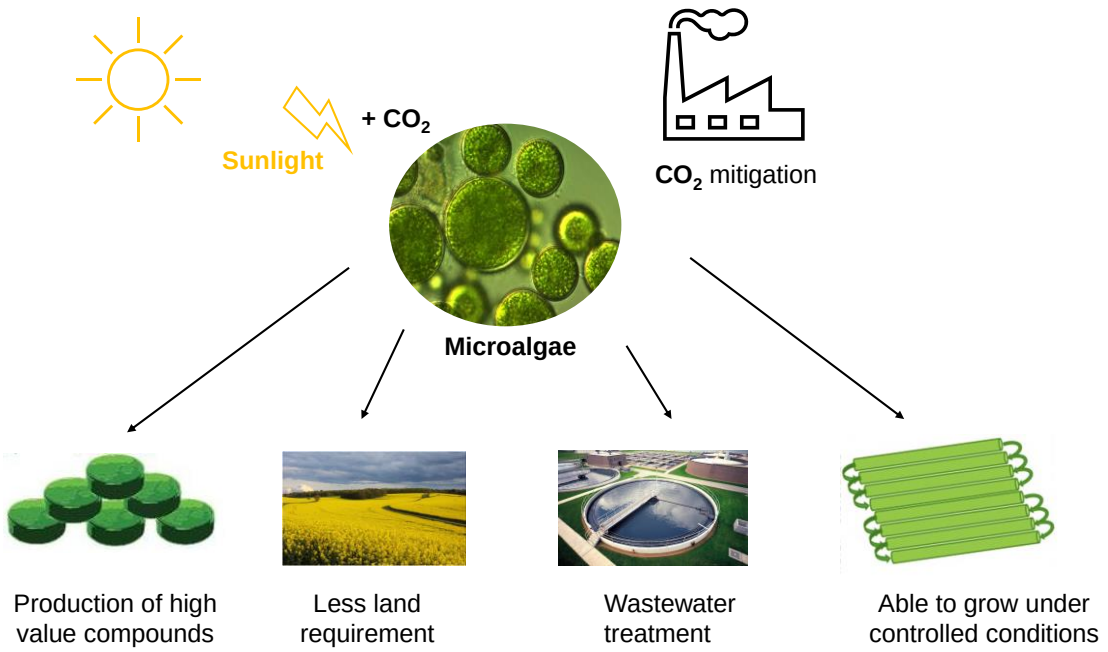

Figure 1.3 – Beneficial outputs of culturing microalgae.

1.2 Cultivation of microalgae

Sustainable and effective cultivation systems appropriate for each microalgae species are a requisite to achieve the full potential of microalgae biomass, especially for large scale industrial applications. There are three distinct microalgae production systems: photoautotrophic, heterotrophic, and mixotrophic. Photoautotrophic cultivation means that inorganic forms of carbon (CO_2 or bicarbonates) are supplied to the cultures as a carbon source to generate organic compounds by using energy from light through photosynthesis [23,26,27]. On heterotrophic cultivation, microalgae depend on organic carbon substrates to provide both carbon source and energy [26,28]. Mixotrophic cultivation employs a combination of autotrophic and heterotrophic production, thus microalgae use light, CO_2 to photosynthesis and organic carbon in the aerobic respiration [26,29]. Taking into consideration the costs for organic supply and artificial light, the photoautotrophic system using sunlight is the most viable option for the production of microalgae biomass on a large scale [26,30].

1.2.1 Microalgae cultivation techniques

Microalgae can grow easily in natural environments, thus the artificial production should replicate and improve the optimum natural conditions in order to improve biomass concentrations and biomolecules production [3]. In this line, the design and optimization of artificial production to allow light penetration and an efficient supply of carbon for the rapid microalgae cultivation are important requirements to make viable the commercialization of these microorganisms. Microalgae are cultivated in two different aqueous systems, namely open ponds and photobioreactors (PBRs) [1,31].

Open ponds are the most basic cultivation systems and comprise lake and natural ponds, as well as circular ponds and raceways. The open-air systems are easier to build, are less expensive, and have larger production capacity than most PBR, being the most widespread microalgae growth system. They can utilize sunlight and the nutrients provided through waters from nearby land areas or by using the water from sewage/water treatment plants thus making it the cheapest method of large-scale algal biomass production [32]. However, this cultivation method is only promising for large scale commercial production of robust microalgae species. Some delicate species, such as *Porphyridium purpureum*, are damaged by the circulation system of circular ponds [33], limiting their application. Moreover, these systems present other technical challenges, since they are vulnerable to weather conditions, making unfeasible the control of temperature or light. They are also vulnerable to other microalgal or other microorganisms contamination, and are vulnerable to contaminations from waters, as heavy metals, limiting the commercial output of microalgae [1,31].

Photobioreactors (PBRs) are close systems for cultivating microalgae biomass on a laboratory and industrial scale. Close PBRs normally consist of vessels made from glass/fibre/plastic and the light passes through the transparent reactor walls to reach the microalgae cells culture [34]. PBRs allow to control and standardize of almost all biotechnology important growth paraments, with the additional advantage of allowing to reduce risk of contaminations and CO_2 losses [1,6,31]. The controlled growth conditions led to a reproducible cultivation, as well as to higher biomass concentrations, which are requisites for the production of high-value products [1]. Strains such as *Chlorella*, *Porphyridium, Scenedesmus, Dunaliella*, *Spirulina,* and *Haematococcus* have been widely cultured using PBRs [35]. There are several designs of PBRs, namely tubulars, flat panels or wall PBRs, columns, and stirred tank reactors. Tubular and flat panel PBRs have the

advantage of providing a good balance of irradiation area per unit of reactor volume and an efficient stirring effect. In addition, since flat panel PBRs are built of thin layers, this might contribute to an even higher light intensity [6,36]. Due to design limitations, tubular reactors, such as the ones presented in Figure 1.4 for the production of *Chlorella vulgaris* and *Porphyridium purpureum*, are the bioreactors that have been widely used in industrial scale, yielding reasonable energy and cost efficiency [1].

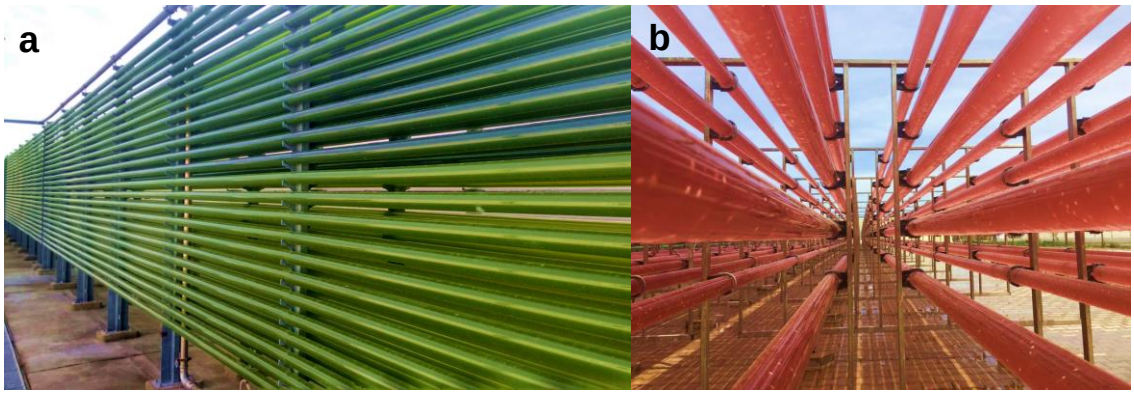

Figure 1.4 – Tubular PBR cultivation for microalgal cultures: a) *Chlorella vulgaris* culture produced by Allmicroalgae, S.A. (Pataias, Portugal); b) *Porphyridium purpureum* culture produced by Necton, S.A. (Olhão, Portugal).

1.2.2 Growth factors affecting microalgal cultures

The culture media used to produce microalgal biomass must supply all the necessary environmental conditions required for cells during the different growth phases (e.g. lag, and exponential phases), and for the microalgae maintenance (stationary phase). Thus, the most important parameters that regulates microalgal growth include the nutrients, CO_2, light, temperature (optimal temperature generally between 20-24 ºC), pH (most of the microalgae grow in the pH range of 6-9), turbulence (to promote appropriate distribution of nutrients, light and CO_2), and salinity, that strongly depends on the ecological origin of the microalgae [1–3,37]. Culture media should contain carbon, nitrogen, and phosphorous sources and some other macronutrients, such as Na, Mg, Ca, and K. Micronutrients, such as Mo, Mn, B, Co, Fe, S, and Zn, chelating agents, and vitamins [1,2,38–40] are also required. Light intensity, spectral quality, and photoperiod (light/dark period) are also important variables for proper growth.

The salinity levels of the growth medium is another important aspect to culture microalgae [41,42]. However, it has been less exploited. Furthermore, salinity tolerance is an important parameter since avoiding the use of freshwater, can make the system more environmental friendly [26]. High salinity levels in culture media could imply an osmotic stress, and consequently, microalga can alter their cell metabolism, which influences the biomass productivity [43–45]. Indeed, the sodium chloride (NaCl) concentration of culture medium influences the growth behaviour of the marine microalgae, namely *Porphyridium* species. Different optimal NaCl water culture concentrations, namely 20, 24.5, and 41.8 g/L [46–48], were achieved by different studies to promote an optimal biomass production of *Porphyridium* species, which are nearly included in the optimal range of 26 to 47 g/L proposed by Cohen *et al.* [49]. The differences in optimal NaCl concentrations could be related with the additional environmental conditions that possibly affects the growth/salinity relationship [50]. The salinity levels, as well as the other abiotic factors necessary for cells growth, also can have influence on the pattern, pathway, and activity of cellular metabolism to protect cells from salt injury by changing the cellular composition. Consequently, the salinity levels affect the production of high-value biomolecules [26,40,51]. Different osmotic levels revealed influence on biomass composition of *Porphyridium* species, such as proteins [47] and free amino acids [52], fatty acids, namely on eicosapentaenoic acid (EPA) and arachidonic acid (AA) [48,53,54], phycoerythrin [55], and carbohydrates [56], namely starch and sulfated extracellular polysaccharides (sEPS) [47]. Regarding to the latter biomolecules, the only information available concerns to the fact that at 20 g/L of NaCl *P. marinum* produces lower content of sulfated polysaccharides but higher content of starch.

Different marine and freshwater species of microalgae have different growth media requisites, consequently, optimal growth parameters should be determined individually to achieve optimal biomass and high-added value molecules production.

1.3 High-added value molecules

Recently, the principal field of microalgae research and applications has changed, being more focused on the production and valorization of high-added value molecules, instead of biofuels production or environmental applications [9]. This trend may be due to the high cost

of microalgae production even at large scale, mainly due to the expensive downstream processing to recover the biomass [9].

Actually, microalgae are recognized as a tremendous source of a large plethora of biomolecules with high-added value due to their extremely phylogenetic diverse collection that results in a great diversity of the chemical composition of these organisms [21,57,58]. Among the many high-added value biomolecules known to be produced by microalgae are the lipids, proteins, pigments (like chlorophylls, carotenoids, and phycobiliproteins), and polysaccharides, which can be applied using whole biomass or as isolated bioactive molecules [6,59–61]. Moreover, biomolecules of microalgae can be sequentially co-extracted and valorised in different applications, increasing their bio-economic viability for industrial exploitation.

Microalgae possess two main groups of lipids: the storage lipids (mainly triglycerides), which are produced by photosynthesis and stored in the cells, and the structural lipids (phospholipids and sterols), which are an integral part of the cell structure [62]. These photosynthetic microorganisms are able to produce varied classes of fatty acids, such as C14–C22, saturated and unsaturated fatty acids [5], which profile is relatively preserved within a phylum [63], but their contents varies within species according to environmental factors [64]. For instance, *C. vulgaris* when cultivated under nitrogen limitation growth conditions is able to accumulate up to 63% of total lipid in dry weight, consisting primarily of neutral lipids, mostly triglycerides [65]. On the other hand, *P. purpureum* produces 1-11% of total lipids, possibly due to the differences on culture media composition or/and difference in strains [56,66].

Eukaryotic microalgae contain generally more unsaturated fatty acids [5]. Within them, polyunsaturated fatty acids (PUFAs) are of special interest for both food and pharmaceuticals applications, as nutritional supplements for the prevention of cardiovascular diseases [67,68]. Prominent microalgae PUFAs include docosahexaenoic acid (DHA 22:6 *n*-3), eicosapentaenoic acid (EPA 20:5 *n*-3), arachidonic acid (AA 20:4 *n*-6), α-linolenic acid (ALA 18:3 *n*-3), and γ-linolenic acid (GLA 18:3 *n*-6) [26]. *Chlorella* species showed high proportion of medium chain FAs (<C20), producing mainly palmitic acid (16:0) and oleic acid (18:1) and only minor portions of polyunsaturated fatty acids, namely linoleic and linolenic acids (18:2 and 18:3, respectively) [65,69]. Other species such as *Porphyridium purpureum* are a promising long chain PUFAs producer (> C20) [5,40], such as arachidonic

acid and eicosapentanoic acid, which can comprises up to 37% [70,71] and 36% of total fatty acids, respectively [49].

Proteins are other biomolecules that microalgae can produce in higher amounts. Indeed, these microorganisms are able to accumulate protein up to 70% of their dry weight, depending on culture conditions, although most microalgae have protein contents around 50% [72]. Proteins in *C. vulgaris* could represent 35–58% of biomass dry weight [72–74], while *P. purpureum* has the capacity to accumulate proteins up to 56% of their dry weight [75]. Microalgae proteins have also a rich and varied composition of essential amino acids that contributes to a high biological value [6,76,77]. Hence, microalgae biomass, such as *Chlorella* and *Porphyridium* compare favourably with the standard protein/amino acids requirement profile for human nutrition proposed by World Health Organisation (WHO) and Food and Agricultural Organisation (FAO) (Table 1.1). It is estimated that proteins derived from as algae or insects, will be an important source in a near future food supply market [78].

Table 1.1 – Amino acid profile (content per 100g) of *Chlorella vulgaris* [79] **and *Porphyridium purpureum*** [75]**, compared with the FAO/WHO/ONU** [80]**, as a reference pattern.**

Source	His	Ile	Leu	Lys	Met+ Cys	Phe + Tyr	Thr	Val	Trp	Ala	Arg	Asp	Glu	Gly	Pro	Ser
FAO /WHO	1.9	2.8	6.6	5.8	2.5	6.3	3.4	3.5	1.1							
C. vulgaris	2.2	4.5	9.8	7.1	1.9	7.8	4.6	7.9	1.2	11.5	6.0	10.1	14.4	5.3	5.2	3.3
P. purpureum	1.1	5.2	5.8	5.5	3.1	9.4	6.2	2.5	1.4	6.7	7.8	11.2	8.2	6.9	2.5	8.1

1.3.1 Pigments

Pigments are chromatic chemical substances that are part of the photosynthetic system of autotrophic organisms, including microalgae [81], due to the ability to capture solar energy to be transformed into chemical energy [82]. They are also responsible to repair the photosynthetic apparatus [26,64]. Pigments can be distinguished into three different categories: chlorophylls, carotenoids, and phycobiliproteins, which are responsible for green, yellow/orange, and red/blue color, respectively [9,62]. These pigments, including those from microalgae, are being exploited for different applications in a variety of industries, from food natural colorants to health products [83]. Although their great potential for biotechnological

purposes, the use of these products still faces some challenges, like the high cost of production and the instability of the isolated pigments. Nevertheless, it has been made efforts to provide promising prospects for the use of microalgae as a source of pigments [84].

1.3.1.1 Chlorophylls

In eukaryotic microalgae, chlorophylls are located in the chloroplast (similar to higher plants), while in Cyanobacteria they are located in the photosynthetic lamellae. Structurally, chlorophylls are constituted by a large aromatic tetrapyrrole macrocycle, with a centrally bound Mg ion (that maximizes excited state lifetime of chlorophyll) and a hydrocarbon tail (that anchors and orients the pigment in thylakoids), the phytol (Figure 1.5) [85,86]. There are five kinds of chlorophyll in microalga: *a*, *b*, *c*, *d* and *f*, which have some small differences in their absorption spectra, and, consequently, in their tonality. Chlorophyll *a* (Chl *a*) has a blue-green color and occurs universally in algae of all classes. Chlorophyll *b* (Chl *b*) is a brilliant green and it is largely or entirely restricted to green algae (Chlorophyta), such as *C. vulgaris*; chlorophylls *c* is yellow-green and occur in many classes, chlorophyll *d* is a brilliant/forest green and it is present in Rhodophyta, and chlorophyll *f* is emerald green and it is present in Cyanobacteria [81,87]. The Chl *a*:Chl *b* ratio ranges from 2:1 to 3:1 in green algae [88]. The difference between Chl *b* and Chl *a* is attributed to a methyl functional group on porphyrin ring in Chl *a* and an aldehyde (formyl) group in Chl *b* [89], as shown in Figure 1.5. This makes chlorophyll *b* slightly more polar than chlorophyll *a*.

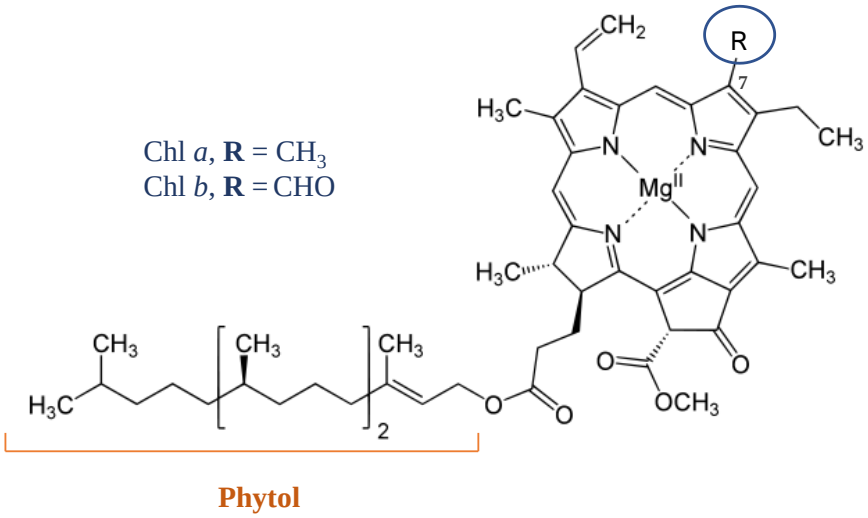

Figure 1.5 – Schematic representation of Chlorophyll *a* and Chlorophyll *b*. In Chl *a* the side group in the C7 is a methyl group (-CH_3) while in Chl *b* it is an aldehyde group (-CHO) [86].

All chlorophylls have two main absorption bands, 450-475 (blue light) and 630-675 nm (red light) [84]. The solvents may also influence the maximum absorption wavelength of chlorophylls' spectra. Different ethanol concentrations (1-60% of ethanol) have a maximum absorbance of Chl *a* between 420 and 432 nm [90].

Chlorophylls has been used by food industry as a natural pigment ingredient in processed foods. Indeed, due to their strong green pigmentation and consumers demand for natural foods, chlorophylls are gaining a major importance as food additives [91]. However, it is difficult to keep green color of chlorophyll extracts or processed food products. These pigments are chemically unstable to pH variations and are vulnerable to heat, oxygen or intense light, which can lead to the formation of a large number of degradation products. Acidification and/or thermal processing result in a perceivable discoloration of chlorophylls from bright green to an olive-green or olive-yellow color, known as pheophytinization (Figure 1.6). During this reaction, hydrogen ions can transform the natural chlorophylls to their corresponding pheophytins by substitution of the Mg^{2+} in the porphyrin ring [81,92–94]. The formation of chlorophyllides from chlorophylls can also occur, involving the saponification of the phytol side chain with sodium hydroxide [95] (Figure 1.6). Other chemical degradation routes are oxidation or photo-oxidation, if light is implicated [94].

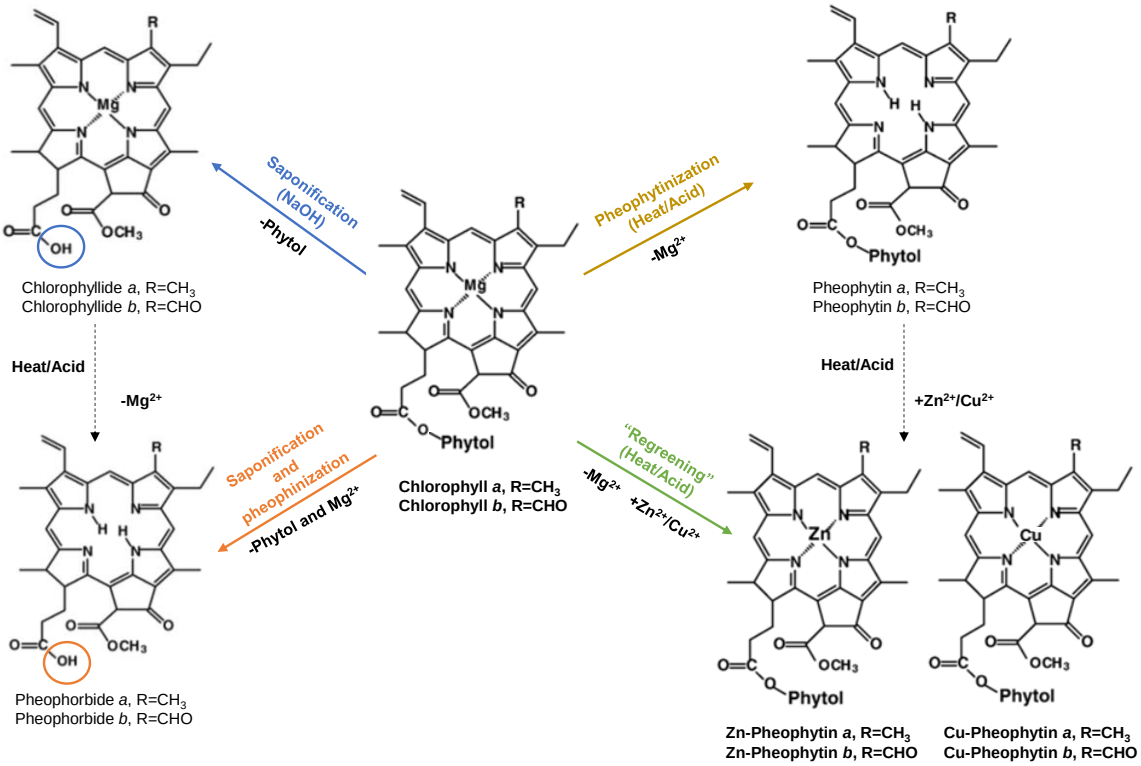

Figure 1.6 – Major Chl *a* and Chl *b* degradation and derivatization routes. Saponification results in water-soluble chlorophyllides that can be further degrade through heating and acidification to pheophorbides. The exposure to heat/ acid results in loss of central Mg^{2+} metal through pheophytinization reaction, forming pheophytins. The inclusion of divalent metals such as Zn^{2+} and Cu^{2+} results in a "regreening" by generation of Zn-pheophytins and Cu-pheophytins.

Color plays a dominant role on the appearance and acceptance of food matrices and their change could be perceived by consumers as a loss of quality [96]. Thus, efforts in preserving the green chlorophylls in foods [97–102] or solvents extracts, such in acetone [103] or ethanol [90], have been carried out though pH control [97,98,102], enzymatic treatments [100], temperature control [90,97–99,102,103], and addition of metal ions Cu^{2+} and Zn^{2+} [97,101].

Regarding to the legal aspects, European legislation (Commission Directive 95/45/EC) allows the use of two natural green colorants in foods, E140 and E141 [104]. E140 consist of Mg-containing chlorophylls and their direct chlorophyll derivatives, obtained from edible natural source materials with organic solvents. E140i colorant represents liposoluble Mg-Chls *a* and *b* as well as their pheophytins directly extracted from the natural sources, whereas E140ii colorant represents water soluble chlorophyllins (Na or K-chlorophyllins without phytol and with or without the central Mg^{2+}), which is obtained by alkali treatment (saponification) followed by the neutralization with K and/or Na salts [105]. The E141

colorant is classified in the lipid-soluble E141i, consisting of copper chlorophylls (Cu-pheophytin, Figure 1.6), and in the water-soluble E141ii, consisting of copper chlorophyllins [106].

Besides the use of chlorophylls in food industry due to their high green pigmentation [82], these pigments can be also employed in pharmaceutical and cosmetic industries, due to their health benefits, such as antioxidant, stimulation of the immune system, and anti-inflammatory properties [93,107].

It has been demonstrated that microalgae can produce chlorophylls in an economically feasible way [108]. Thereafter, species such as *C. vulgaris* are able to grow rapidly and achieve 4% of chlorophylls on a dry weight basis (Table 1.2) [62,81]. In fact, due to its chlorophyll content, which is one of the highest found in nature, *C. vulgaris* is known as the "emerald food" [92,109,110]. Moreover, chlorophylls can be isolated as a co-product, which can potentiate their valorization, representing an increase of the revenue stream of microalgae [111].

Table 1.2 – Pigment content in *C. vulgaris* grown under different conditions.

Pigments	µg/g (DW)	References
Chlorophyll *a*	250 - 32 444	[112,113]
β-Carotene	7 - 12 000	[10,112]
Lutein	52 - 9 820	[10,114,115]
Chlorophyll *b*	72 - 5 770	[10,116]
Pheophytin *a*	2 310 – 5 640	[10,116]
Violoxanthin	10 - 3 700	[10,117]
Astaxanthin	2 200	[10,118]
Canthaxanthin	145 - 1 448	[10,118]
Zeaxanthin	440	[117]

1.3.1.2 Carotenoids

Carotenoids are other class of pigments that, beyond chlorophylls, are found abundantly in microalgae. Their maximum wavelength absorption is in the visible region, ranging

between 400 and 550 nm [82,84]. Carotenoids are colored lipid-soluble compounds that consist of yellow to orange-red tetraterpenoid piments. Oxygen-free hydrocarbon carotenoids are named carotenes whereas oxygenated derivatives are recognized as xanthophylls. In the latter, oxygen can be present forming hydroxyl, keto and/or epoxy groups [93,119,120]. Some carotenoids are found only in certain algal divisions or classes, and, consequently, these carotenoids, as well as some chlorophylls, can be used as chemotaxonomic markers [121]. The main source of carotenoids is from microalgae belonging to the Chlorophyceae class. Among these green microalgae, *Dunaliella salina* and *Haematococcus pluvialis* are largely studied for β-carotene and astaxanthin production, respectively, which biomass accumulation yields depends on culture conditions, namely high light intensities [62,81,82,122]. In Table 1.2 is represented the carotenoids content specifically for *C. vulgaris*, depending on growth conditions. These carotenoids have been extensively used in food industry and in animal and aquaculture feed, as natural color enhancers in alternative to synthetic pigments [123–125].

1.3.1.3 Phycobiliproteins

Phycobiliproteins are brilliantly colored, autofluorescent, and water-soluble pigments, mainly present in Cyanobacteria and Rhodophyta. Due to their role in light harvesting, phycobiliproteins are able to maximize their absorption when exposed to external factors such as changes in pH and ionic composition. Phycobiliproteins are composed of proteins and covalent bound, via cysteine amino acid, to chromophores called phycobillins, which belong to a linear tetrapyrroles, conferring them a very stable structure [126]. According to their amino acid sequences and spectroscopic properties, they can generally be divided into three classes, consisting of red-colored phycoerythrin (PE; λmax = 560–570 nm), blue-colored phycocyanin (PC; λmax = 610-620 nm), and bluish green-colored allophycocyanin (APC; λmax = 650-660 nm) [93,127]. These classes are structurally distinguished by only small differences in the groups attached to the pyrrole rings [108]. The phycobiliproteins are usually organized to form complexes called phycobilisomes, which contain hundreds of protein-bound phycobilins, and are attached to the surface of the thylakoids membranes for photosynthesis [93,108]. Unlike chlorophylls and carotenoids, the phycobilin pigments are only found in algae [58].

Phycobiliproteins can represent up to 13% of the dry microalgal biomass, under certain conditions [128]. Phycocyanin from *Spirulina* spp. and phycoerythrin from *Porphyridium* spp. are two of the most well-known phycobiliproteins that have been produced on an industrial scale [58]. Phycobiliproteins are used as natural food colorant and as markers for immunological methods, such as in flow cytometry, microscopy, and DNA test, due to their highly sensitive fluorescent properties and high photostability [9,64,82,128,129].

1.3.2 Polysaccharides

Microalgae polysaccharides are synthesized intracellularly and represent a major part of the biomass compounds. In eukaryotes, polysaccharides are formed inside chloroplasts, and in prokaryotes are formed in cytosol [20]. Once synthesized, these polysaccharides can operate in several biological functions. They can be distinguished in three different classes: energy reserve, structural (i.e. cell wall related polysaccharides), and extracellular polysaccharides [9,130]. This different type of polysaccharides that exhibit different functions in microalgae cells, also reveals different uses in food, nutraceuticals, and pharmaceuticals industries. Even although they have been mainly determined as a total carbohydrate content, it is important to analyse them separately.

1.3.2.1 Structural characteristics of polysaccharides

Reserve polysaccharides can provide stored energy needed for the microalgal cells metabolic processes and allow, if necessary, temporary survival in the dark conditions. Overall, storage compounds, such the carbohydrates, proteins, and lipids, permit the microalgal growth adjustment to the changing of environmental conditions [20]. There are five types of glucan storage polysaccharides in microalgae, which are species-dependent: starch, floridean starch, glycogen, chrysolaminarin, and paramylon and organized by the degree of branching and type of glycosidic linkages (Figure 1.7). Starch, floridean starch, and glycogen consist of α-1,4 and α-1,6 glucose linkages in different ratios, meaning that they have different degrees of branching. Starch is a complex polysaccharide composed of two distinct α-glucans: amylose, a low branched polysaccharide, and amylopectin, a highly branched one. Amylopectin possesses 5‑6% of α-1,6-linkages, which is about one branch

point for every 20 glucose residues. The ratio amylose/amylopectin of starch varies according to the species origin. Floridean starch is at times referred as amylopectin-rich starch, typically contains little or no amylose (0‑5%), and consequently its granules are composed of more branched polymers compared to starch. In other hand, glycogen has the higher degree of branching, with one branching point for 10 glucose residues. Chrysolaminarin and paramylon are composed of β-1,3-linked glucose residues. The linear paramylon polymers are only composed of β-1,3-linked glucose residues, whereas chrysolaminarin has a high degree of branching points, with one β-1,6-linked glucose for 11 glucose residues [130–135].

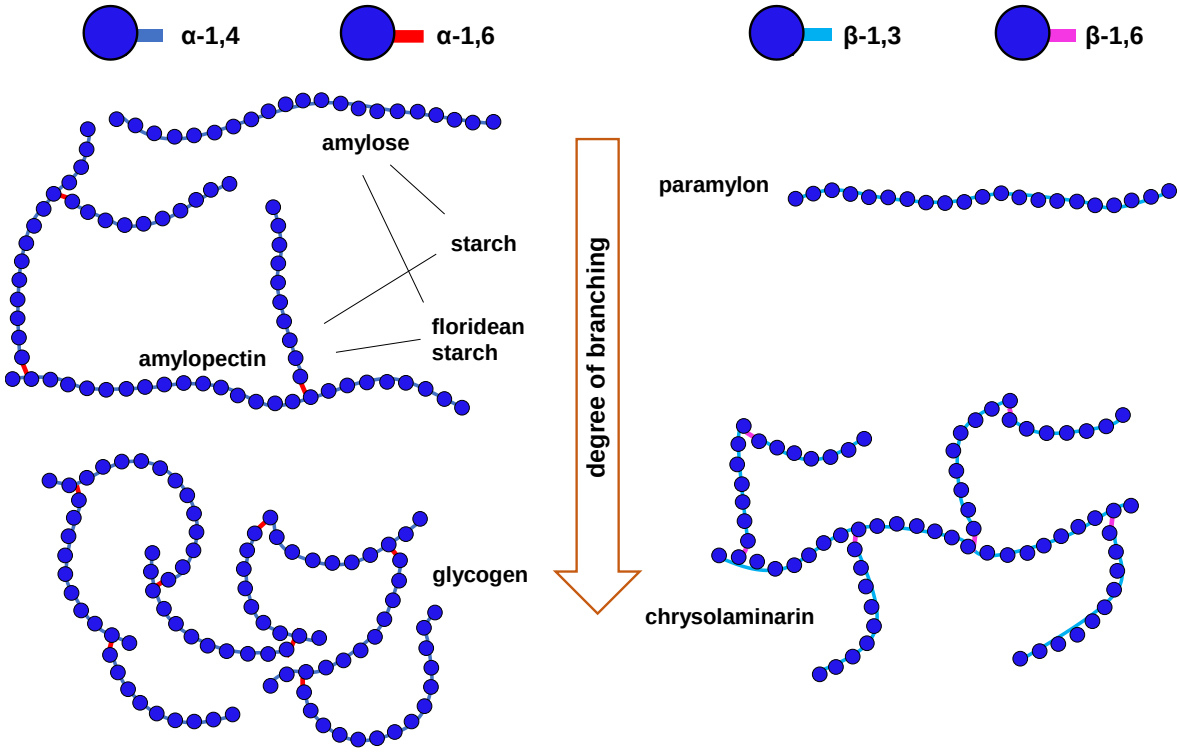

Figure 1.7 – Schematic representation of the five types of storage polysaccharides in microalgae and cyanobacteria, adapted from Bernaerts *et al.* [130].

Chlorophyta (green microalgae), as *C. vulgaris*, synthesizes starch; Rhodophyta, such as *P. purpureum*, and Glaucophyta synthetizes floridean starch [136]; cyanobacteria, such as *Spirulina platensis*, produces glycogen; the linear β-1,3-glucan paramylon is characteristic of Euglenophyta species [137]; and species belonging to the Ochrophyta

phylum, such diatoms and chrysophytes, and to Haptophyta phylum produce chrysolaminarin [138]. The location of these types of storage polysaccharides in the microalgal cell also differs. While starch granules are typically stored in the chloroplasts, chrysolaminarin is accumulated in the vacuoles of the cells. The other three types (floridean starch, paramylon, and glycogen) are located as granules in the cytoplasm outside the chloroplast [139].

The accumulation amount of reserve polysaccharides is dependent of the microalgae species and growth conditions. For instance, *C. vulgaris* is able to produce starch between 9 to 41% in its dry matter content and *P. purpureum* is able to produce up to 4 pg/cell of floridean starch [140].

Structural polysaccharides include the polysaccharides that composes the cell wall that surrounds most of microalgae. The microalgae cell wall is responsible for preserving the integrity of the cell and protecting against unfavourable conditions or invaders [141,142]. Literature related with the quantification and characterization of cell wall polysaccharides is scarce when compared with the other microalgae macromolecules, which could be due to the difficulty in the extraction of these polysaccharides and structural complexity [130]. While glucose is the predominant sugar in reserve polysaccharides, the cell wall related polysaccharides are usually polymers with a heterogeneous monosaccharide composition and different glycosidic linkages. Additionally, these polysaccharides are usually highly branched and can have different substituents in the backbone or in the side chains, such as sulfate or methyl groups [143]. Cell wall composition differs within a phylum, class, species, or even genus [130,144]. Indeed, according to the composition of their rigid cell wall, the genus *Chlorella* can be divided into two distinct groups: one composed by glucosamine residues and the other composed by glucose-mannose polysaccharides. *C. vulgaris*, along with *C. kessleri* and *C. sorokiniana,* belongs to the group that contains glucosamine, as chitin [145–147]. The flexible sugar matrix of chitin-type species is dominated by the neutral sugar residues rhamnose and galactose, being other sugar residues as uronic acids, xylose, mannose, glucose, present in minor amounts. Some polysaccharides such as a glucuronorhamnan [148], β1,3-galactan with 1,6-linkages in the side chains [149], and an arabinomannan [150] were also already reported in *C. vulgaris* cell walls.

In diverse microalgae species, such as the eukaryotic red microalgae *P. purpureum*, the cell wall is surrounded by an external part of polymers, that can either remain associated to

the cell surface or be released into the growth culture, depending on several factors such as the growth stage of the microalgae. These polysaccharides are called exopolysaccharides or extracellular polysaccharides (EPS). The EPS have a commercial advantage over structural polysaccharides, since they can be easily separated and extracted from the culture medium [151–153]. Several potential functions have been attributed to those EPS hydrophilic matrix. Extracellular polysaccharides promote the formation of cell adhesion, forming aggregates that plays a role in the development of biofilms. Moreover, their production is an adaptative response of microalgae to several stresses, such as osmotic stress, having the capacity to retain water and trap cations, which allows the microalgae to resist to desiccation [9,14]. There are still limited information about the structural characterization of the EPS due to their very complex structure, similarly to observed for the structural polysaccharides [9,130]. Microalgae are recognized as an attractive source of EPS, since they can excrete high amounts these polysaccharides [154,155]. For instance, the red microalga *Porphyridium* is able to release soluble exopolysaccharides in a concentration of 0.1–3.4 g/L [156,157] that are in the range of relatively high producing photosynthetic microorganisms such as *Arthrospira platensis* (0.03-0.29 g/L [155]), *Botryococcus braunii* (0.25–1 g/L) and *Dunaliella salina* (0.06-0.94 g/L [158]).

The extracellular polysaccharides of *P. purpureum* are not fully characterized, however, some studies have been made in order to disclose their composition and structure. These extracellular polysaccharides are heteropolymers mainly composed of D-xylose, D- and L-galactose, and D-glucose that have reach a very high molecular mass (2 to 7×10^6 Da) [159–161]. The polysaccharides are anionic due to the presence of glucuronic acid (about 9%) and sulfate groups (about 8%), which are located mainly at the *O*-6 position of glucose [159,161,162]. The *Porphyridium* sp. biopolymer has been found to contain a disaccharide of 3-(α-D-glucuronic acid)-L-galactose, an aldobiouronic acid common in polysaccharides from another red microalgae species [163]. This disaccharide is part of a tetrasaccharide fragment of β-D-Xyl*p*-(1-3)-α-D-Glc*p*-(1-3)-α-D-Glc*p*A-(1-3)-L-Gal*p*. The authors were unable to distinguish between 2- and 4-Xyl sugar residues, and, therefore, two structural possibilities were suggested (Figure 1.8a and b). Moreover, the sulfate groups, as well as the non-reducing Xyl and Gal residues, are attached to *O*-6 Glc of the main chain [159].

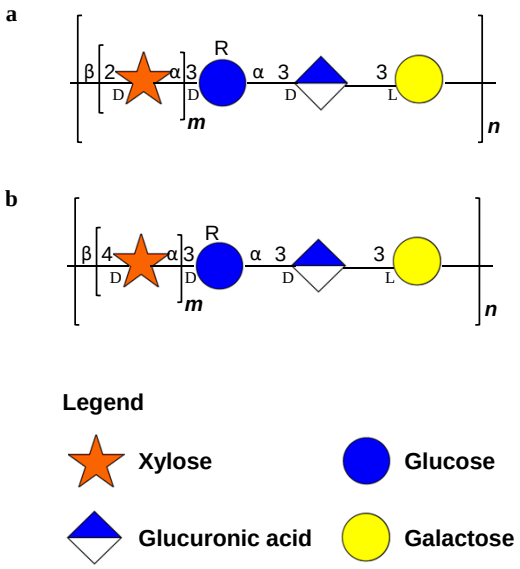

Figure 1.8 – Proposed structures of a linear building block of the *Porphyridium* sp. polysaccharide, R=H, SO_3, terminal Gal or terminal Xyl, with m=2 or 3, where a) corresponds to (1-2)-β-D- Xyl*p*-(1-3)-α-D-Glc*p*-(1-3)-α-D-Glc*p*A-(1-3)-L-Gal*p*, and b) corresponds to (1-4)-β-D- Xyl*p*-(1-3)-α-D-Glc*p*-(1-3)-α-D-Glc*p*A-(1-3)-L-Gal*p* [159].

Gloaguen *et al.* [160] also attempted to elucidate the structure of *Porphyridium* sp. by uronic degradation with lithium in ethylenediamine, resulting in two neutral oligosaccharides fragments (Figure 1.9). Both tetra and hexasaccharide revealed Xyl residues in branches linked to Gal by *O*-2, and the 3 and 4- Xyl residues in the linear polysaccharide chain. It is important to note that both proposed structures (Figure 1.8 and Figure 1.9) are different, maybe due to the use of different methods in the two studies, or due to a difference of origin of alga strains [159].

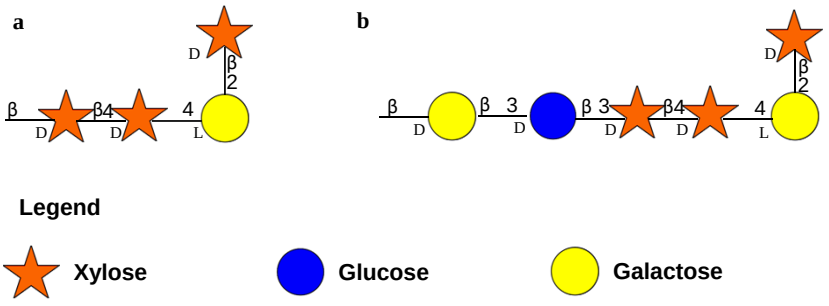

Figure 1.9 – Neutral a) tetra and b) hexasaccharide structures belonging to anionic polysaccharides produced by *Porphyridium* sp. [160].

The green microalgae *C. vulgaris* is also able to excrete polysaccharides to the growth medium, although they have been widely less studied than EPS produced by *Porphyridium* species. Bernaerts *et al.* [164] found that *C. vulgaris* excrete polysaccharides containing mainly glucose, mannose, and galactose, while Noda *et al.* [165] described a glycoprotein with a polysaccharide fraction of β1,6-D-galactopyranose backbone. More recently, a highly branched α-L-arabino-α-L-rhamno-α,β-D-galactan structure was described for *C. vulgaris* EPS [166].

The great diversity of microalgae structural features of their polysaccharides is related with the diverse biological properties attributed to these polysaccharides [6,11,167,168].

1.3.2.2 Immunostimulatory activity of polysaccharides

Biological activities of microalgae polysaccharides have been recently explored. *C vulgaris* structural polysaccharides and EPS have been reported to present anti-inflammatory [166,169], antitussive [169], antitumor [170], antioxidant [170,171], and immunostimulatory properties [172,173]. The sulfated extracellular polysaccharides produced from *P. purpureum* have a wide range of biological activities due to their antiglycaemic [174], antiviral [175–179], antioxidant [180], antitumor [181,182], and immunostimulatory properties [183–185]. Indeed, immunostimulatory activities have been widely attributed to the polysaccharides [186], which can influence both innate and adaptive or acquired immunity. The innate immunity, the first line of defence that does not require a previous encounter with pathogens, includes the activation of phagocytic cells, such as monocytes, macrophages, neutrophils, and dendritic cells, as well as natural killer (NK) cells, while the adaptive immunity can be directly activated by the stimulation of B and T lymphocytes, or indirectly activated by the response of the innate immune cells (Figure 1.10). Thus, polysaccharides are able to activate the innate and adaptive immunity that operates in cooperative and interdependent ways [186,187].

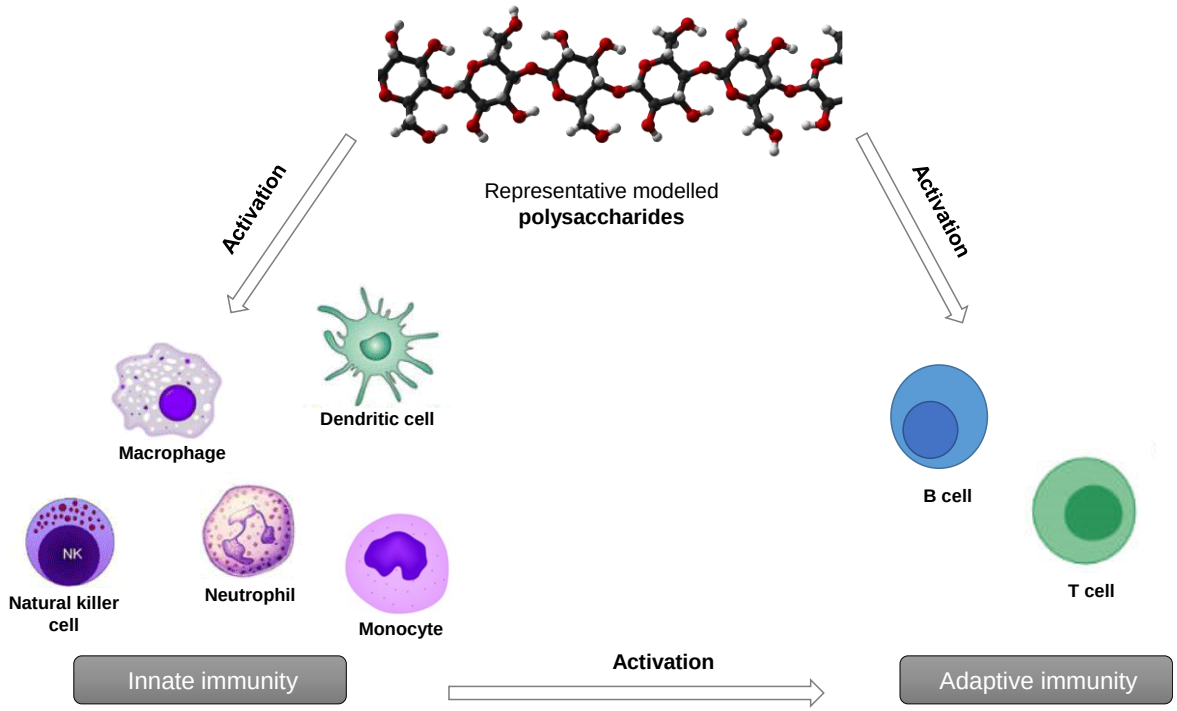

Figure 1.10 – Illustration of innate and adaptive immune system activation by immunostimulatory polysaccharides

The polysaccharides biological properties and applications are dependent on their detailed structure, namely, their composition in monosaccharides, type of linkages, branching, molecular weight, and the presence of functional groups, such as sulfate esters [186,187]. Consequently, the study of detailed structure of the bioactive compounds becomes increasingly important to understand their function. The study of immunostimulatory active polysaccharides involve complementary fields in chemistry and life sciences, which results on just few studies concerning of polysaccharides' structure-function relationship. Some studies only state the immunostimulatory effect, lacking on polysaccharides purification, as for example occurs in the studies where the enhancement of the resistance against infection of *Escherichia coli* [188,189], *Listeria monocytogenes* [190], and murine *cytomegalovirus* [191], via augmentation of cell-mediated immunity, as polymorphonuclear lymphocytes, NK of spleen cells, and T cells were achieved with *C. vulgaris* hot water extracts. *C. vulgaris* microalga also regulated the immune function of shrimp, where polysaccharides biomolecules were speculated to be the main active ingredient [192]. However, the immunostimulatory effect of both studies could be also due

to the other compounds present in this microalga, such as proteins or polyphenols or due to some contaminants like lipopolysaccharides (LPS).

Although very few have been rigorously studied, some recent reports have revealed the structure of polysaccharides that are possibly related with their immunostimulatory activities. *C. vulgaris* contains 1,6-linked glucan with branches at *O*-3 positions able to stimulate macrophage cells, in a dose-dependent manner [172]. *C. vulgaris* polysaccharides of relatively low molecular weight (23.9 kDa) containing terminally linked, 1,3, 1,6, and 1,3,6-galactose and 1,3, 1,6, and 1,3,6-glucose residues [173] also showed immunostimulatory activity on chicken immune cells.

P. cruentum sEPS are able to stimulate macrophage in a dose-dependent and molecular weight-dependent way, since the lower molecular weight (MW) sEPS fragment (6.53 kDa) had the strongest immunoenhancing activity on peritoneal macrophage. while fragments with MW > 903.3 kDa failed to promote the nitric oxide (NO) release from macrophages [183]. *P. cruentum* polysaccharides with galactose, xylose, arabinose and glucose residues are reported to have *in vitro* stimulation of human peripheral blood lymphocytes and hamster splenocytes [185]. Although the sulfate esters are a structural feature that also influences immunostimulatory effect of polysaccharides [186,193], there is no information concerning the influence of the sulfation of *C. vulgaris* and *P. purpureum* polysaccharides on this biological activity.

The ability of microalgae polysaccharides to improve the immune function, and the concomitantly non toxicity effects on normal cells, make them attractive, for instance, to develop nutraceutical or functional feed and food [194].

1.4 Applications of microalgae

Owing to their chemical composition in compounds that exhibit attractive bioactivities, microalgae are regarded as potential feedstock to be used in diverse applications, namely as live feed in aquaculture and for human consumption.

1.4.1 Microalgae in aquaculture

The aquaculture plays an important role in the sustainable growth of fish for human consumption [195]. Microalgae are the foundation of the aquatic food chain and can be supplemented directly to aquaculture or indirectly as live feed to *Zooplankton* [196]. Hence, microalgae can be used as an alternative feed to bivalve molluscs, juvenile fish, and crustaceans in aquaculture due to their rich nutritional value, which promotes growth and improves the reproductive performance [197,198] (Figure 1.11). Furthermore, the use of microalgae in aquaculture as nutraceutical is having great industrial acceptation, since marine invertebrates have an immature immune system [199]. Therefore, microalgae have been used to enhance the defense mechanism systems of these organisms and reduce infectious diseases, due to the immunostimulatory activity of their polysaccharides [186]. Consequently, the use of these natural immunostimulants can avoid the use of antibiotics that could be threat to human health [195]. Some microalgae such as *Chlorella*, *Spirulina*, *Haematococcus*, *Nannochloropsis*, and *Isochrysis* have been grown routinely for aquaculture [200]. Other microalgae that are easy to cultivate, with good nutritional value, with high content of immunostimulatory polysaccharides, and digestible cell wall, need to be considered [14,199,201–203].

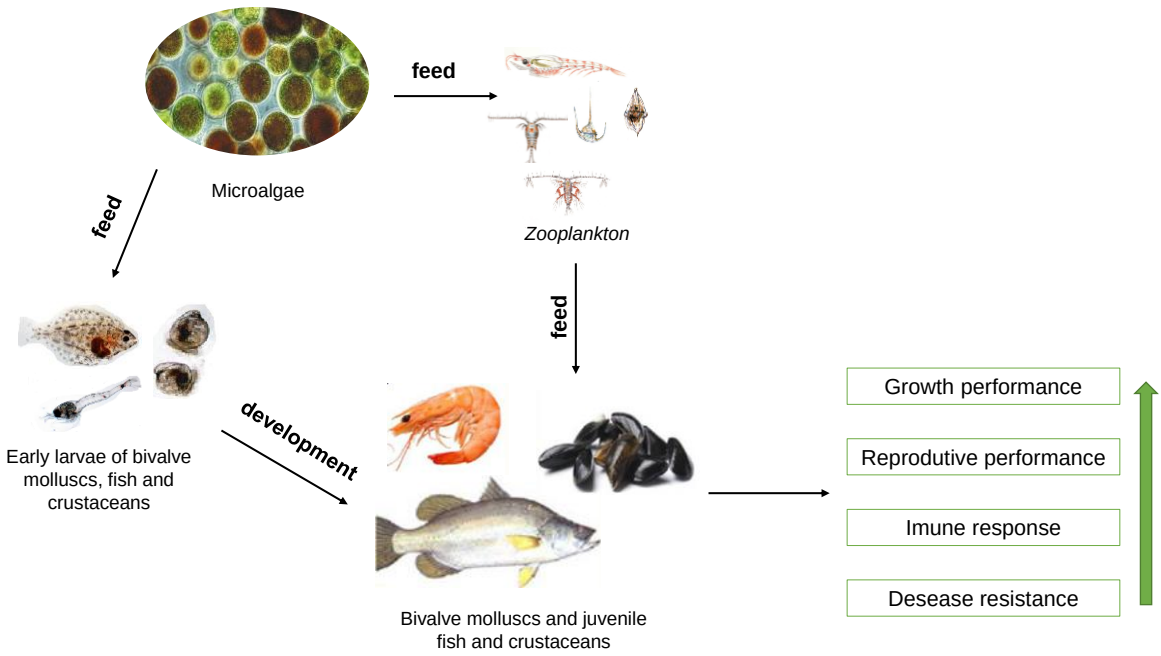

Figure 1.11 – The direct use of microalgae as a feed to bivalve mollusks, and juvenile fish and crustaceans, and indirectly as feed to Zooplankton used in the aquaculture food chains.

1.4.2 Microalgae for human consumption

Achieving an efficient, sustainable, and nutritious food is a growing global concern with the increase of world population. Microalgae represents an opportunity to develop new, more efficient, and healthier food resources that could complement the traditional agriculture to meet the world food supply. Firstly, microalgae to be consumed by humans need to be considered safe. There are only a few microalgae that have the Generally Recognized As Safe (GRAS) status given by the Food and Drug Administration, a status that considers substances or whole organisms safe for human consumption in United States. These microalgae include: *Arthrospira platensis* (*Spirulina platensis*), *Chlamydomonas reinhardtii*, *Chlorella protothecoides*, *Chlorella vulgaris*, *Dunaliella bardawil*, and *Euglena gracilis* [204,205]. In European Union, the European Food Safety Authority (EFSA) oversees the food safety regulations and consider as "novel foods" and "novel food ingredients", the foods which have not been used for human consumption to a significant degree before the Regulation of May 1997. Thus, the microalgae *C. vulgaris*, *C. luteoviridis*, *C. pyrenoidosa*, and the cyanobacteria *A. platensis* and *Aphanizomenon flos-aquae* are not considered a "novel food" but yet approved for human consumption due to the history of their commercialization and consumption by a prolonged period [206]. In other hand, DHA rich oil extracted from *Schizochytrium* sp. [207], oil extracted from *Ulkenia* sp., astaxanthin extracted from *Haematococcus pluvialis* [208], or the phycocyanin extracted from *Spirulina* [209] are considered a novel food product pursuant to Regulation (EU) 2015/2283. Moreover, the microalgae *Odontella aurita*, *Tetraselmis chuii*, and *Euglena gracilis* have been authorized to be exploited as whole cells [206].

Currently, the health food market has been using *Chlorella* and *Spirulina* in the formulations of functional foods and nutraceuticals. Nevertheless, the unpleasant fish flavor, which is a bottleneck to their application in food products, limits the incorporation of the biomass to small quantities and, consequently, reducing their health benefits [72,210]. Moreover, the incorporation of whole cells could hinder the bioaccessibility of nutrient and bioactive compounds during consumption [211,212]. Thus, using microalgae extracts as food additives, such as in forms of polysaccharides or pigments is one of the strategies that possibly overcomes the consumers acceptance and nutrients bioaccessibility barriers.

1.5 Hypothesis, aims and outline of this thesis

It is hypothesized that microalgae can growth under controlled conditions to produce valuable compounds, such as pigments and polysaccharides, that could have potential to be valorized as food or feed ingredients with health benefits. This study was focused on *C. vulgaris*, commercially produced by Allmicroalgae for food and feed markets and *P. purpureum*, commercially produced by Necton S. A. for feed aquaculture.

Chlorophylls were extracted from *C. vulgaris* and since they are instable and their color vanish rapidly, compromising their application, the stability of *C. vulgaris* ethanolic solution was evaluated to disclose the most appropriated storage conditions, to ultimately understand their potential to be applied as food colorant. Moreover, the polysaccharides of *C. vulgaris* and *P. purpureum* were extracted, purified, and characterized. The stimulation effect of extracellular polysaccharides on splenocyte T cells (for cell-mediated, cytotoxic adaptive immunity), and B cells (for humoral, antibody-driven adaptive immunity) were also evaluated to understand their application as health promoters.

The present PhD thesis is organized in four chapters, according to the organizational sequence illustrated in Figure 1.12.

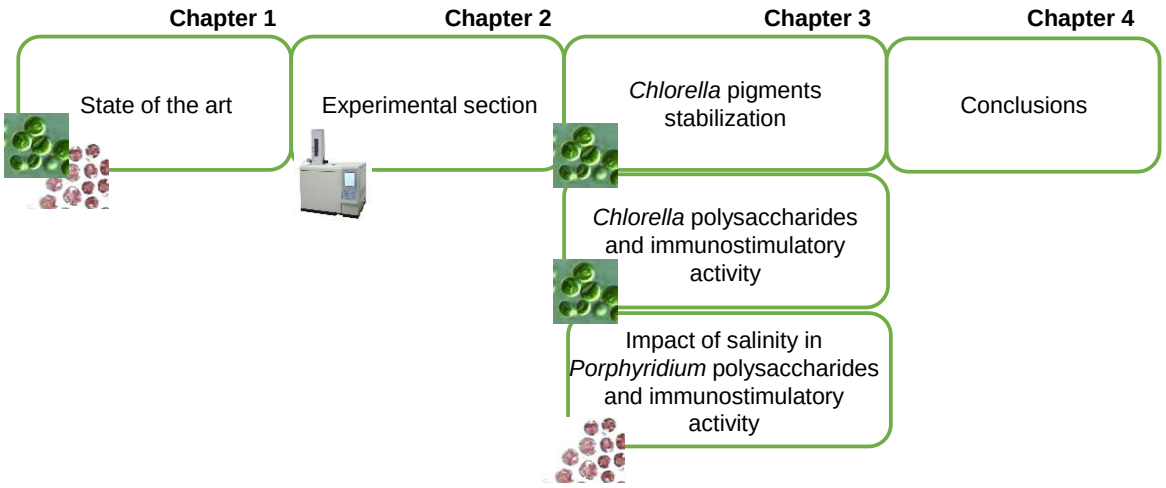

Figure 1.12 – PhD thesis workflow.

Chapter 1 reviewed the most important literature data on production of biomolecules by microalgae, namely *Chlorella vulgaris* and *Porphyridium purpureum*, for food and aquaculture applications. The biological properties, with particular attention to

immunostimulatory activity, of the polysaccharides produced by the two microalgae analyzed under this thesis were also reviewed.

Chapter 2 concerns to the experimental section of this thesis.

Chapter 3 is divided in 3 subsections: **Chapter 3.1** is devoted to the study of the stabilization of *C. vulgaris* pigments in ethanol solution at different storage conditions: temperature, light, alkaline conditions, and modified atmosphere (argon and oxygen), in order to evaluate which conditions have higher effect on the color preservation. **Chapter 3.2** is related to the extraction, purification and characterization of the reserve, structural and extracellular polysaccharides of *C. vulgaris* microalga. Moreover, the immunostimulatory effect of the extracellular polysaccharides were also evaluated. **Chapter 3.3** discusses the effect of three different salinity levels (18, 32, and 50 g/L NaCl) on *P. purpureum* growth rate, and sEPS productivity, structural features, and immunostimulatory activity. Moreover, the viability to produce those sEPS in large scale wall photobioreactor (800 L) for their commercial exploitation was also assessed.

Chapter 4 highlights the main conclusions of the data obtained in all subsections of chapter 3.

CHAPTER 2. Experimental section

2.1 *Chlorella vulgaris* production and biomass fractionation

2.1.1 Culture conditions

Chlorella vulgaris was kindly provided by Allmicroalgae, S.A. (Pataias, Portugal). *C. vulgaris* was cultivated in autotrophic media using the Guillard's F2 culture medium that was adapted to the local water. The culture was supplemented with the concentrated culture medium to reach 4 mM of nitrate. Microalgae cells were transferred to 250 mL Erlenmeyer flasks that were placed in an orbital shaker to further inoculate a 2 L round flask, that was subsequently transferred to 5 L round flasks. The experiments were carried out at room temperature (25 ± 1 ºC), under low light intensity (50 µmol photons s^{-1} m^{-2}), using a photoperiod of 24:0 h (light: dark). The pH was maintained between 7 and 8 by periodic injection of CO_2. The microalgal culture was then subsequential inoculated to an outdoor 125 L flat panel, which was then used to seed a 1 m^3 outdoor photobioreactor. Each scale-up step lasted 7 days [213].

2.1.2 *C. vulgaris* pigments extraction, characterization, and application

Extraction

Different solvents and extraction methodologies were tested to obtain the pigments (green color) from *C. vulgaris* microalgae dry biomass. Thus, 10 mL of ethanol 96%, acetone, or chloroform:methanol (2:1, v/v) were added to 100 mg of biomass, and the respective suspensions were homogenized for 10 min. Moreover, one other extraction with chloroform:methanol (2:1, v/v) was also performed by ultrasound assisted for the first 5 min. The suspensions of all extractions were centrifuged for 3 min (4000 rpm) and the supernatant collected. Two other extractions with 5 mL were performed and all supernatants combined.

Total chlorophylls content determination

Absorption measurements of chlorophyll were made on an Eon Microplate Spectrophotometer (BioTek Instruments, Inc). The equations proposed by Wellburn [214] and Lichtenthaler [215,216] were used for the determination of chlorophyll concentration in the extracts of *C. vulgaris*. The absorbance was measured at 649 and 664 nm to determine chlorophyll a (Chl *a*) and b (Chl *b*) contents when ethanol was used as extraction solvent

[215]. For acetone extract, the absorbance was measured at 647 and 663 nm [216]. For chloroform:methanol extract, the absorbance was measured at 648 and 666 nm [214]. The total chlorophyll content was determined as the sum of Chl *a* and Chl *b* and expressed as mg/g dry weight [91].

Pigments identification by thin layer chromatography (TLC)

To identify the pigments of *C. vulgaris* extracted with ethanol 96%, a thin layer chromatography (TLC) was performed. Thus, *C. vulgaris* ethanolic extract was applied into a 4 cm × 10 cm silica plates. Two different eluents were used, namely petroleum ether:1-propanol:water (100:10:0.25, v/v/v) and *n*-hexane:acetone (7:3, v/v).

Evaluation of pigments stabilization and color loss

C. vulgaris pigments were extracted with ethanol to evaluate their storage stability under different conditions, namely temperature, light, atmosphere, and alkaline environment. In data set 1, 4 g of *C. vulgaris* biomass were mixed with 300 mL ethanol 96% and stirred for 15 min to extract pigments. Thereafter, the ethanolic solution was centrifuged and filtered with glass fiber filters under vacuum. More ethanol 96% was added until the absorbance at 418 nm reach 0.6 (addition of about 800 mL ethanol). NaOH 1 M (100 μL) was added to 300 mL of the solution. The ethanolic extracts were distributed to glass bottles (25 mL). Eight bottles (4 with and 4 without NaOH addition) were placed at 4 ºC and other 8 bottles at 60 ºC in a bath with paraffin (to avoid long term evaporation). In each temperature, 4 bottles were protected from the light (2 with and 2 without NaOH addition) and 4 bottles were subjected to light with a photoperiod of 24 h (about 3500 lx). In each temperature, half of the bottles were under air atmosphere and the other half were under an argon atmosphere, according to the scheme represented in Figure 2.1. The absorbance (300-700 nm, Jenway 6405 UV/Vis) and color through CIELAB system (PerkinElmer, Lambda35-UVWinLab program to obtain the transmittance spectra at 380-780 nm, and COLOR-UVWinLab program for CIE L*a*b*determination, illuminant D65, 10 °) of each solution were measured along 9 days (at 0, 48, 96, 168, and 216 h). CIELAB system expresses color in a three-dimensional space, with three axes: L* for the lightness from black to white, a* from green (-) to red (+), and b* from blue (-) to yellow (+).

To statistically analyze the data, an unreplicated 2^4 full factorial design with two levels was used to evaluate, after 48 h of storage, the effect of temperature (X_1, 4 ºC and 60 ºC), light (X_2, presence or absence of light), modified atmosphere (X_3, presence or absence of oxygen), and alkaline environment (X_4, with or without NaOH). The two levels are coded (+1) and (-1) for the higher and lower limits of each one, respectively. In a two-level full factorial design, 2^k runs are required, where k represents the number of factors to be analyzed, which results in 16 runs performed. The experimental data were statistically analyzed using Minitab v17 software. The Pareto charts were developed for the linear terms and for their interactions that showed statistically relevance to simplify the model. The Pareto chart with the linear and all the 2-way interactions terms are presented in the Annex.

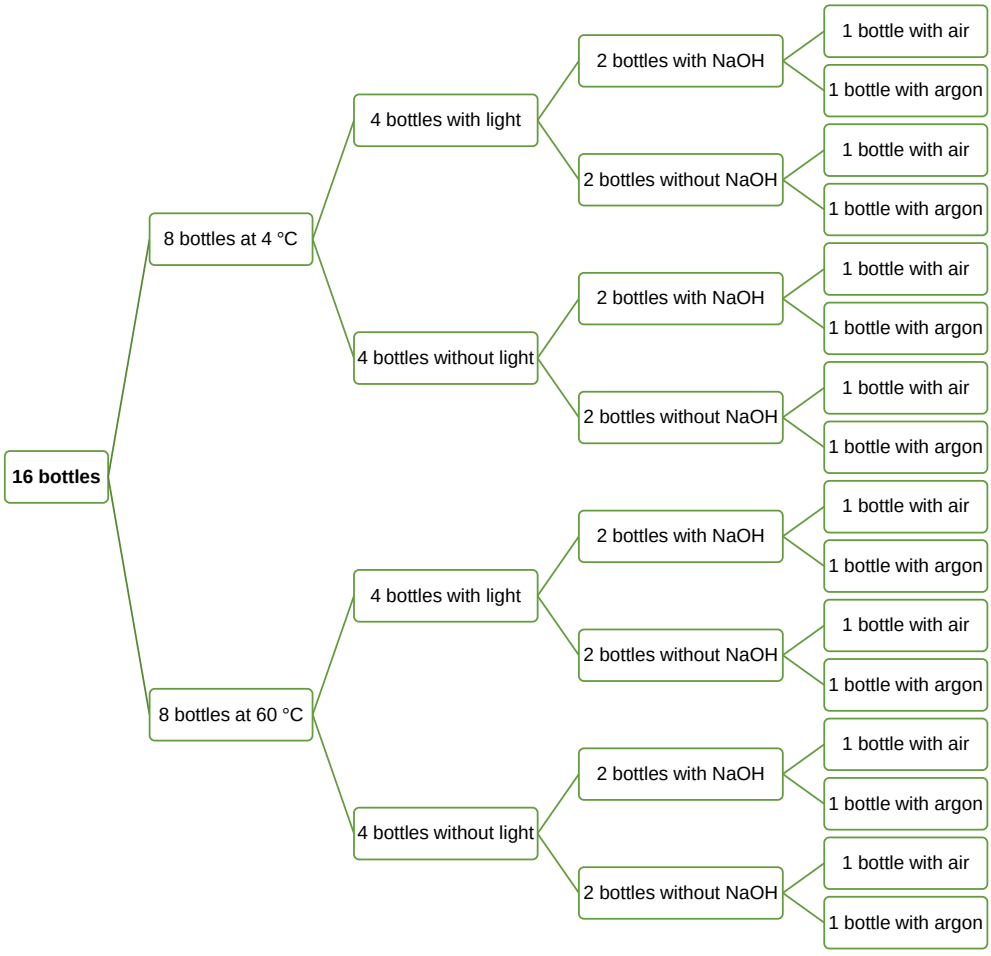

Figure 2.1 – Schematic representation of the study of the stability of *C. vulgaris* pigments at different storage conditions for data set 1.

A second set of experiments (data set 2) was performed with an unreplicated 2^3 full factorial design with two levels to evaluate the effect of temperature (X_1, 4 ºC and 28 ºC), light (X_2, presence or absence of light), and alkaline environment (X_3, with or without NaOH) for 9.5 and 65.5 h, using a more concentrated *C. vulgaris* ethanolic solution (8 g of *C. vulgaris* biomass extracted with 600 mL of 96% of ethanol), resulting in 8 runs performed. The preparation of the bottles with the ethanolic extract was performed as described for data set 1, except for the use of a water bath to monitor the temperature at 28 ºC, instead of a bath with paraffin. The absorbance and color stability were evaluated along 14 days (at 0, 9.5, 19, 36, 65.5, 138, 156, 184, 229, and 324 h, Figure 2.2a).

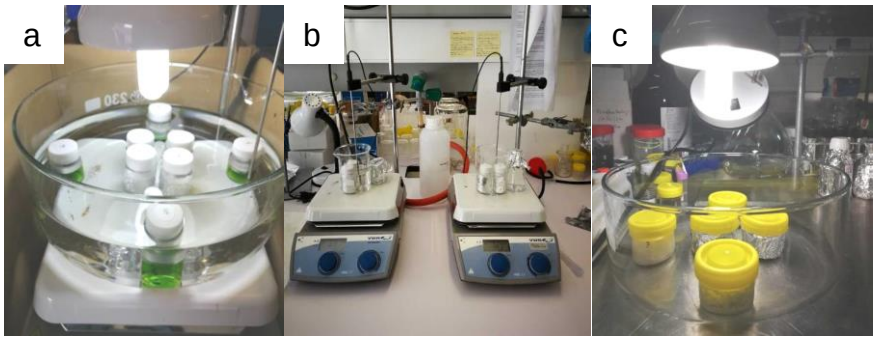

Figure 2.2 – a) Evaluation of *C. vulgaris* pigments storage stability carried out at 28 ºC; b) Evaluation of kinetic degradation of green color at 45 ºC and 60 ºC in a paraffin bath; c) Evaluation of color degradation of green cooked rice (with the incorporation of *C. vulgaris* ethanolic extract).

Degradation kinetic of green color

The bottles with ethanolic extract (data set 2) were placed at five different temperatures: 4, 15, 28, 45, and 60 °C (Figure 2.2b), protected from the light. The color of each solution was measured along 4 days (0, 6, 24, 29, 47, and 102 h). Since green is the major color of *C. vulgaris* ethanolic extract, the increase of parameter "a*" values from a more negative value towards zero (-a*) were considered a visual parameter to describe the green color degradation at different temperatures [98]. The first-order reaction rate constant (*k*) was calculated using the following equation:

$$\ln\left(\frac{-a*}{-a*_0}\right) = -kt$$

where $-a*$ is the "-a*" value measured at different times (t) and $-a*_0$ is the "-a*" value measured at time zero.

Temperature dependence of green color degradation was determined by the Arrhenius equation:

$$k = k_0 e^{-E_a/RT}$$

where E_a is the activation energy (kJ mol^{-1}), k is the first-order reaction rate constant (s^{-1}), k_0 is the pre-exponential factor, R is the universal gas constant (8.3145 J mol^{-1} K^{-1}), and T is the absolute temperature (K).

Food application of C. vulgaris pigments

An ethanolic extract of *C. vulgaris* was obtained using 1 g of biomass and 10 mL of ethanol 96%. This extract (1 mL) was added to 2 containers with 18 g of cold cooked rice. Moreover, 2 mL were also added to 2 containers with the same amount of rice. A fifth container was used as control, only containing the cooked rice. All containers were placed at 4 ºC, 2 in the presence of light in a 24 h photoperiod and 2 in the absence of light. The control was maintained at 4 ºC in the presence of light. The color visually evaluated through photographs along 13 days.

2.1.3 Biomass fractionation

C. vulgaris biomass was fractionated to obtain different extracts with different compositions. A schematic representation of the extraction and purification procedures of polysaccharides from *C. vulgaris* is shown in Figure 2.3. Firstly, *C. vulgaris* biomass was separated by centrifugation (4,696×*g*, 4 °C, 15 min) from the growth medium (that was kept for further analysis). Then, the biomass was defatted exhaustively (13 times, until a faded green color was obtained) with a mixture of chloroform:methanol (2:1 v/v). The lipid fraction was used for further analysis of fatty acid composition. The defatted biomass was subsequently submitted to different polysaccharide extractions.

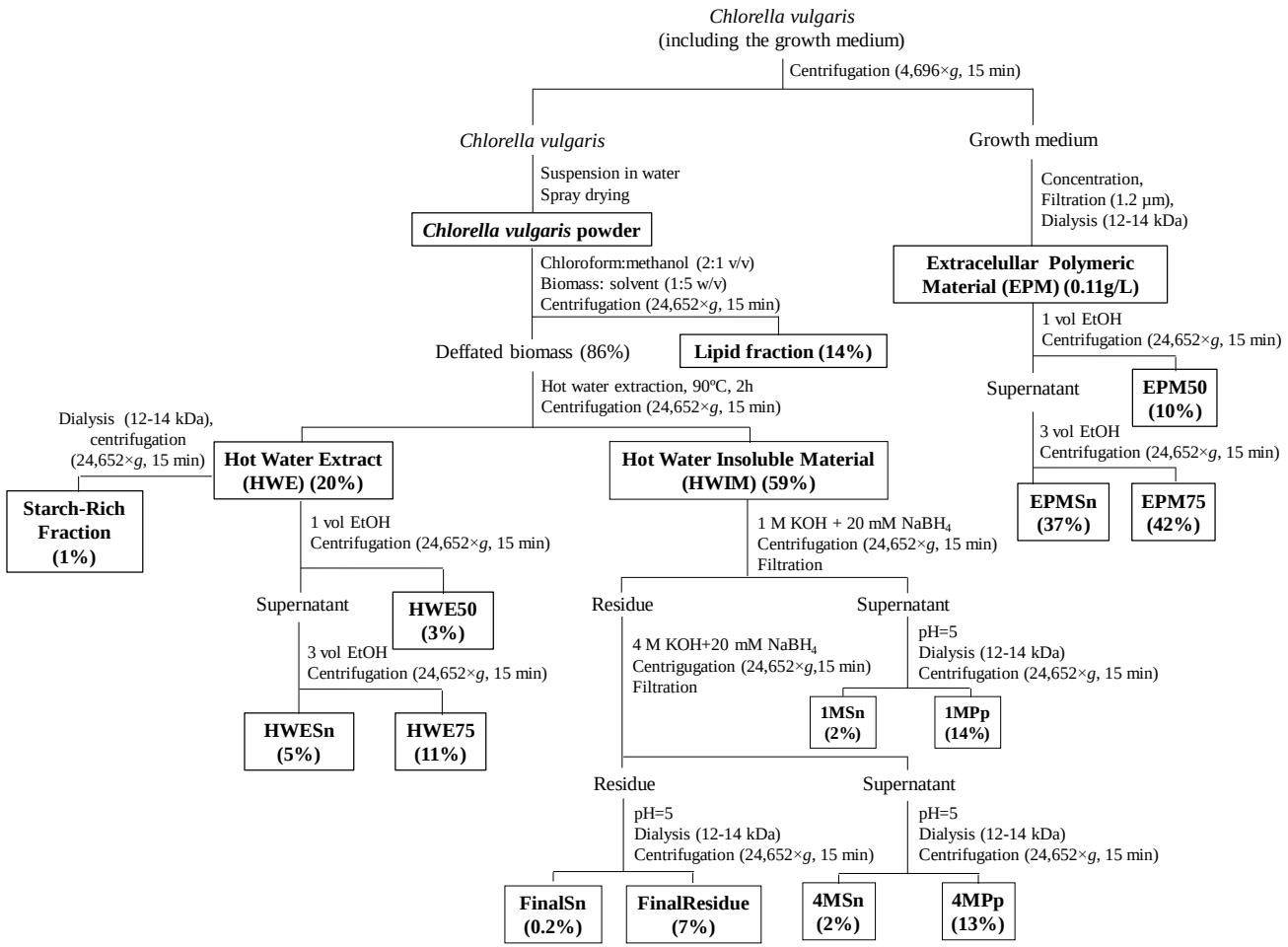

Figure 2.3 – Schematic representation of *C. vulgaris* polysaccharides extraction and fractionation (extraction yields are represented in relation to the *C. vulgaris* powder or extracellular polymeric material). Samples analyzed are represented in bold inside the square boxes. HWE50 – Hot Water Extract precipitated at 50% ethanol; HWE75 – Hot Water Extract precipitated at 75% ethanol; HWESn – Hot Water Extract supernatant; 1MSn – Supernatant of 1 M KOH extraction; 1MPp – Precipitate of 1 M KOH extraction; 4MSn – Supernatant of 4 M KOH extraction; 4MPp – Precipitate of 4 M KOH extraction; FinalSn – Final Supernatant of 4 M KOH extraction; FinalResidue – Final Residue of 4 M KOH extraction; EPM50 – Extracellular Polymeric Material precipitated at 50% ethanol; EPM75 – Extracellular Polymeric Material precipitated at 75% ethanol; EPMSn – Extracellular Polymeric Material supernatant.

Hot-water soluble polysaccharides

The defatted microalgae were extracted twice with distilled water at 90 °C for 2 h. The mixture was centrifuged (24,652×*g*, 4 °C, 15 min) and the supernatants were combined and concentrated in a vacuum evaporator to obtain the hot water extract (HWE). The hot water insoluble material (HWIM) was also recovered and freeze-dried for further analysis. The HWE was dialyzed (12-14 kDa dialysis bag) at 4 ºC, allowing to recover a precipitate by centrifugation (24,652×*g*, 4 °C, 15 min), the starch rich fraction (named as StarchRF). The polymeric material of HWE was also precipitated with 50% (HWE50) and 75% ethanol (HWE75), allowing to obtain the compounds that remain soluble in 75% ethanol solution (HWESn) [217].

KOH-soluble polysaccharides

The hot water insoluble material (HWIM) was subsequently extracted with O_2-free alkaline solutions under N_2 atmosphere at room temperature, according to Nunes *et al*. [218]. The HWIM was extracted for 2 h, firstly with 500 mL of 1 M KOH and then with 500 mL of 4 M KOH, both containing 20 mM $NaBH_4$. The solubilized material was separated from the insoluble residue by centrifugation (24,652×*g*, 4 °C, 15 min), followed by filtration of the supernatant through a glass fiber filter (Whatman GF/C). The extracts were neutralized with glacial acetic acid at pH 5, dialyzed (12-14 kDa) at 4 °C, and centrifuged (24,652×*g*, 4 °C, 15 min). The precipitates (1MPp, and 4MPp) and supernatants (1MSn, and 4MSn) were collected separately and freeze-dried. The final residue was suspended in water, neutralized (pH 5) and dialyzed at the same conditions. The soluble material retained in the dialysis membrane, named final supernatant (FinalSn), was recovered separately from the final residue (FinalResidue) by centrifugation (24,652×*g*, 4 °C, 15 min) and both samples were freeze dried.

Extracellular polymeric material (EPM)

The growth medium of *C. vulgaris* biomass was centrifuged and the recovered supernatant was concentrated using a rotary evaporator, filtered through a glass fiber filter (Whatman GF/C), and dialyzed (12-14 kDa), obtaining the extracellular polymeric material (EPM). A graded ethanol precipitation was performed following the procedure described

earlier section 2.1.2.1 allowing to obtain fractions that precipitate at 50% ethanol (EPM50), at 75% ethanol (EPM75), and that remain soluble in the supernatant (EPMSn).

2.2 *Porphyridium purpureum* growth and sulfated extracellular polysaccharides recovery

2.2.1 Culture conditions

Porphyridium purpureum microalga was obtained from the collection of microalgae cultures from Necton, S.A., (Olhão, Portugal). The culture medium (Nutribloom ®), contained: 1.0 mM $ZnCl_2$, 1.0 mM $ZnSH_4{\cdot}H_2O$, 1.0 mM $MnCl_2{\cdot}4H_2O$, 0.1 mM $Na_2MoO_4{\cdot}2H_2O$, 0.1 mM $CoCl_2{\cdot}6H_2O$, 0.1 mM $CuSO_4{\cdot}5H_2O$, 6.4 mM EDTA-Na, 2.0 mM $MgSO_4{\cdot}7H_2O$, 20.0 mM $FeCl_3$, 20.0 mM EDTA-Na, 2.0 mM $NaNO_3$, and 100.0 mM KH_2PO_4. The nitrate concentration was maintained at 4 mM along all culture time. This culture medium was sterilized by autoclaving at 121 ℃, 1 bar, for 40 min. Three different sodium chloride (NaCl) concentrations were tested: 18, 32, and 50 g/L. The salinity of 32 g/L (0.46 M NaCl) was chosen as a control, corresponding to the salinity of Ria Formosa, Portugal, used in the production plant of Necton S.A.. The salinity of 18 g/L (0.31 M NaCl) approaches the lower salinity value of Ria Formosa, whereas the salinity of 50 g/L (0.92 M NaCl) corresponds to the higher salinity that allows the growth of *Porphyridium* [219]. The salt water with 32 g/L concentration came from Ria Formosa, Portugal, and it was subjected to several sterilization processes: ultrafiltration with a pore size of 0.2 μm, sodium hypochlorite treatment with further sodium thiosulfate neutralization, and by autoclaving at 121 ℃ and 1 bar for 40 min. The water medium with 18 g/L was performed by diluting the treated water of Ria Formosa (salinity 32 g/L NaCl) with tap water and the water medium with 50 g/L was performed by adding NaCl from Necton S.A. salt pans.

P. purpureum cells inoculated at 10^6 cells/mL were maintained in 5 L plastic flasks, containing 0.5 L inoculum and 2 L culture medium (salt water + Nutribloom ®) for 24 days, in 20-21 ºC climate room, with an average pH of 9.2, and subjected to air bubbling and natural sunlight to maintain a photoperiod of 12:12 h light:dark (Figure 2.4a). Each salinity level culture was performed in triplicate.

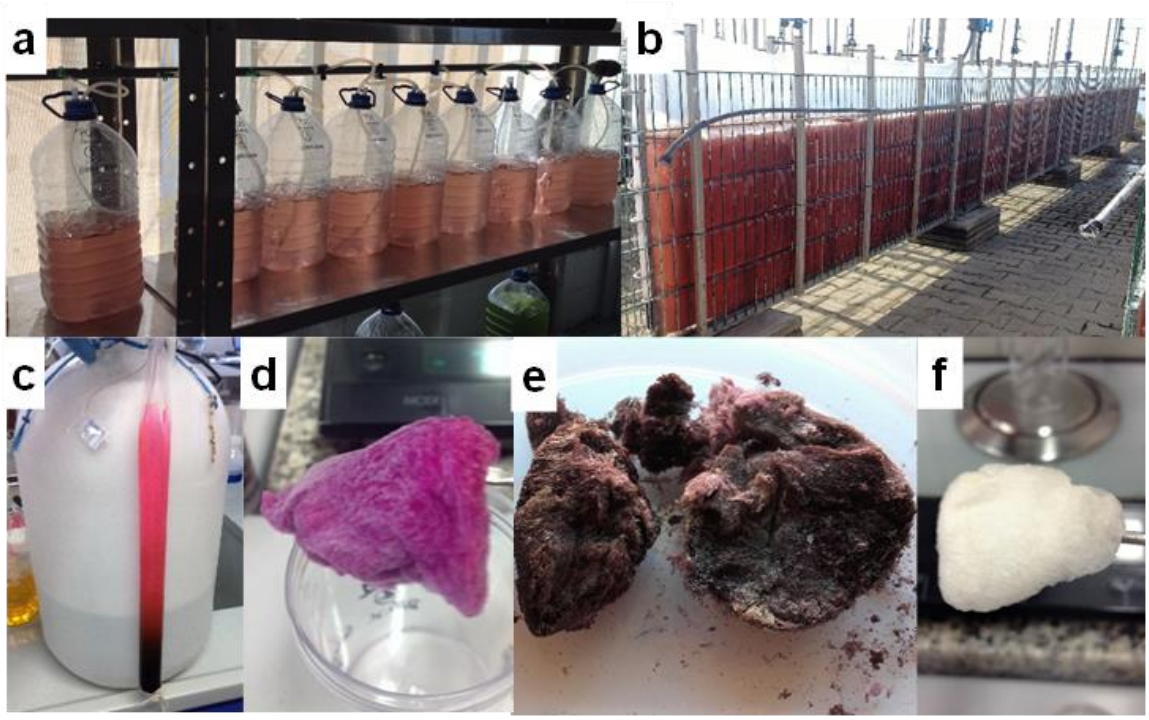

Figure 2.4 – *P. purpureum* cultures and resulting biomass and extracellular polysaccharides. a) Lab scale plastic flask reactor; b) scale-up to 800 L flat panel photobioreactor operated outdoors; c) dialysis bag with *P. purpureum* biomass; d) supernatant of *P. purpureum* biomass dialysis; e) *P. purpureum* biomass after dialysis; f) extracellular polysaccharides of *P. purpureum* purified with graded ethanol.

For scale-up in the outdoor cultivation, Ria Formosa treated water (32 g/L NaCl) and culture medium were used as described for laboratorial scale. A scale up from 2.5 L to 800 L was performed using an outdoor flat panel photobioreactor (Figure 2.4b). The outdoor photobioreactor has a light path of 55 mm with controlled pH and temperature by a pH/Temperature probe. The temperature was controlled (cooled down) with water sprinkles. The growth rate and extracellular polysaccharides released after 16 days, once the stationary phase was reached, were evaluated.

2.2.2 Growth measurement

Microalgae growth was determined by optical density (OD) at 540 nm and it was performed three times for each culture. The OD can be directly related to dry weight and cell density [220], therefore calibration curves of OD vs dry weight (g/L) and OD vs cell density (cells/mL) with aliquots of the 3 salinities were developed (Figure 2.5a and Figure 2.5b),

verifying a linear relationship (r^2=0.9935 and r^2=0.9806, respectively). Dry weight (g/L) was determined by filtering 10 mL of properly homogenized culture. The filters with 0.45 μm pore size were previously washed with distilled water and 0.5 M ammonium formate, dried at 60 ºC until a constant weight, and weighted. Dry weight was calculated by dividing the filtered biomass after drying at 60 ºC until a constant weight by the filtered volume. Cell density (cells/mL) was determined by cell counting under an optical microscope (40 ×) using a mirrored Neubauer chamber with two counting grids. The central quadrant was chosen for cell counting, due to cell size and density. The calculations of growth rates (μ) were done using equation 1 [47], and the generation time or doubling time (g) was calculated using equation 2 [221],

$$\mu = \frac{\ln(Nt) - \ln(N0)}{t - t0} \quad (1)$$

$$\mathrm{g} = \ln 2 \times \mu^{-1} \quad (2)$$

where Nt and N0 correspond to cell density at time t and t0, respectively.

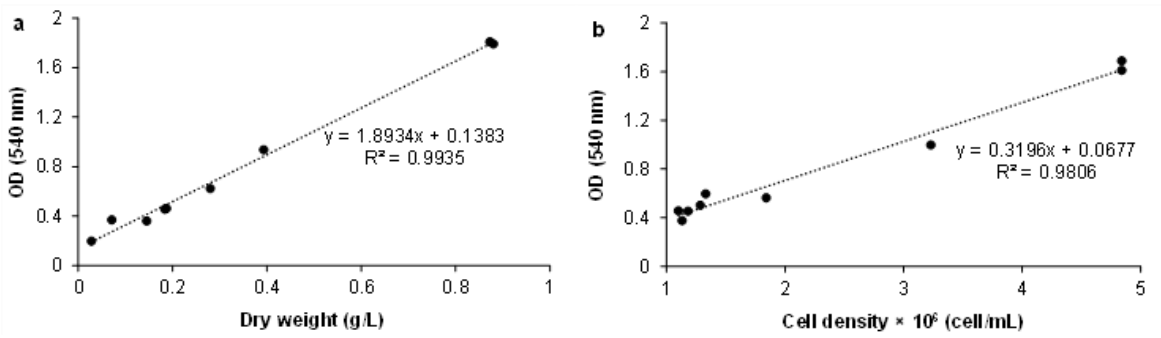

Figure 2.5 – Calibration curves relating optical density (540 nm) with a) dry weight (g/L) and b) cell density (cells/mL).

2.2.3 Recovery of biomass and sulfated extracellular polysaccharides

P. purpureum biomass and culture media were recovered separately by centrifugation (3894×*g* for 10 min, twice). The biomass was then dialyzed against distilled water (12-14 kDa dialysis bag, Figure 2.4c), to obtain the insoluble biomass (Figure 2.4e) and a soluble polymeric material (Figure 2.4d) by centrifugation, which were both freeze-dried for further analysis. The culture media were stabilized by boiling for 30 min, centrifuged, dialyzed (12-14 kDa dialysis bag) and freeze dried (Initial sEPS). Extracellular polysaccharides present in the culture media were purified by the addition of five volumes of graded ethanol, and the resulting precipitate (Purified sEPS) was recovered, washed, freeze dried, and stored for further analysis.

2.3 Analytical methods

2.3.1 Protein analysis

Total protein content of *C. vulgaris* and *P. purpureum* biomasses was estimated by the determination of total nitrogen (N) using elemental analysis (Leco TruSpec 630-200-200 with a TCD detector, USA). Nitrogen-to-protein conversion factor of 6.35 was used for *C. vulgaris* biomass and extracts [73], while a conversion factor of 4.78 was used for *P. purpureum* biomass [222]. The soluble protein content of extracellular polymeric material extracts of *P. purpureum* was measured by the bicinchoninic acid assay [223]. Bovine serum albumin (BSA) was used as a standard in measuring absorbance at 562 nm. The content of phycobiliproteins was estimated by absorbance at 565 nm [224].

For amino acid composition analysis of *C. vulgaris* biomass, the protein was solubilized in 50 mM phosphate buffer pH 7.0 containing 1% (w/w) Pronase from *Streptomyces griseus* (10165921001, PRON-RO, Roche, Switzerland), and incubated at 37 ºC [225,226]. After 24 h, 10 µg of Prolidase from porcine kidney (P6675, Sigma-Aldrich, USA) was added and incubated at 37 ºC for 2 h. After enzymatic hydrolysis, the amino acids were derivatized with ethyl chloroformate according to the method described by Qiu *et al*. [227] and subsequently analyzed by gas chromatography quadrupole mass spectrometry (GC-qMS) (GC-2010 Plus, Shimadzu, Japan) using a non-polar column DB1 (30 m length, 0.25 mm internal diameter and 0.10 µm stationary phase, Agilent, USA), by injection of 1 µL in split

mode (split ratio 2.0) with an injection temperature of 260 ºC. The initial column temperature was 70 ºC, and the temperature increased to 260 ºC at 10 ºC/min and then to 300 ºC at a rate of 20 ºC/min. The carrier gas (helium) was maintained at a constant flow rate of 1.51 mL/min. The transfer line temperature was 300 ºC and the temperature of the ionization source was 250 ºC. Mass spectra were acquired in the full-scan mode (50-700 *m/z*) after ionization by electron impact with 70 eV.

2.3.2 Fatty acids analysis

Lipidic fractions of *C. vulgaris* and *P. purpureum* biomasses were extracted using a mixture of chloroform:methanol (2:1, v/v) [228] that was stirred and treated in an ultrasound bath for 15 min, and quantified by gravimetry. To characterize the fatty acids profile, fatty acid methyl esters (FAMEs) were prepared by transesterification with sodium methoxide [229], using heneicosanoic acid (C21:0) prepared in *n*-hexane as internal standard. FAMEs were then analyzed and separated on a gas chromatograph (Perkin Elmer Clarus 400, Massachusetts, USA), equipped with a 30 m × 0.32 mm, 0.25 μm film thickness DB-FFAP fused silica capillary column (J&W Scientific Inc., Folsom, CA, USA) and a flame ionization detector. (GC-FID). The GC injection port was programmed at 245 °C, and the detector at 250 °C. Oven temperature was programmed in three ramps, from 75 to 155 °C at 15 °C/min, from 155 to 180 °C at 3 °C/min, and from 180 to 220 °C at 40 °C/min, and held isothermal for 3 min. The carrier gas was hydrogen at 50 cm^3/min [230]. The compounds were identified by comparing their retention times with a commercial FAME mixture of reference (C8-C24) (Supelco, USA).

2.3.3 Ash content

The inorganic material was determined by placing microalgae biomasses in a muffle furnace at 700 °C for 6 h, under air atmosphere in a pre-weighed dry porcelain crucible. After cooling down, ash content (%) was determined by gravimetry.

2.3.4 Thermal gravimetric analysis

Thermal gravimetric analysis (Setaram, setsys Ev 1750 ITGA) was performed to *P. purpureum* biomass under nitrogen atmosphere with a caudal of 200 mL/min. The temperatures ranged from 25 to 700 °C at 10 °C/min.

2.3.5 Sulfate content

The content of ester sulfates in the Initial sEPS and Purified sEPS *P. purpureum* extracts was determined by the turbidimetric method proposed by Dodgson and Price [231,232]. The extracts were accurately weighed (usually 2–4 mg) and dissolved in the respective amount of hydrochloric acid 1 M. The mixture was submitted to a hydrolysis at 105–110 °C for 5 h. A portion (0.2 mL) was transferred to a tube containing 3.8 mL of 3% (w/v) trichloroacetic acid. Barium chloride-gelatin reagent (1 mL) was added, and, after mixing, the whole was kept at RT for 15–20 min. The barium chloride-gelatin reagent was previously prepared by mixing gelatin (1 g) with 200 mL of hot water (60–70 °C) and was allowed to stand at 4 °C overnight. Barium chloride (1 g) was dissolved in the semigelatinous fluid and the resultant cloudy solution was allowed to stand for 2–3 h before use. The solution was then analyzed at 360 nm (microplate reader Eon, Biotek, USA) against reagent blank containing distilled water instead of sample. A second 0.2 mL portion of the hydrolysate was mixed with 3.8 mL of trichloroacetic acid, as described above, and with 1 mL of gelatin solution (i.e., containing no barium chloride). The extinction of this "control" solution was then measured at 360 nm against a reagent blank consisting of distilled water instead of sample and 1 mL of gelatin solution. The concentration of sulfate esters was determined by building a K_2SO_4 calibration curve, containing between 20 and 200 μg of SO_4^{2-} ion.

The content of ester sulfates in the *P. purpureum* biomass and *C. vulgaris* EPM extracts was determined by elemental analysis in a Truspec 630-200-200 with a TCD detector.

2.3.6 Carbohydrate analysis

Neutral sugars were determined as alditol acetates as described by Coimbra *et al.* [233]. Briefly, a pre-hydrolysis of *C. vulgaris* freeze-dried extracts was performed with 72% (w/w)

sulfuric acid for 3 h at room temperature, followed by a hydrolysis with 1 M sulfuric acid for 2.5 h at 100 °C. 2-deoxyglucose (1 mg/mL) was used as internal standard. Monosaccharides were reduced with $NaBH_4$ and acetylated with acetic anhydride using methylimidazole as catalyst [234]. The formed alditol acetate derivatives were analyzed in a Perkin Elmer chromatograph (Perkin Elmer Clarus 400, Massachusetts, USA) equipped with an FID detector and a DB-225 column (30 m × 0.25 mm and 0.15 μm of film thickness, J&W Scientific, Folsom, CA). The temperature of the injector was 220 °C while the detector operated at 230 °C. The following oven temperature program was used: initial temperature was set at 200 °C and then rises to 220 °C at 40 °C/min, standing for 7 min, and reaches 230 °C by a 20 °C/min rate maintaining this temperature for 1 min. The carrier gas (H_2) had a flow rate set at 1.7 mL/min. [235]. Uronic acids (UA) were quantified by the 3-phenylphenol colorimetric method using a calibration curve made with D-galacturonic acid (10-80 μg/mL) [234].

Glycosidic-substitution analysis was performed using a GC-qMS of the partially methylated alditol acetates, as described by Ciucanu and Kerek [236] and Oliveira *et al.* [237]. The different *C. vulgaris* extracts and *P. cruentum* extracellular polysaccharides were dissolved in anhydrous dimethylsulfoxide and then powdered NaOH was added under an argon atmosphere. The samples were methylated with CH_3I during 20 min with stirring (this procedure was repeated twice). Chloroform: methanol (1:1, v/v) was added and the solution was dialyzed (12–14 kDa) against 50% EtOH. The retentate was evaporated to dryness. The methylation procedure was repeated to assure a complete methylation. The remethylated sample was hydrolyzed with 2 M TFA at 120 °C for 1 h, and then reduced and acetylated as described for neutral sugar analysis, using $NaBD_4$ instead of $NaBH_4$ to mark the anomeric carbon and facilitate MS identification. The partially methylated alditol acetates were separated and analyzed by GC-qMS (GC-2010 Plus, Shimadzu, Japan) using the chromatographic conditions described by Martin-Pastor *et al.* [238]. The GC was equipped with a DB-1 (J&W Scientific, Folsom, CA, USA) capillary column (30 m length, 0.25 mm of internal diameter, and 0.10 μm of film thickness). The samples were injected in "split" mode with the injector temperature at 250 °C. The temperature program used was as follows: an initial temperature of 80 °C; an increase of 7.5 °C/min until 140 °C, and a hold time of 5 min; an increase of 0.2 °C/min until 143.2 °C; an increase of 12 °C/min until 200 °C; an increase of 50 °C/min until 250 °C and a hold time of 5 min. The carrier gas has helium with

a flow of 8.5 mL/min. The GC was connected to GCMS-QP 2010 Ultra Shimadzu mass quadrupole selective detector operating with an electron impact mode at 70 eV and scanning the range m/z 50–700 in a 1 s cycle in a full scan mode acquisition.

To evaluate the sulfate position of *P. cruentum* sEPS, the sulfated extracellular polysaccharides (10 mg) were dissolved in 1.8 mL of dried dimethyl sulfoxide, with the sequential addition of 0.1 mL pyridine, 13 mg of pyromellitic acid, 12 mg of NaF, and 0.2 mL of pyridine, allowing the desulfation of polysaccharides. The mixture was stirred at 120 °C for 3 h, cooled and poured into 1 mL of 3% of $NaHCO_3$ aqueous solution [159,239]. The solution containing the desulfated polysaccharide was dialyzed and freeze-dried. Afterwards, the desulfated polysaccharides were submitted to methylation analysis, as described above.

2.3.7 *In vitro* digestion of starch and estimation of glycemic index (GI)

Total starch content was determined by enzymatic degradation of starch to glucose with α-amylase and amyloglucosidase according to Fernandes *et al*. [240]. For *C. vulgaris* biomass the pigments were previously removed with 80% (v/v) ethanol. The total glucose released was derivatized to glucitol hexaacetate and quantified by GC-FID (Perkin Elmer Clarus 400, Massachusetts, USA) as described in section 2.3.5.

Glycemic Index (GI) represents the glycemic response of a fixed amount of available carbohydrate to simulate the effect on postprandial blood glucose [241]. *In vitro* digestion of raw and boiled *C. vulgaris* biomass and starch rich fraction (StarchRF) was performed using a multiple-enzymatic method [242,243]. Commercial potato starch, boiled potato, and white bread were used as reference. The starch samples, *C. vulgaris* biomass, and white bread were homogenized in HCl-KCl buffer (pH=1.5) (about 20 mg/mL). *C. vulgaris* biomass and potato (about 20 mg/mL) were boiled during 20 min. The final volume of all samples was adjusted for 15 mL adding KCl-HCl buffer (pH=1.5). Thereafter, 400 µL of pepsin from porcine gastric mucosa (P7000, Sigma-Aldrich, USA) prepared in KCl-HCl buffer (approximately 80 U) were added and left to react during 60 min at 37 ºC. After cooldown at room temperature, 0.1 M phosphate buffer (pH 6.9) was added to reach the final volume of 30 mL and an aliquot was taken (T0). Then, 1 mL of α-amylase (18 U, 10070, Fluka, USA), prepared in phosphate buffer, was added and the samples were incubated at 37 ºC. Aliquots of 1 mL were taken from each sample every 30 min along 3 h. The samples

were placed at 100 °C during 5 min to inactivate the enzyme. The reducing sugars content was determined by the 3,5-dinitrosalicylic acid (DNS) method. A standard curve with maltose was prepared (0.05 and 1 mg/mL) and starch content was calculated by multiplying the maltose amount by 0.9. The kinetics of starch hydrolysis was described by the non-linear model $C=C\infty(1-e^{-kt})$ (C is the percentage of starch hydrolysed at time t; C∞ corresponds to the equilibrium percentage of starch hydrolysed after 180 min; k is the kinetic constant; and t is the time, in min). The hydrolysis index (HI) was calculated by dividing the area under the hydrolysis curve (AUC) of each sample by the AUC of white bread (reference sample), expressed in percentage. GI was then estimated by using the equation: GI=39.71+(0.549×HI), established by Goñi *et al*. [242].

2.3.8 Intrinsic viscosity

The intrinsic viscosity of Initial sEPS and Purified sEPS extracts of *P. purpureum* was determined by dissolving the samples in ultrapure water (0.5 mg/mL), overnight. A Cannon-Fenske routine glass capillary viscometer (serie 50, nº 2110) equipped in a viscometer bath was used to measure the passage time of extracellular polymeric solutions flowing through the capillary. The capillary viscometer was filled with 7 mL equilibrated at 25 ºC for 15 min. Viscosity measured in this way was converted in dynamic viscosity (cP).

2.3.9 Starch characterization

Amylose content

The determination of amylose content was carried out according to the ISO 6647 [244] with some slight modifications. About 10 mg of starch rich fraction (StarchRF) were mixed with 0.1 mL of ethanol solution 95% and 0. 9 mL of 1 M NaOH and placed at 100 ºC during 10 min. The samples volume was completed with distilled water to 10 mL. Three aliquots of 500 µL were transferred to test tubes and 100 µL of 1 M acetic acid, 200 µL of iodine solution (prepared with 20 mg/mL of potassium iodide and 2 mg/mL of iodine crystals) and 9.20 mL of distilled water were added. The absorbance at 620 nm was determined using the microplate reader (Eon, Biotek, USA). The same procedure was applied to commercial

amylose in order to get the standard curve (1 to 6 mg/mL). A blank solution was prepared replacing the sample by 500 µL of 0.09 M NaOH.

Fourier-transform infrared spectroscopy (FTIR)

FTIR spectra of the *C. vulgaris* StarchRF and commercial potato starch were obtained using a GoldenGate single reflection diamond ATR system in a Perkin Elmer Spectrum BX spectrometer (USA). Spectra were recorded at the absorbance mode from 4000 to 500 cm^{-1} (mid-infrared region) at a resolution of 16 cm^{-1}. Five replicates (64 co-added scans) were collected for each sample.

Thermogravimetric analysis (TGA)

Thermogravimetric analysis (TGA) was performed to *C. vulgaris* StarchRF and commercial potato starch under nitrogen atmosphere with a caudal of 200 mL/min using a Setaram, setsys Ev 1750 ITGA equipment (France). The temperatures ranged from 30 to 700 °C at 10 °C/min.

X-ray diffraction

C. vulgaris StarchRF and commercial potato starch were equilibrated in a moisture chamber (40 and 80% of relative humidity) for 24 h at room temperature. X-ray diffractograms of dry, 40, and 80% RH samples were conducted using a PANalytical Empyrean X-Ray diffractometer (UK). The radiation used was Cu-Kα (wavelength of 0.15406 nm). The scan was carried out at 45 kV and 40 mA for 2θ range of 5-40º with a step size of 0.04º and a collection time of 196 seconds at each step.

Size distribution

Size distribution of *C. vulgaris* StarchRF and commercial potato starch granules was measured in a COULTER, LS 230 model (USA), applying light scattering, with a detection limit of 0.04-2000 µm. Three replicates were collected for each sample.

Scanning Electron Microscopy (SEM)

The morphologic characteristics of *C. vulgaris* StarchRF and commercial potato starch were examined using a SEM Hitachi (SU-70, Japan) microscope at an accelerated voltage of 1-4 kV. Samples were deposited onto carbon tape before observation.

2.4 Immunostimulatory activity

2.4.1 Mice

BALB/c mice were purchased from Charles River (Barcelona, Spain) and were kept at the animal facilities of i3S (University of Oporto). All experiments were performed according to the Portuguese rules (DL 113/2013), and according to the European Convention for the Protection of Vertebrate Animals used for Experimental and Other Scientific Purposes (ETS 123) and directive 2010/63/EU of the European parliament and the council of 22 September 2010 on the protection of the animals used for scientific purposes.

2.4.2 Flow cytometry analysis of *in vitro* lymphocyte stimulating effect

The preparation of spleen lymphocytes for stimulation tests and flow cytometry analysis was performed according to Pandeirada *et al.* [245]. In a first batch, cells were stimulated with RPMI (negative control), 2.5 µg/mL of *Escherichia coli* lipopolysaccharides (B cells positive control), 2.5 µg/mL of concanavalin A (ConA, T cells positive control) or 25, 100 and 250 µg/mL of EPM75. Co-incubation with 100 µg/mL polymyxin B (PB) was parallelly done to evaluate possible contamination by endotoxins. In a second batch, beyond positive e negative control, 2.5, 25, 100 and 200 µg/mL of Purified sEPS native (N) and desulfated (D) obtained from *P. purpureum* grown at 32 g/L of NaCl. The different concentrations were tested to evaluate the existence of a dose response manner of the native and desulfated polysaccharides. The concentration of 200 µg/mL of Purified sEPS native (N) and desulfated (D) obtained from *P. purpureum* grown at 18 and 50 g/L NaCl were also tested to access the differences between sEPS obtained from the culture salinities. Co-incubation with 100 µg/mL polymyxin B (PB) was performed in parallel for all samples to evaluate possible contamination by endotoxins. Monoclonal antibodies used (diluted from 1:100) were: anti-

CD19 (PE- conjugate; clone 1D3; Biolegend, USA), anti-CD3 (PE-Cy7-conjugate; clone 145-2C11; BD Bioscience, USA), and anti-CD69 (FTIC-conjugate; clone H1.2F3; Biolegend, USA). Lymphocytes were analysed in a BD FACSCanto II flow cytometer using BD FACSDiva Software (Biosciences BD). The collected data files were analysed using FlowJo v10.3 software (Tree Star Inc., Ashland, OR, USA). The gating strategy used to select B and T lymphocytes expressing the molecule CD69 is shown in Figure 2.6.

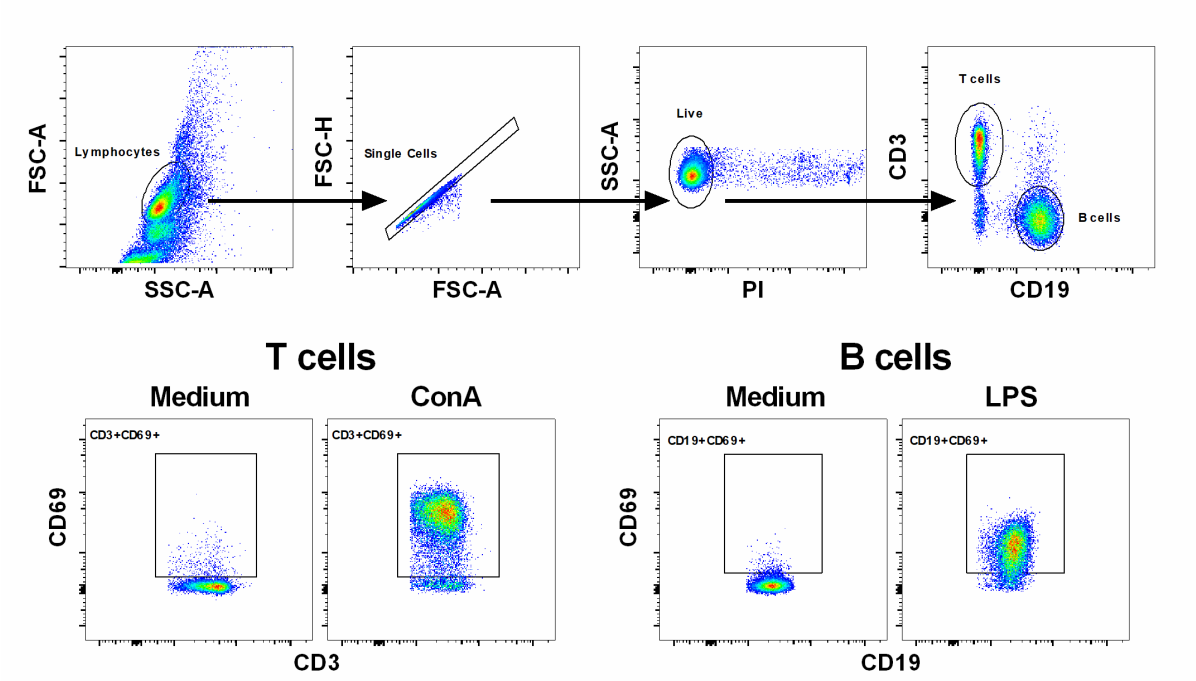

Figure 2.6 – A sequential gating strategy was used to identify lymphoid cell populations by flow cytometry based on their surface expression of specific markers (upper row). Lymphocytes were gated above cell debris based on FSC and SSC characteristics (Lymphocytes); then, doublets were excluded (Single cells), followed by dead cell exclusion (Live), based on propidium iodide (PI) incorporation; T lymphocytes were gated based on CD3 expression (T cells) and B lymphocytes were selected based on CD19 expression (B cells). The percentage of T and B cells expressing the early activation marker CD69 was determined in gated T and B cells (CD3+CD69+ and CD19+CD69+, respectively). Examples (lower row) of the expression of CD69 in gated T and B cells non-stimulated (Medium) or stimulated with Concanavalin A (ConA) and Lipopolysaccharide (LPS), that were respectively used as positive controls for T and B cell activation, are shown.

2.5 Statistical analysis

Statistical analyses were performed using One-Way ANOVA in Minitab 17, for 95% confidence level, using Tukey's comparisons tests. Principal Component Analyses (PCA) were performed in the online platform MetaboAnalyst 3.0 [246], applying a normalization by the total of each sugar residue of *P. purpureum* extracts.

CHAPTER 3. Results and Discussion

3.1 Stabilization of *Chlorella vulgaris* chlorophylls in ethanol

As *C. vulgaris* has a high chlorophyll content, one of the highest found in nature among all species, its pigments have the potential to be used as a natural coloring additive in food products, a major sensorial quality responsible for visual recognition of foods. However, when chlorophylls are out of the chloroplasts, they can easily degrade, decreasing their green color intensity. Consequently, adequate storage conditions are of utmost importance to preserve the color of chlorophylls. Thus, to obtain a suitable green extract to incorporate in food products, *C. vulgaris* pigments were extracted with ethanol, a food grade solvent. The influence of combined storage conditions, namely, temperature, light, atmosphere, and alkaline environment, on the stability of ethanol solutions of *C. vulgaris* chlorophylls/color was studied. This will allow to set the most appropriate storage conditions of *C. vulgaris* ethanolic extract to be further applied as coloring agent in food products.

3.1.1 Evaluation of the efficiency of different technologies to extract *C. vulgaris* pigments

The liposoluble chlorophylls can be extracted from thylakoid membranes of chloroplasts of *C. vulgaris* with organic solvents such as chloroform, methanol, ethanol, and acetone or their mixtures [60,85,89]. Therefore, different solvents, namely ethanol, acetone, and chloroform:methanol (2:1, v/v), and different extraction methodologies, namely ultrasound-assisted extraction, were used to evaluate the *C. vulgaris* chlorophyll´s extraction yield (Figure 3.1). The solvent mixture of chloroform:methanol (2:1, v/v) allowed to obtain a total chlorophylls content of 7.9 mg/g, agreeing with literature [247]. Although extractions assisted by ultrasound has been reported to improve chlorophylls extraction yield [91], it has already been verified that application of high energies may lead to pigment decomposition due to thermal effect [248], which may explain the extraction yield of 8.2 mg/g, similar to the non-treated sample. The extraction with acetone revealed a lower extraction yield of total chlorophylls content (1.1 mg/g). Although this solvent is used for extraction of chlorophylls from plants [249] for dried *C. vulgaris*, it is not the most appropriate solvent.

The extraction of chlorophylls from *C. vulgaris* with ethanol also resulted in a poor extraction (1.7 mg/g), much lower than the extraction yield of the chloroform:methanol, but higher than the yield obtained with acetone. Despite this lower yield, due to its food grade

label, ethanol was used to extract chlorophylls in order to study their storage stabilization for further application as ingredient in the food sector.

Independently of the extraction solvents used, Chl *a* content was always higher than Chl *b* content (Figure 3.1), which agrees with the higher content of Chl *a* in *C. vulgaris* biomass [112]. This allows to use ethanol to obtain a representative extract of the chlorophylls of *C. vulgaris* for further studies.

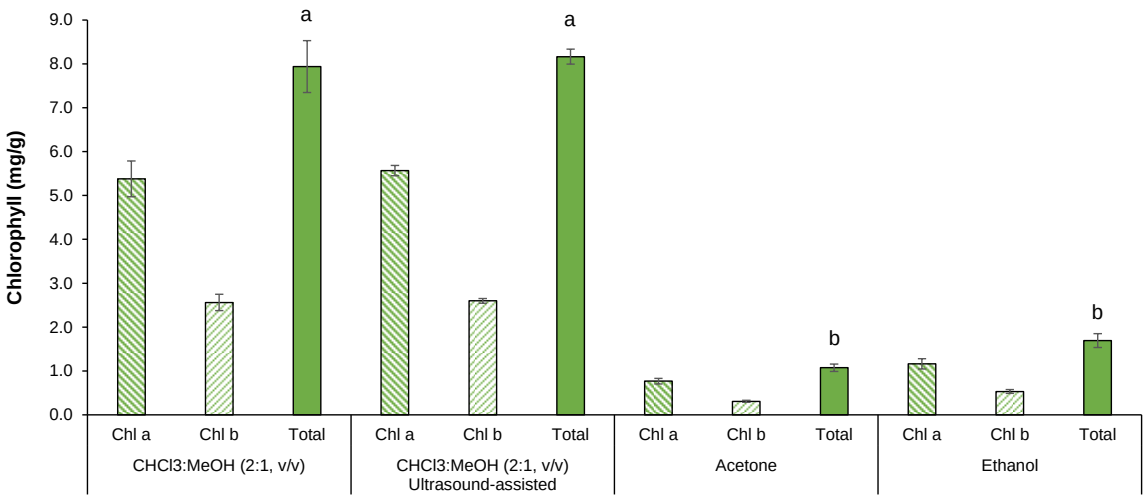

Figure 3.1 – Extraction yield of chlorophyll *a* (Chl *a*, mg/g), chlorophyll *b* (Chl *b*, mg/g), and total chlorophylls (Chl *a* + Chl *b*, mg/g) from *C. vulgaris* biomass, using chloroform:methanol (2:1, v/v), chloroform:methanol (2:1, v/v) assisted with ultrasound, acetone, and ethanol. Mean values ± SD, *n*=9. The different characters above bar indicate statistical differences ($p<0.05$) between compared groups (One-Way ANOVA, Tukey's multiple comparisons test).

3.1.2 *C. vulgaris* pigments identification

To evaluate the pigments composition of the ethanolic extract, a thin layer chromatography (TLC) was performed using two mobile phases with different polarities: petroleum ether:1-propanol:water (100:10:0.25, v/v/v) and *n*-hexane:acetone (7:3, v/v). The separation was carried out on the principle of affinity of substances to the stationary phase and solubility in the mobile phase according to their polarity as follows: the fastest mobility compound was carotene, pheophytin, Chl *a*, Chl *b*, and xanthophylls (Figure 3.2), according with literature [89,250]. The petroleum ether:1-propanol:water eluent allowed the separation and identification of four different pigments (Figure 3.2a), while the less polar eluent, *n*-hexane: acetone, allowed the separation and identification of 5 pigments: the same

previously identified with the addition of the pheophytin (Figure 3.2b), identified by its Rf and color [89]. Despite of the additional band identification, the separation of the most polar compounds with *n*-hexane: acetone was not as efficient (Figure 3.2a) as in the TLC with the organic phase with low water content, since a slight overlap of xanthophylls and Chl *b* was observed (Figure 3.2b). Xanthophylls may correspond to lutein and zeaxanthin, due to their polarity similitude and due to the broad yellow band verified in TLC plate on Figure 3.2a, as reported in literature [89], agreeing with the composition of *C. vulgaris* pigments [115,117].

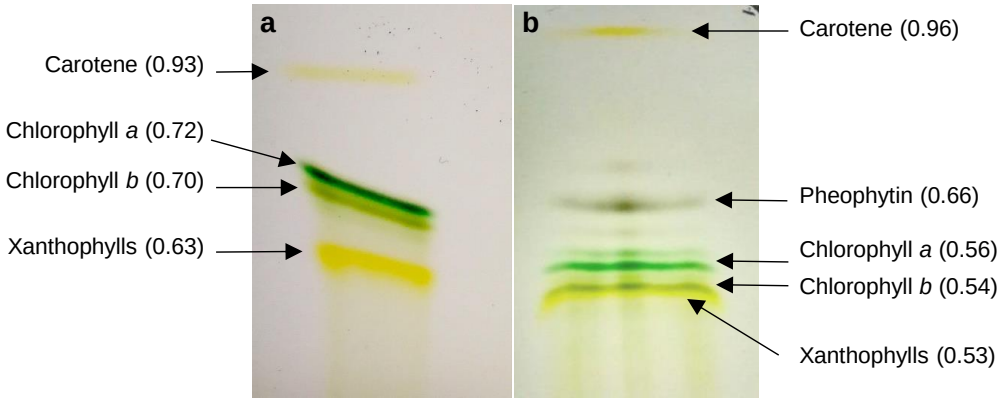

Figure 3.2 – TLC of ethanol *C. vulgaris* extract with two different eluents a) petroleum ether:1-propanol:water (100:10:0.25, v/v/v); b) *n*-hexane:acetone (7:3, v/v). The number between parentheses corresponds to the Rf value).

Albeit a large number of pigments are present, chlorophyll *a* as the most abundant pigment *in C. vulgaris* and responsible for the dark green color, was used as diagnostic pigment to study the stability *of C. vulgaris* pigments in ethanol solutions.

3.1.3 Evaluation of *C. vulgaris* pigments stability

Since Chl *a* present in *C. vulgaris* ethanolic extract is susceptible to chemical degradation, resulting in a decrease of color intensity [251], the evaluation of pigments stability under different storage conditions are necessary for further application as a natural colorant in food products. Therefore, this investigation was undertaken to study the influence of temperature (4 and 60 ºC), light (in the presence and absence of light), alkaline

environment (with or without NaOH), and atmosphere (oxygen-rich or argon-rich atmosphere) on the stability of ethanol solutions of *C. vulgaris* pigments along 9 days (216 h). The evaluation of pigments/green color degradation over time was carried out with 16 experiments in total, measuring the absorbance.

As the maximum absorption of chlorophylls strongly depends on the type of solvent [214], the ultraviolet-visible spectrum (300 – 700 nm) of *C. vulgaris* ethanolic extract was performed (Figure 3.3). The wavelength of 418 nm corresponded to the maximum absorbance absorption, the maximum absorption of Chl *a* in ethanol [90], corroborating the majority of this pigment in the ethanolic extract. In this sense, the evaluation of pigments stability over time was recorded at 418 nm.

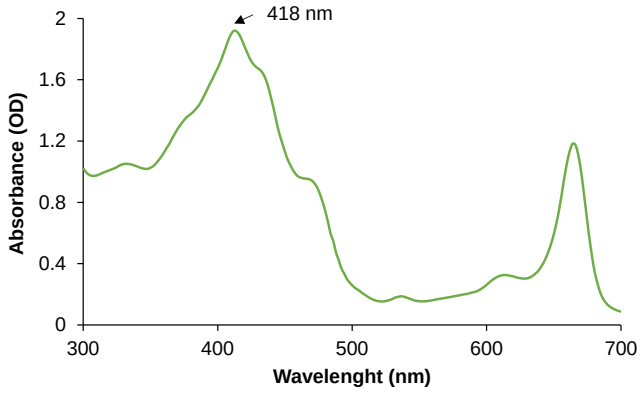

Figure 3.3 – Ultraviolet-visible spectrum of *C. vulgaris* ethanolic extract.

The decrease of absorbance over time (0, 48, 96, 168, 216 h) for the 16 experimental storage conditions is represented in Figure 3.4, where it is possible to observe that after 9 days of storage, although the absorbance decreased for all conditions, showing the instability of green color, the absorbance decrease for the temperature of 4 ºC in the dark, was only 41.3% for 216 h in a rich argon atmosphere, with or without NaOH addition or in the presence of air-rich atmosphere with NaOH addition. A slightly higher decrease of absorbance (53.8%) was observed for the sample in air atmosphere without the addition of NaOH (Figure 3.4a). This was much lower when compared with 60 ºC in the dark, which for the same period presented a decrease of 73.8 % (Figure 3.4b), as well as for the presence of light at 4 ºC (Figure 3.4c), 79.4% decrease, and at 60 ºC (Figure 3.4d), 89.4% decrease.

The use of modified atmosphere and alkaline environment seemed not to have high influence on the degradation of chlorophylls.

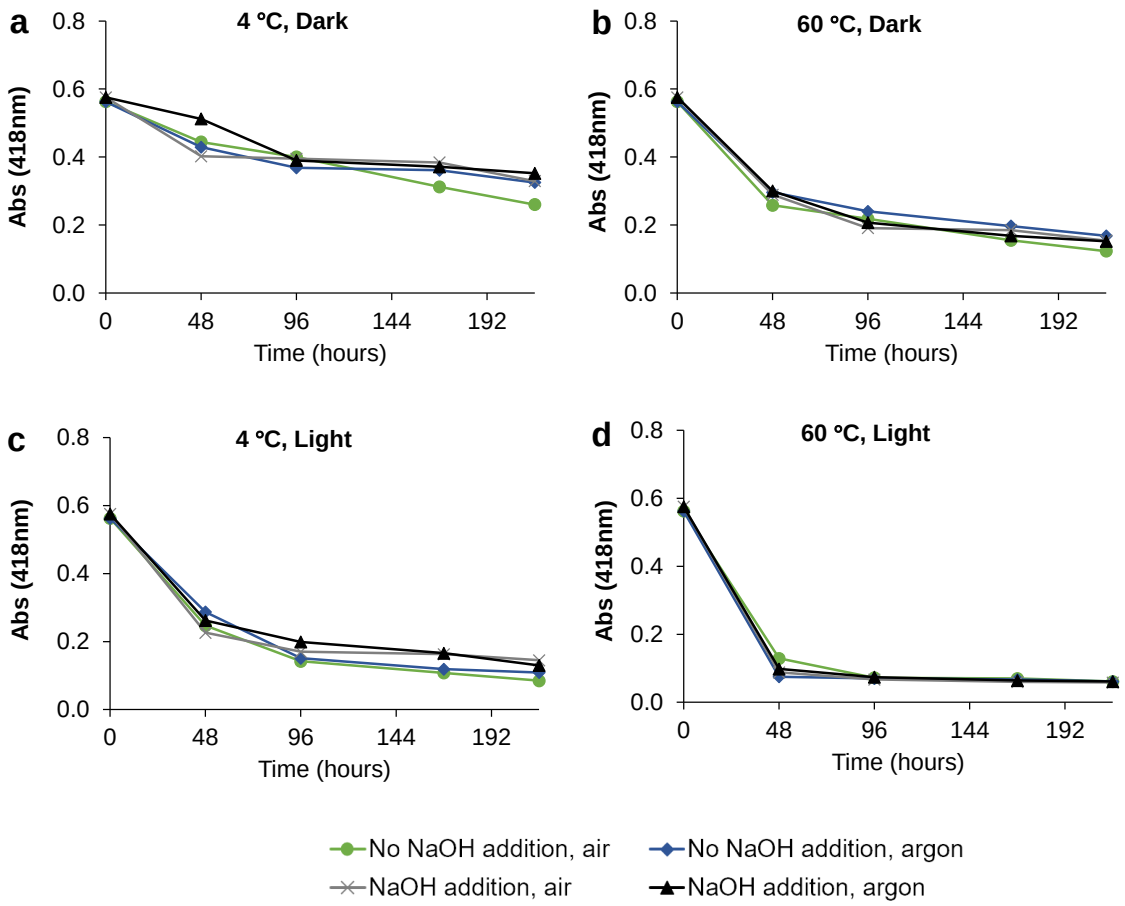

Figure 3.4 – Absorbance (418 nm) measured over time for the 16 experimental conditions a) 4 ºC, Dark, b) 60 ºC, Dark, c) 4 ºC, Light, d) 60 ºC, Light.

The major absorbance decrease was observed for the first period measured, 48 h of storage. In the conditions that have in common the temperature of 4 ºC in the dark, it was observed that with the addition of NaOH in the presence of argon a lower absorbance decrease (-0.001 Δabs/h) was obtained when compared with the other ones (average of -0.003 Δabs/h) (Figure 3.4a). Nevertheless these slopes were lower than those observed for all other conditions, -0.006 Δabs/h at 60 ºC in the dark (Figure 3.4b), -0.007 Δabs/h at 4 ºC in the presence of light (Figure 3.4c), and -0.010 Δabs/h at 60 ºC in the presence of light (Figure 3.4d). Thus, the presence of light and high temperature appears to be the factors that contributed more for the Chl *a* degradation.

The color of *C. vulgaris* ethanolic extract was also measured using the CIELAB system that complement the spectrophotometric method, since color vision is a complex phenomenon and its measurement can be more complex than the absorption at specific wavelengths [98]. Thus, the measurement of -a* is a parameter that have been used to evaluate over time the green color loss of ethanolic solutions [90,98]. In Figure 3.5 is represented the decrease of -a* value over time. As verified for the absorbance measurements, it is possible to observe that after 9 days of storage, the -a* decrease for the temperature of 4 ºC in the dark, was only 51.9% for 216 h (Figure 3.5a), which was much lower when compared with 60 ºC in the dark, which for the same period presented a decrease of 86.7% (Figure 3.5b), as well as for the presence of light at 4 ºC (Figure 3.5c), 91.7% decrease, and at 60 ºC (Figure 3.5d), 100% decrease. In agreement with the data obtained for the absorbance measurement, the color decrease was mainly observed for 48 h of storage.

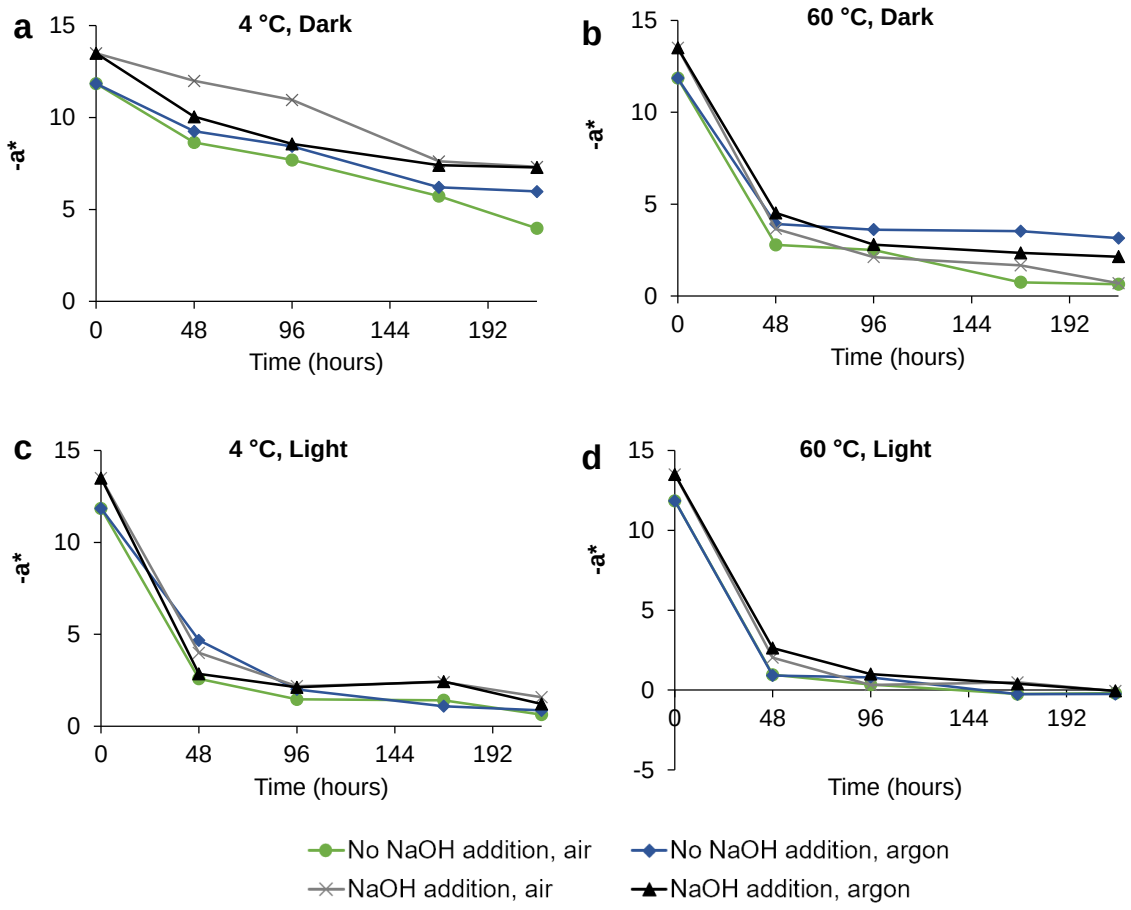

Figure 3.5 – Value of greenness (-a*) measured over time for the 16 experimental conditions a) 4 ºC, Dark, b) 60 ºC, Dark, c) 4 ºC, Light, d) 60 ºC, Light.

In order to better understand which conditions have more influence in Chl *a* degradation and to understand the way that those conditions interact between them, an unreplicated 2^4 full factorial design with two levels was performed for 48 h of storage. The two levels are coded (+1) and (-1) for the higher and lower limits of each one, respectively. The absorbance at 418 nm (Y_1) and -a* (Y_2) for the full factorial design is represented in Table 3.1.

Table 3.1 – Absorbance at 418 nm (Y_1) and -a* (Y_2) settled according to full factorial design for 48 h of *C. vulgaris* ethanolic extract.

Run	X_1 (T, ºC)	X_2 (Light)	X_3 (Atm)	X_4 (Alkaline)	Y_1 (A418)	Y_2 (-a*)
1	-1 (4)	-1 (Dark)	-1 (Air)	-1 (No NaOH addition)	0.444	8.65
2	+1 (60)	-1 (Dark)	-1 (Air)	-1 (No NaOH addition)	0.258	2.78
3	-1 (4)	+1 (Light)	-1 (Air)	-1 (No NaOH addition)	0.247	2.58
4	+1 (60)	+1 (Light)	-1 (Air)	-1 (No NaOH addition)	0.129	0.96
5	-1 (4)	-1 (Dark)	+1 (Argon)	-1 (No NaOH addition)	0.429	9.26
6	+1 (60)	-1 (Dark)	+1 (Argon)	-1 (No NaOH addition)	0.296	3.92
7	-1 (4)	+1 (Light)	+1 (Argon)	-1 (No NaOH addition)	0.287	4.67
8	+1 (60)	+1 (Light)	+1 (Argon)	-1 (No NaOH addition)	0.075	0.91
9	-1 (4)	-1 (Dark)	-1 (Air)	+1 (NaOH addition)	0.402	12.00
10	+1 (60)	-1 (Dark)	-1 (Air)	+1 (NaOH addition)	0.289	3.66
11	-1 (4)	+1 (Light)	-1 (Air)	+1 (NaOH addition)	0.226	3.99
12	+1 (60)	+1 (Light)	-1 (Air)	+1 (NaOH addition)	0.088	2.03
13	-1 (4)	-1 (Dark)	+1 (Argon)	+1 (NaOH addition)	0.512	10.05
14	+1 (60)	-1 (Dark)	+1 (Argon)	+1 (NaOH addition)	0.300	4.52
15	-1 (4)	+1 (Light)	+1 (Argon)	+1 (NaOH addition)	0.262	2.85
16	+1 (60)	+1 (Light)	+1 (Argon)	+1 (NaOH addition)	0.098	2.63

Pareto chart (Figure 3.6a) represents the effects on color stability measured by the absorbance at 418 nm. The linear terms of the variables light (X_2) and temperature (X_1) exhibited significant effect on pigments degradation. This is shown by the bars of the standardized effect that are beyond the vertical red line, representing the statical significance at 95% confidence level, which does not happen when considering their interactions. Moreover, Pareto chart evidenced that linear light variable exerts the most preponderant effect. Accordingly, Pareto chart in Figure 3.6b reveals that the linear terms of the variables

light (X_2) and temperature (X_1) showed significant effect on the green color vanishing (-a*) of *C. vulgaris* ethanolic extract, being the presence of light the most significant factor as well. According to both Pareto charts (Figure 3.6), under the studied conditions, the variables atmosphere (X_3) and the alkaline environment (X_4) on ethanolic solutions had no statistical impact on the color loss. Contrary to Pareto chart of the response at Abs 418 nm (Figure 3.6a), the Pareto chart of the -a* response (Figure 3.6b) showed a significant two 2-way interactions between temperature and light (X_1X_2). When an interaction is significant, it means that the effect of a term on the response is distinct at different levels of another independent variable [252].

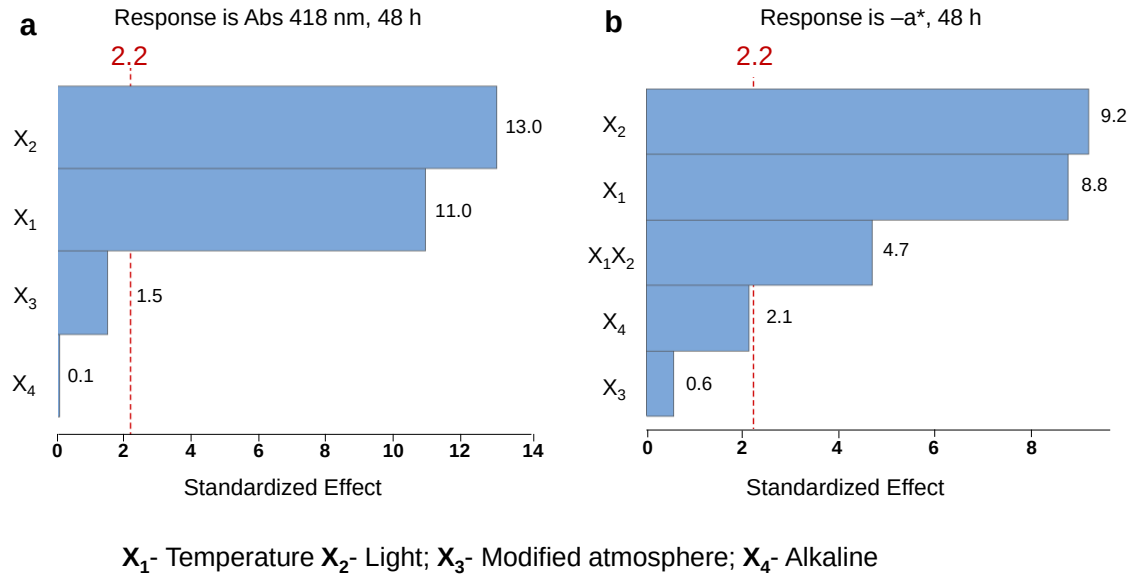

Figure 3.6 – Pareto charts of the standardized effects: a) response is Abs (418 nm), 48 h (p<0.05); b) response is -a*, 48 h (p<0.05).

When chlorophyll in organic solvents such as ethanol, acetone or benzene is exposed to light in the presence of oxygen, it is irreversibly bleached by photo-oxidation, resulting in colorless derivates [253]. The presence of an argon rich atmosphere, instead of an oxygen-rich atmosphere, did not have a significant effect on the protection of chlorophylls degradation, possibly due to the fact that there are oxygen molecules present in the solution, which could be enough to promote photo-oxidation reactions. The lack of effect of modified atmosphere was also verified on the stability of pigments (Chl *a*, Chl *b*, and lutein) of

pistachio kernels, since no differences were observed during storage, irrespective to the use of oxygen scavengers and high gas barrier plastic films [99].

Temperature is also a well-stablished main factor influencing the stability of chlorophylls [97], since high temperatures, 60 ºC in this study, could promote the formation of pheophytins, leading to a green color loss [96]. It was also already reported [90] that the rate of color loss of Chl *a* in ethanolic solutions increases with temperature (tested from 20 to 50 °C). Moreover, the stability of Chl *a* or green color with temperature in broccoli and green beans treated from 40 up to 96 °C [254] and spinach puree in a temperature range of 50–120 °C [98] was also affected. The pH also has influence on stability of chlorophyll pigments mainly changing their structures by pheophytinization. When an acidic solution was added to the *C. vulgaris* ethanolic extract, the solution changed immediately from bright green to olive brown (results not shown). However, the addition of NaOH did not significantly influence the chlorophylls degradation in the present study. Alkaline conditions have been reported to induce oxidation of the isocyclic ring and de-esterification of phytol in chlorophylls. These reactions do not significantly affect the color of the product since these compounds retain intact the basic structure of the chromophore group with Mg linked to the porphyrin ring [255]. Consequently, chlorophyll is reported to be stable at alkaline conditions [98] or even more stable, as verified for the chlorophylls in coriander leaf puree that was found to be most heat stable at pH 7.5 [102].

To evaluate the effect of pigments concentration in the *C. vulgaris* ethanolic extract in different storage conditions, another set of experiments were performed, starting with a higher concentrated ethanolic pigments solution. Since presence of NaOH seemed to prevent the degradation of long-term chlorophyll at 4 ºC in the dark under air atmosphere (Figure 3.4a), the argon-rich atmosphere was no longer tested. Moreover, 28 ºC was tested instead of 60 ºC since higher temperatures greatly promoted Chl *a* degradation. The first batch of experiments also revealed that after 48 h of storage, most experiments had already a faint green color, thus, in the second set, beyond the higher concentration of pigments in the ethanol *C. vulgaris* extract, the time span of the experiments was enlarged with points at 9.5, 36, 65.5, 138, 155.5, 184, 228.5, and 324 h. Thereafter, the total of eight storage conditions were tested throughout the measurement of the absorbance at 418 nm and -a* (Figure 3.7 and Figure 3.8, respectively). According to Figure 3.7a, the lower decreasing of Abs at 418 nm occurred in the absence of light, while the higher degradation rate occurred at the

presence of light (Figure 3.7b). The two temperatures (4 ºC and 28 ºC) seemed to have no impact on the pigment's degradation. Moreover, the addition of NaOH also appeared to have no influence in the maximum absorbance at 418 nm. The measured of -a* (Figure 3.8) also revealed the major importance of the dark to protect chlorophyll degradation as well as the addition of NaOH although in less extent for long periods of time (Figure 3.8a). This protection effect is also noticed in the presence of light (Figure 3.8b).

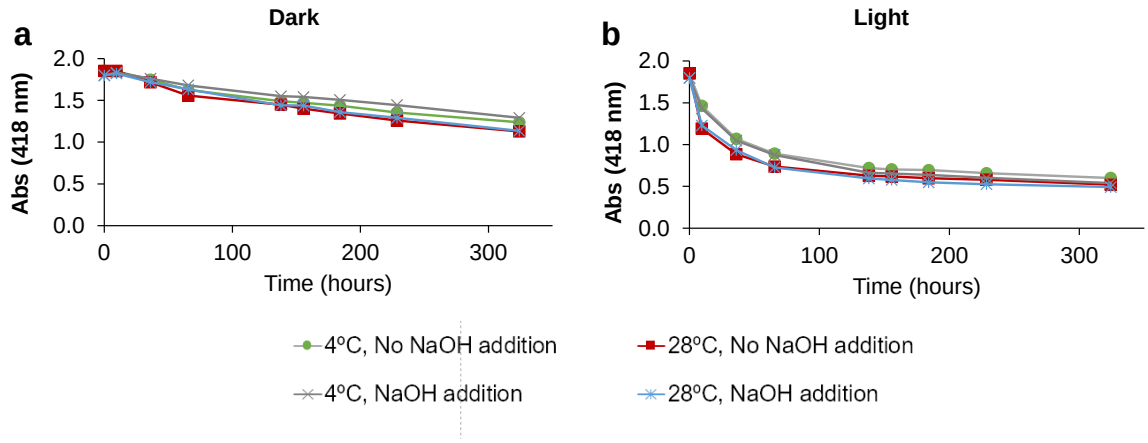

Figure 3.7 – Absorbance (418 nm) measured over time for the 8 experimental conditions a) in the dark, b) in the light.

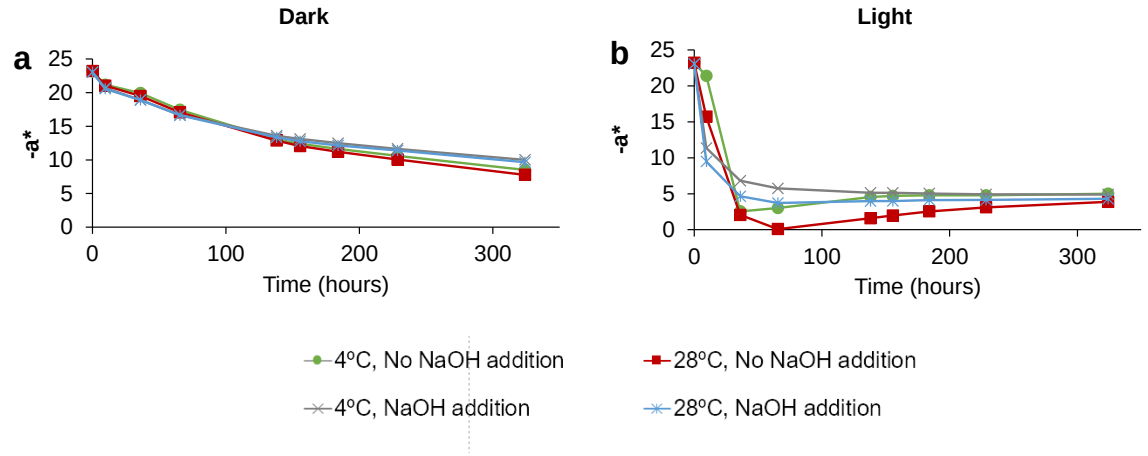

Figure 3.8 – Value of greenness (-a*) measured over time for the 8 experimental conditions a) in the dark, b) in the light.

To understand the influence of pigments concentration on their degradation rate, the degradation at 4 ºC with and without NaOH in the dark and in the presence of light were evaluated. Hence, the analyzed parameters at time 48 h were estimated Table 3.2.

Table 3.2 – Degradation rate (slope) of Chl *a* and green color (-a*) of 4 experiments of each set of experiments at 4ºC for the first 48 h. Set 1 refers to the first batch of experiments (0.6 of absorbance) and set 2 refers to the second batch of experiments (1.8 of absorbance).

Conditions	Runs	A418			-a*		
		Set 1	Set 2	%dif	Set 1	Set 2	%dif
No NaOH additon, dark	1	-0.0025	-0.0029	13.8	-0.0667	-0.0892	25.2
No NaOH addittion, light	2	-0.0066	-0.0163	59.5	-0.1931	-0.4264	54.7
NaOH addition, dark	3	-0.0036	-0.0012	-66.7	-0.0313	-0.1048	70.1
NaOH addition, light	4	-0.0073	-0.0170	57.1	-0.1981	-0.3470	42.9

From Table 3.2 it is possible to observe that set 2, the samples with higher chlorophyll concentration, had a higher degradation rate of Chl *a* (A418) and green color (-a*) higher, in the presence of light, with higher slopes, in accordance with the difference in the initial concentration of the solutions. In dark conditions, the slopes were much lower and similar between sets, allowing to infer the stabilization of chlorophylls in these ethanolic solutions.

The full factorial analysis was employed at 9.5 h and at 65.5 h and the responses Y_1 (abs 418 nm) and Y_2 (-a*) are represented in Table 3.3.

Table 3.3 – Absorbance at 418 nm (Y_1) and -a* (Y_2) settled according to full factorial design for 9.5 and 65.5 h of *C. vulgaris* ethanolic extract (data set 2).

Run	X_1 (T,ºC)	X_2 (Light)	X_3 (Alkaline)	9.5 h		65.5 h	
				Y_1 (A418)	Y_2 (-a*)	Y_1 (A418)	Y_2 (-a*)
1	-1 (4)	-1 (Dark)	-1 (No NaOH addition)	1.846	21.19	1.624	17.45
2	+1 (28)	-1 (Dark)	-1 (No NaOH addition)	1.852	21.04	1.556	17.07
3	-1 (4)	+1 (Light)	-1 (No NaOH addition)	1.463	21.40	0.893	3.02
4	+1 (28)	+1 (Light)	-1 (No NaOH addition)	1.191	15.71	0.737	0.09
5	-1 (4)	-1 (Dark)	+1 (NaOH addition)	1.833	20.72	1.679	16.69
6	+1 (28)	-1 (Dark)	+1 (NaOH addition)	1.822	20.58	1.631	16.64
7	-1 (4)	+1 (Light)	+1 (NaOH addition)	1.434	11.37	0.876	5.75
8	+1 (28)	+1 (Light)	+1 (NaOH addition)	1.229	9.48	0.727	3.72

Full factorial design allowed to demonstrate the statistical relevance (at 95% confidence level) of the presence of light (X_2) on de decreasing of absorbance (418 nm) at 9.5 h of storage, as shown in the Pareto chart (Figure 3.9a), and the statistical irrelevance of the other linear terms, namely temperature (X_1) and alkaline environment (with or without NaOH, X_3). For the same time of storage (9.5 h) of *C. vulgaris* ethanolic extract, similar behaviour was observed in the stability of -a* parameter (Figure 3.9b), where only the presence of light had a slight influence. After longer period of storage (65.5 h), the presence of light greatly influenced the degradation of pigments and green color in the ethanolic solution, verified by the statistically relevance on both absorbance and -a* parameter, as demonstrated by the Pareto charts in Figure 3.9a and b. Moreover, after this period, the linear variable temperature (X_1) also exhibited a lower preponderant influence on the decreasing of absorbance, without statistically affecting the decreasing of -a*. The evaluation of the CIELAB parameter, -a*, reflects the vanishing of green color, which is a crucial visual parameter to take into account for further application of these colorants in the food industry.

A significant two 2-way interactions between the terms light (X_2) and temperature (X_1) it was not observed, contrarily to the experiments performed at 60 ºC, allowing to infer that the temperature of 28 °C did not promote a significant extent of chlorophyll degradation as observed at 60 ºC. It was reported that both refrigerator and room temperatures are suitable to store Chl *a* dissolved in acetone, that was kept for 84 days in the dark [103]. The degradation rate of Chl *a* of pistachio kernels was only slightly different at 10 and at 25 °C [99].

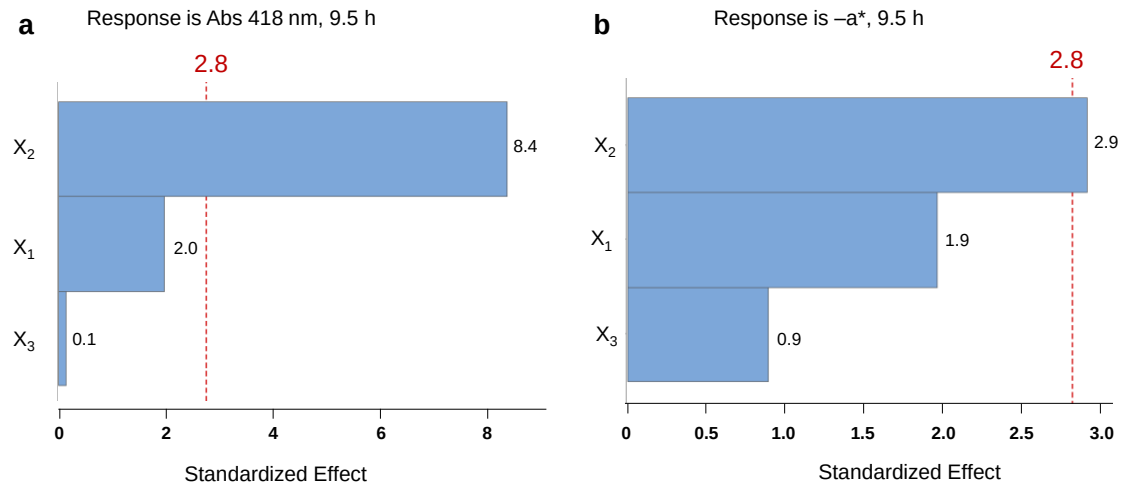

Figure 3.9 – Pareto charts of the standardized effects: a) response is Abs (418 nm), 9.5 h (p<0.05); b) response is -a*, 9.5 h (p<0.05).

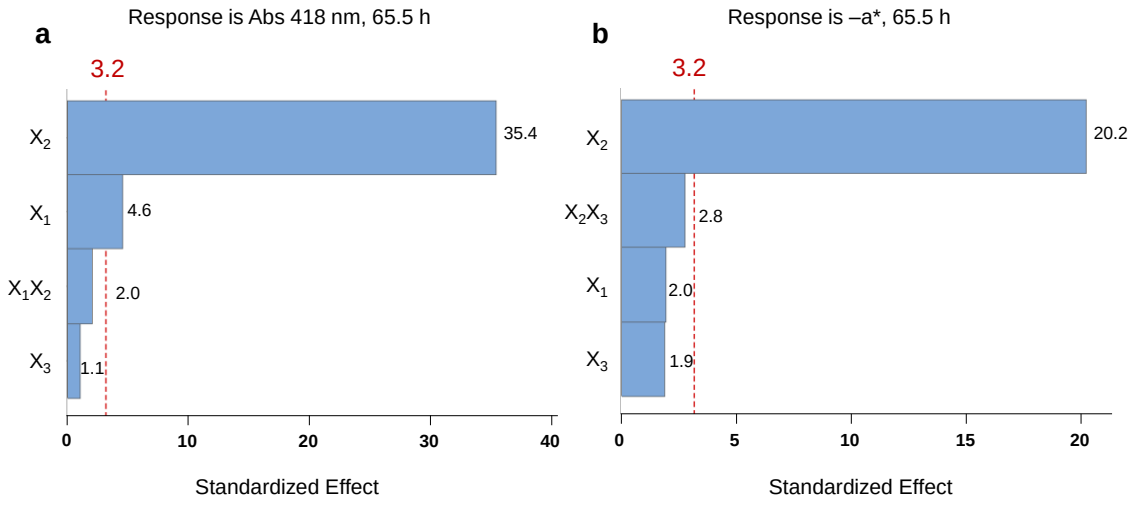

Figure 3.10 – Pareto charts of the standardized effects: a) response is Abs (418 nm), 65.5 h, p<0.05; b) response is -a*, 65.5 h, p<0.05.

3.1.4 Degradation kinetic of green color at different temperatures.

The CIELAB -a*/-a*0 value is a good way to measure chlorophylls degradation and color loss with temperature [256]. Using linear regression, the data were analyzed to determine the overall order and rate constant for the degradation reaction of green pigments. Accordingly, ln (-a*/-a0*) was plotted *vs* time (0, 6, 24, 29, 47, and 102 h), from which the rate constants (*k*) were calculated. Figure 3.11a shows the representative values for the first order plots for the degradation of greenness (-a*) for *C. vulgaris* ethanolic extract preserved in the dark at different temperatures, namely 4, 15, 28, 45 and 60 ºC. The correlation coefficient was > 0.84 in all cases, confirming that the degradation of the visual green color indeed followed a first order kinetics at all temperatures. These results are in line with the first order reaction found for Chl *a* degradation in solutions with different percentages of ethanol (1-60%) [90] and in vegetables, such as spinach puree [98], broccoli juice [257], and green peas [94].

From the rate constants obtained in Figure 3.11a, it was possible to develop a semi-logarithmic plot of *k vs* the inverse of temperature. The Arrhenius plot for color loss of *C. vulgaris* pigments in ethanol revealed that the main color loss occurred between 28 and 60 ºC, under the studied conditions, emphasizing the importance of the higher temperatures in the green color degradation. When plotting the three higher temperatures it was an activation energy of 74 kJ/mol (Figure 3.11b). As no significant degradation has been observed for the temperatures of 4 ºC and 15 ºC, these values were not taken into consideration for the calculation of the activation energy of chlorophyll degradation. This emphasizes the stability of pigments bellow room temperature and their higher degradation rate at temperatures higher than room temperature in ethanol solutions.

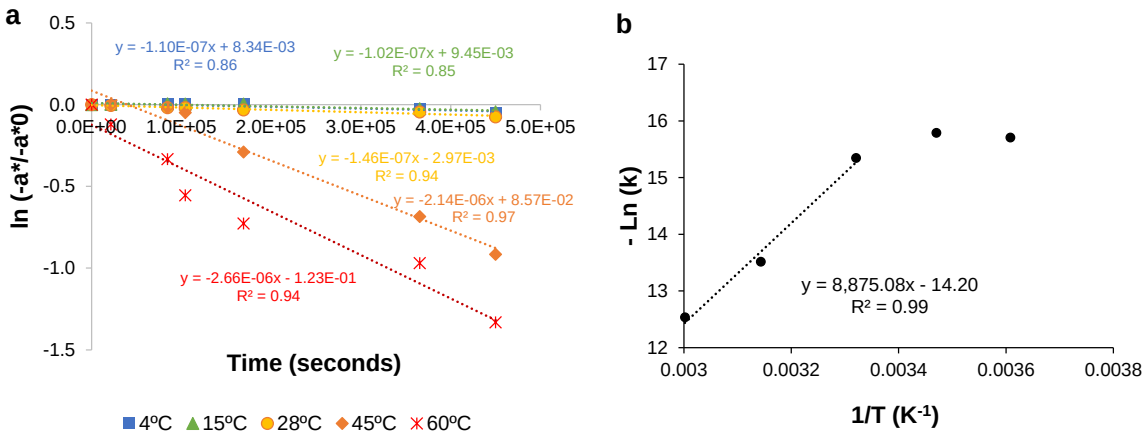

Figure 3.11 – a) First order plot of color (-a*) degradation in *C. vulgaris* ethanolic solution at different temperatures; b) Arrhenius plot for color loss of ethanolic solutions of *C. vulgaris* chlorophylls.

The activation energy in the present study is of similar magnitude of previous studies. An activation energy from 18.4 to 85.1 kJ/mol was achieved for the degradation of Chl *a*, that varied with the ethanol concentration, reaching the maximum at 40% ethanol concentration, since at this concentration the interaction between ethanol and water molecules is stronger [90]. However, most of the studies of chlorophylls degradation have been done in whole foods, not in isolated chlorophylls. Activation energies of 28.7 kJ/mol have been reported for spinach puree, 41.6 kJ/mol for mustard leaves, and 34.0 kJ/mol for mixed puree in a range of temperatures between 75 and 115 °C [258]. Activation energies for color loss in broccoli juice for temperatures between 80 and 120 °C [257] was 71.0 kJ/mol, 11.4-16.0 kJ/mol for green chili puree tested at temperatures between 60 and 90 °C [259], and 34.0-49.8 kJ/mol for blanching of green peas tested at temperatures between 70 and 100 °C [94]. These values shows that the degradation of chlorophylls when in the native matrix are minimized, although variations for the different matrices occur. Beyond the influence of the matrices, the temperature ranges used in these studies have also influence in the determination of the activation energies for chlorophylls' degradation.

3.1.5 Food application

The green *C. vulgaris* ethanolic extract (1 and 2 mL) was added to cooked cold white rice to obtain green rice to be used in sushi. The visual color stability was observed over

time at 4 °C and is shown in Figure 3.12. At time 0 (Figure 3.12a), the addition of chlorophylls' extract, principally the addition of 2 mL, originated an appealing bright green rice. After 3 days of storage (Figure 3.12b), the cooked rice maintained the green color, without presenting the bright color as in the moment of the extract addition. After 7 (Figure 3.12c) or 13 days (Figure 3.12d) of storage, the rice color change from the bright green to a slight olive green, possibly due to the formation of pheophytins, since the pH was not controlled [96].

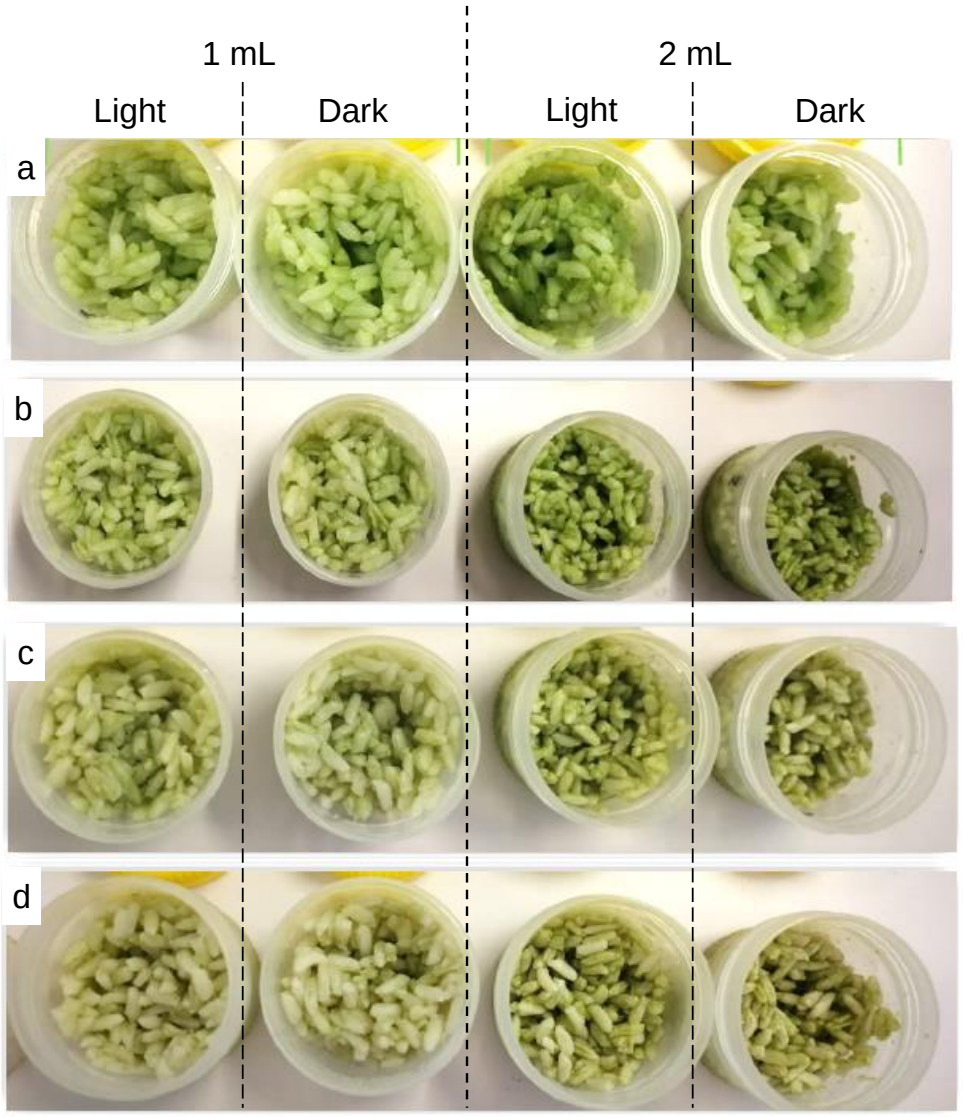

Figure 3.12 – Addition of 1 and 2 mL of *C. vulgaris* ethanolic extract to white rice and evaluation of visual color during storage at 4 ºC in the presence and absence of light at a) day 0; b) day 3; and c) day 7, and d) day 13.

The color of the rice in the presence of light remained visually unchanged (Figure 3.12), similarly to the rice maintained in the dark. Thus, although the light has a great influence in the degradation of color of *C. vulgaris* ethanolic extract, it does not have influence when applied to the rice.

The application of the green extract in cooked cold rice to be used in sushi proved the potential of *C. vulgaris* as a source of a food color additive, mainly for the immediately addition and consumption of the processed food, meeting the need of consumers for natural colorants.

3.1.6 Concluding remarks

The assessment of the color stability of a *C. vulgaris* ethanolic extract, composed mainly by Chl *a* in different storage conditions, allowed to conclude that the light was the main variable that negatively affect the green color, followed by temperature, under the studied conditions. The alkaline environment and an inert atmosphere (argon-rich atmosphere) had no statistical effect on the green color preservation. The loss of color in the ethanol with temperature followed the first-order kinetic, being more significant between 28 and 60 °C, with an activation energy of 74 kJ/mol. These results show that *C. vulgaris* chlorophylls can be preserved in ethanol solutions at room or lower temperatures, allowing them to be preserved in a food grade solvent easy to handle and be used as food ingredient.

The *C. vulgaris* ethanolic extract revealed to be a suitable natural food colorant for cooked rice, up to 3 days of storage at 4 ºC, either is the presence or absence of light. Thus, *C. vulgaris* is a great source of natural pigments that can be employed to colored or enhance the green color of processed foods, playing an important role in the market success of a product.

3.2 Reserve, structural, and extracellular polysaccharides of *Chlorella vulgaris*: a holistic approach

Beyond the biological value of *C. vulgaris* due to the high content of chlorophylls, this microalga is rich in starch and structural polysaccharides that could also have potential to be valued as food ingredients. Despite the potential of *C. vulgaris* biomass in human diet [212], the particular relevance of its polysaccharides still needs to be definitely assessed as a source of energy or even as health-promoting products. Here, the starch digestibility in raw and boiled biomass was evaluated and compared with its extractability with hot water and alkali solutions, after the pigments and lipidic fraction were removed with chloroform: methanol (2:1, v/v). The cell wall related polysaccharides, as well as extracellular polysaccharides, were structurally characterized to establish a relationship with the assessed immunostimulatory activity. The holistic approach in characterizing *C. vulgaris* polysaccharides will be useful to evaluate their potential as functional food ingredients.

3.2.1 Composition of *Chlorella vulgaris* biomass

The *C. vulgaris* biomass used in the present study was composed by 41% of protein, 29% of sugars, 11% of inorganic material, 8% of fatty acids, and 6% of pigments (Figure 3.13a), which is in accordance with literature [10]. The most abundant amino acids were leucine (17%), phenylalanine and lysine (14%), and tyrosine (13%) (Figure 3.13b). The ratio of essential to total amino acids was almost 2/3, which is clearly above the 1/3 index ratio recommended by FAO/WHO/UNU (1985) for a nitrogenous nutritional equilibrium. The fatty acids corresponded to 8% (w/w) of dried microalgae mass. Although palmitic acid (C16:0) was the main fatty acid residue (19%), polyunsaturated acids were also present in higher quantity, namely 14% linolenic (C18:3), 14% linoleic (C18:2), and 13% oleic (C18:1) acids (Figure 3.13c). The ratio of unsaturated to saturated fatty acids was 3:1, showing the good balance of fatty acids profile reported for *C. vulgaris* [260].

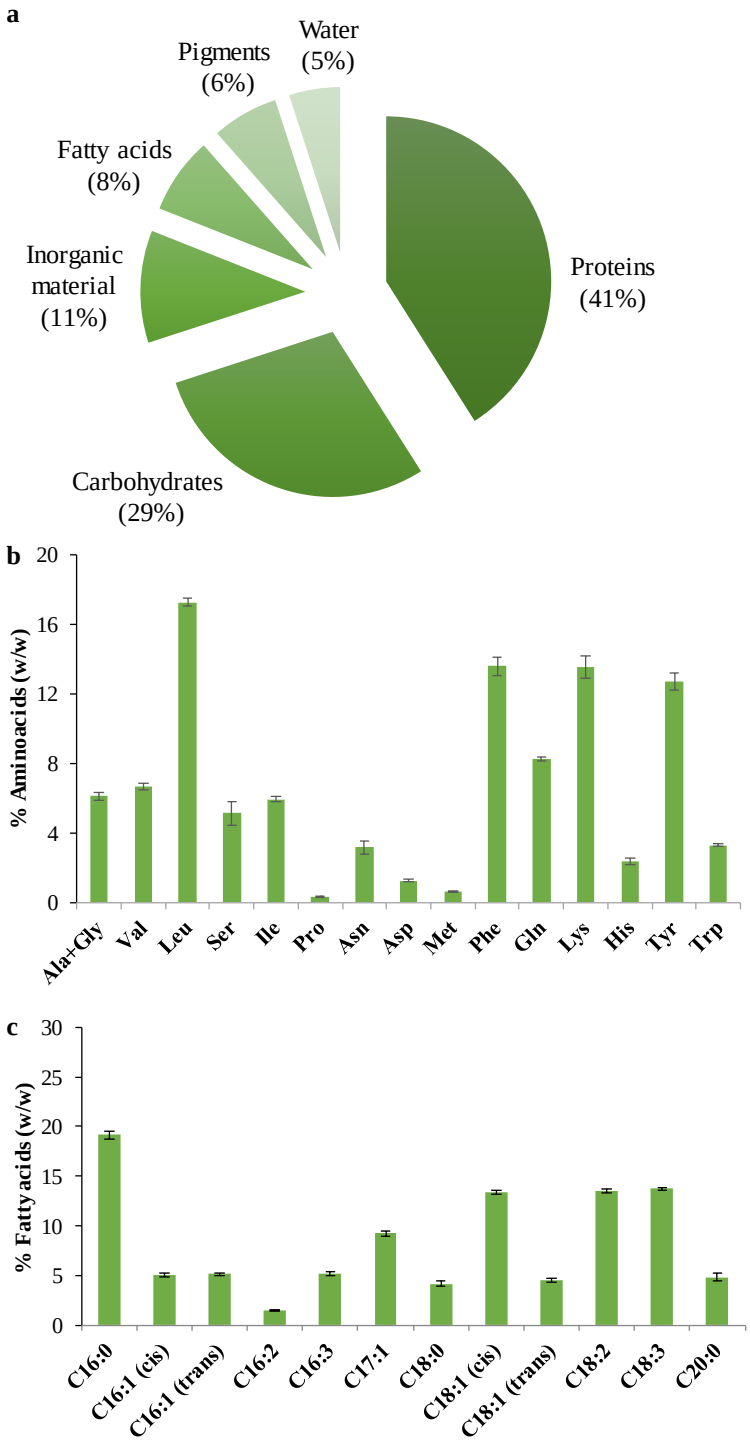

Figure 3.13 – Characterization of *C. vulgaris* biomass: a) *C. vulgaris* composition in proteins, carbohydrates, inorganic material, fatty acids, pigments, and moisture; b) amino acids composition; and c) fatty acids composition. Mean values ± SD, *n*=3.

Carbohydrates were mainly composed by glucose (74%) (Table 3.4), mainly starch, which accounted for 22% of total biomass (quantified enzymatically), which is in accordance with literature, where a starch content up to 55% has been reported [261]. As *C. vulgaris* could represent an important starch source for food purposes, *in vitro* starch digestion and starch extractability was evaluated.

3.2.2 *In vitro* starch digestion of *C. vulgaris* and glycemic index determination

Figure 3.14a shows the starch digestibility of raw and boiled *Chlorella* samples in relation to total starch in dry biomass. It is possible to observe a release of 43% and 71% of total glucose, respectively. This difference promoted by the boiling of microalga biomass should be due to the gelatinization of the inner starch, becoming more available to enzymatic hydrolysis and, consequently, more digestible. Nevertheless, this content of glucose release was lower when compared with the boiled potato and bread, which approach 100% of starch digestibility.

Considering the amount of starch in whole biomass, *Chlorella* showed a low starch digestion when compared with boiled potato and bread (Figure 3.14b). This is in accordance with the lower *Chlorella* glycemic index (GI). *In vitro* digestion of boiled *Chlorella* biomass, with a GI of 56, should be considered a medium ($56 \leqslant GI \leqslant 69$) GI food, whereas raw *Chlorella* biomass (GI=49) should be considered a low ($GI \leqslant 55$) GI food [262]. Since this microalga is usually consumed both raw and cooked, the extent of energy obtained from this microalga can be modulated by processing.

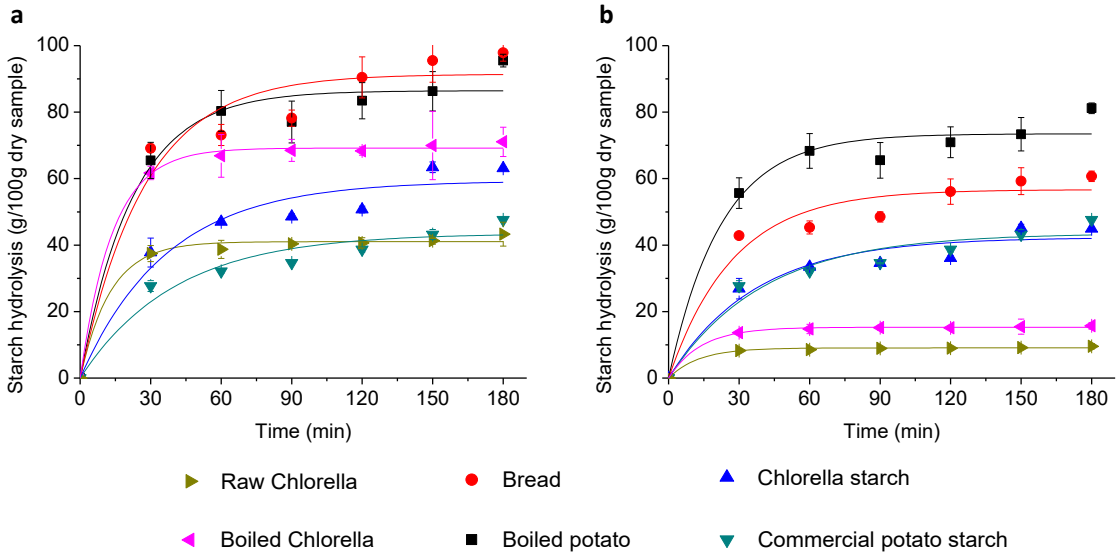

Figure 3.14 – Starch digestibility of different samples in relation to: a) total starch in dry biomass and b) total dry biomass. Mean values ± SD, *n*=3.

3.2.3 *C. vulgaris* starch extraction

A hot water extraction was performed to relate *C. vulgaris* starch extractability with its digestibility. The hot water extract (HWE) obtained was composed by 26% of carbohydrates, mainly glucose (54 %mol) (Table 3.4). Thus, hot water allowed an extraction of 12.5% of total starch, confirmed by blue/purple staining of iodine test (data not shown) and by the presence of characteristic starch 1,4-Glc and 1,4,6-Glc linkages (Table 3.5). The extraction yield obtained was much lower than the 71% of glucose released during the *in vitro* starch digestibility (section 3.2.2). This difference may be due to protein hinderance, since during starch digestibility assay protein was removed by proteases.

Upon dialysis of HWE, it was possible to obtain a precipitate enriched in polysaccharides and also in glucose (87 %mol). Although this fraction accounted only for 1% of total *C. vulgaris* mass (3% of total starch present in *C. vulgaris*), the purity of the starch obtained allowed its further characterization.

In order to extract the starch that still remained in the insoluble material from the hot water extraction (HWIM), alkali extractions with 1 M and 4 M KOH were performed. Upon dialysis, both 1 M and 4 M KOH extracts allowed to obtain a precipitate that was separated from the supernatant by centrifugation (1MPp and 4MPp). The precipitates accounted for an

extraction yield of 24 and 22%, respectively, composed by 45 and 49% of carbohydrates, mainly glucose. The blue/purple staining of iodine test (data not shown) and glycosidic linkage analysis (Table 3.5) allowed to confirm the presence of starch. Sugar and linkage analyses of the supernatants of 1 M and 4 M KOH (1MSn and 4MSn) also revealed the presence of glucose terminally-linked, 1,4-linked and 1,4,6-linked, in accordance with the presence of starch. These glycosidic linkages were also observed in the supernatant resulted from the dialysis of the final residue (FinalSn). Taking into account both dialysis precipitate and supernatant of 1 M and 4 M KOH extractions, it was possible to recover 25 and 26% of the total starch present in *C. vulgaris*, respectively. Aqueous alkali induces swelling and gelatinization of the starch granules at room temperature, since alkali breaks the intramolecular hydrogen bonds, facilitating the penetration of water molecules into the granules. Moreover, alkali solutions were able to dissolve proteins that mainly co-precipitate with starch during dialysis (Table 3.4), allowing a protein network disintegration that benefited the starch extraction [256].

The final insoluble residue (FinalResidue) only contained 3.5% of the initial biomass starch. Therefore, KOH extractions were able to extract starch in higher rate than the digestion simulation, where raw and boiled biomass still contained 12 and 6% undigested starch, respectively (section 3.2.2). Alkali extractions proved to be a good methodology to concomitantly extract starch and proteins of *C. vulgaris* biomass. In order to identify possible food applications for *C. vulgaris* starch, its physicochemical characteristics were evaluated.

Table 3.4 – Sugar composition (%mol), total sugars, starch and protein content (% w/w) of *C. vulgaris* biomass and its fractions (hot water extraction fractions, KOH extraction fractions), and extracellular polymeric material recovered from the *C. vulgaris* growth medium.

	Yield (%)	Sugars (%mol)								Total sugars (% w/w)	Starch[e] (% w/w)	Protein (% w/w)
		Rha	Fuc	Ara	Xyl	Man	Gal	Glc	UA			
***Cv* biomass**		4.0±0.4	0.3±0.0	0.4±0.1	1.7±0.1	2.5±0.2	10.3±1.5	72.9±2.2	8.0±0.3	28.7±0.3	22	41.0±0.4
HWE	20.1[a]	5.1±0.1	1.7±0.0	1.2±0.1	2.3±0.1	4.2±0.2	10.9±0.2	53.9±0.3	20.6±0.3	25.5±0.3	2.8	49.0±0.2
HWE50	15.2[b]	1.5±0.0	0.3±0.0	0.7±0.0	1.3±0.1	1.3±0.1	6.6±2.8	73.9±1.6	14.4±1.2	46.2±3.9	1.0	24.5±0.1
HWE75	52.7[b]	10.4±0.7	3.3±0.2	1.5±0.1	3.2±0.3	6.2±0.4	19.5±1.1	38.2±1.7	17.1±1.1	23.4±0.7	0.9	44.3±0.2
HWESn	26.3[b]	4.6±0.1	1.5±0.0	0.9±0.0	1.5±0.0	8.2±1.4	2.7±0.1	64.5±1.5	16.1±0.2	15.4±0.1	0.5	60.4±1.0
StarchRF	1.0[a]	0.8±0.0	0	0.6±0.0	0.7±0.0	0.2±0.0	0.7±0.0	87.0±1.0	10.0±1.0	74.6±5.4	0.6	9.7±0.0
HWIM	59.3[a]	1.5±0.0	0	0.4±0.1	1.2±0.0	0.9±0.0	3.8±0.1	72.3±0.2	19.8±0.0	38.5±0.6	16.5	49.4±0.8
KOH 1M												
1MSn	3.7[c]	2.5±0.5	0.3±0.0	0.9±0.1	1.7±0.4	4.0±0.4	19.6±0.7	55.2±0.3	15.7±0.8	35.9±1.7	0.4	61.1±3.1
1MPp	24.2[c]	1.6±0.1	0	0.3±0.0	1.2±0.0	0.8±0.1	2.4±0.1	76.5±0.4	17.2±0.4	45.5±1.1	5.0	52.4±0.1
KOH 4M												
4MSn	3.3[c]	1.4±0.0	0.2±0.0	0.9±0.0	1.6±0.0	2.8±0.2	14.7±0.8	66.0±1.0	12.5±0.5	47.0±1.7	0.6	46.7±0.3
4MPp	21.8[c]	1.7±0.0	0	0.3±0.0	1.2±0.0	0.8±0.2	2.9±0.8	79.1±0.6	14.0±0.4	49.4±1.4	5.1	50.2±0.8
FinalSn	0.4[c]	0	0	0.7±0.1	0	1.6±0.2	8.8±0.4	76.5±0.4	12.5±1.2	52.1±4.8	0.1	47.0±1.3
FinalResidue	11.7[c]	1.4±0.1	0	0.4±0.0	0.7±0.0	0.9±0.6	2.0±1.2	83.2±1.3	11.4±0.4	60.2±1.9	3.5	43.9±0.6
EPM		9.5±0.1	0	3.2±0.1	4.4±0.1	12.3±0.3	49.7±1.7	2.3±0.3	19.5±1.0	43.5±0.8		27.9±0.3
EPM50	9.9[d]	8.8±0.6	0	7.1±0.1	6.1±0.0	8.5±0.1	28.6±0.5	8.4±0.3	32.5±0.3	16.6±0.1		53.9±0.6
EPM75	36.6[d]	6.8±0.4	0	2.5±0.0	4.3±0.1	7.2±0.4	58.0±0.8	1.4±0.0	19.8±0.1	44.2±0.2		29.0±0.2
EPMSn	41.5[d]	7.4±0.3	0	3.1±0.3	4.0±0.1	8.1±1.6	50.7±2.2	2.4±0.2	24.2±0.7	37.5±1.1		21.5±0.0

Cv biomass – *Chlorella vulgaris* biomass; HWE – Hot Water Extract; HWE50 – Hot Water Extract precipitated at 50% ethanol; HWE75 – Hot Water Extract precipitated at 75% ethanol; HWESn – Hot Water Extract supernatant of the precipitation at 75% ethanol; StarchRF – Starch Rich Fraction; HWIM – Hot Water Insoluble Material; 1MSn – Supernatant of 1M KOH extraction; 1MPp – Precipitate of 1M KOH extraction; 4MSn – Supernatant of 4 M KOH extraction; 4MPp – Precipitate of 4 M KOH extraction; FinalSn – Final Supernatant of 4 M KOH extraction; FinalResidue – Final Residue of 4 M KOH extraction; EPM – Extracellular Polymeric Material; EPM50 – Extracellular Polymeric Material precipitated at 50% ethanol; EPM75 – Extracellular Polymeric Material precipitated at 75% ethanol; EPMSn – Extracellular Polymeric Material supernatant of the precipitation at 75% ethanol. [a]Extraction yield in relation to *Cv* biomass. [b]Ethanol precipitation yield in relation to HWE. [c]KOH extraction yield in relation to HWIM. [d]Ethanol precipitation yield in relation to EPM. [e]Starch (% w/w) in relation to *Cv* biomass. Mean values ± SD, *n*=3

Table 3.5 – Glycosidic linkage analysis of *C. vulgaris* fractions (hot water extraction fractions, KOH extraction fractions, and extracellular polymeric material).

	HWE	HWE50	HWE75	StarchRF	HWIM	HWIM 1M Sn	HWIM 1M Pp	HWIM 4M Sn	HWIM 4M Pp	HWIM FinalSn	HWIM Final Residue	EPM
t-Rha	3.7	0.5	6.0	vt	0.2	0.4	0.1	0.2	0.2	0.1	0.1	2.3
2-Rha+3-Rha	7.3	1.5	10.2	vt	1.8	1.9	vt	1.5	1.6	vt	1.3	11.3
2,3-Rha	1.7	-	vt	-	-	-	-	-	-	-	-	1.1
Total Rha	***12.7***	***2.1***	***16.2***	***vt***	***2.0***	***2.2***	***0.1***	***1.7***	***1.8***	***0.1***	***1.4***	***14.7***
t-Fuc	0.5	0.1	0.7	-	-	-	-	-	-	-	-	-
3-Fuc	2.0	vt	2.7	-	-	-	-	-	-	-	-	-
Total Fuc	***2.5***	***0.1***	***3.3***	***-***	***-***	***-***	***-***	***-***	***-***	***-***	***-***	***-***
t-Xyl	1.9	vt	0.3	vt	0.1	0.3	vt	0.2	0.1	0.1	vt	1.2
3-Xyl	1.9	vt	2.3	vt	vt	vt	vt	vt	vt	vt	vt	3.1
Total Xyl	***3.8***	***vt***	***2.6***	***vt***	***0.1***	***0.3***	***vt***	***0.2***	***0.1***	***0.1***	***vt***	***4.3***
t-Man	2.2	0.7	1.7	-	0.3	0.8	0.2	0.6	0.2	0.4	0.2	3.3
2-Man	2.0	-	7.0	-	-	-	-	-	-	-	-	3.9
Total Man	***4.2***	***0.7***	***8.8***	***-***	***0.3***	***0.8***	***0.2***	***0.6***	***0.2***	***0.4***	***0.2***	***7.2***
t-Gal	3.0	1.1	4.1	vt	0.5	2.0	0.3	1.8	0.3	1.2	0.2	10.0
3-Gal	3.1	0.3	1.8	vt	vt	3.0	vt	2.7	vt	1.6	vt	10.9
6-Gal	21.5	6.7	20.8	vt	5.0	22.6	1.9	14.3	1.6	10.6	1.0	36.9
3,6-Gal	4.3	0.7	4.3	vt	vt	2.3	vt	1.6	vt	1.1	vt	8.9
Total Gal	***31.9***	***8.8***	***31.0***	***vt***	***5.5***	***29.8***	***2.2***	***20.4***	***2.0***	***14.6***	***1.2***	***66.7***
t-Glc	3.7	7.2	2.9	6.1	5.8	4.5	6.1	5.0	6.1	6.1	5.7	0.9
4-Glc	39.6	78.3	34.2	90.6	79.8	59.3	87.5	68.5	83.2	74.1	85.0	3.3
4,6-Glc	1.6	2.9	1.0	3.3	4.2	2.8	3.0	3.4	4.8	4.5	4.8	-
Total Glc	***44.9***	***88.4***	***38.2***	***100.0***	***89.9***	***66.6***	***96.5***	***76.9***	***94.1***	***84.7***	***95.5***	***4.2***
4-GlcN	vt	vt	vt	vt	2.2	0.3	0.9	0.2	1.9	0.2	1.7	2.9

vt – vestigial; HWE – Hot Water Extract; HWE50 – Hot Water Extract precipitated at 50% ethanol; HWE75 – Hot Water Extract precipitated at 75% ethanol; StarchRF – Starch Rich Fraction; HWIM – Hot Water Insoluble Material; 1MSn – Supernatant of 1M KOH extraction; 1MPp – Precipitate of 1M KOH extraction; 4MSn – Supernatant of 4M KOH extraction; 4MPp – Precipitate of 4M KOH extraction; FinalSn – Final Supernatant of 4M KOH extraction; FinalResidue – Final Residue of 4M KOH extraction; EPM – Extracellular Polymeric Material.

3.2.4 *C. vulgaris* starch characterization

The fraction richest in starch (StarchRF), obtained as a precipitate from the dialysis of hot water extract (HWE), was used to characterize *C. vulgaris* starch. FTIR spectrum (Figure 3.15a) confirmed the presence of starch by exhibiting a carbohydrates fingerprint composed of the overlapping bands between 1200 and 800 cm^{-1} that are characteristics of C–O–H bending, C–O, C–C and O–H stretching. Particularly, vibrations arising from the C–O–C of α-1,4 glycosidic linkages are observed in the infrared peak at 994 cm^{-1} [263,264], showing a FTIR spectra similar to commercial starch (Figure 3.15a). Thermogravimetric analysis of StarchRF and commercial starch (Figure 3.15b) showed two stages of mass loss: the first one occurred at 100 °C, assigned to the loss of structural bonded water; the second stage occurred at 300 ºC, attributed to the degradation of the polymeric material [265]. The differences between starches can be attributed to the presence of inorganic material in StarchRF.

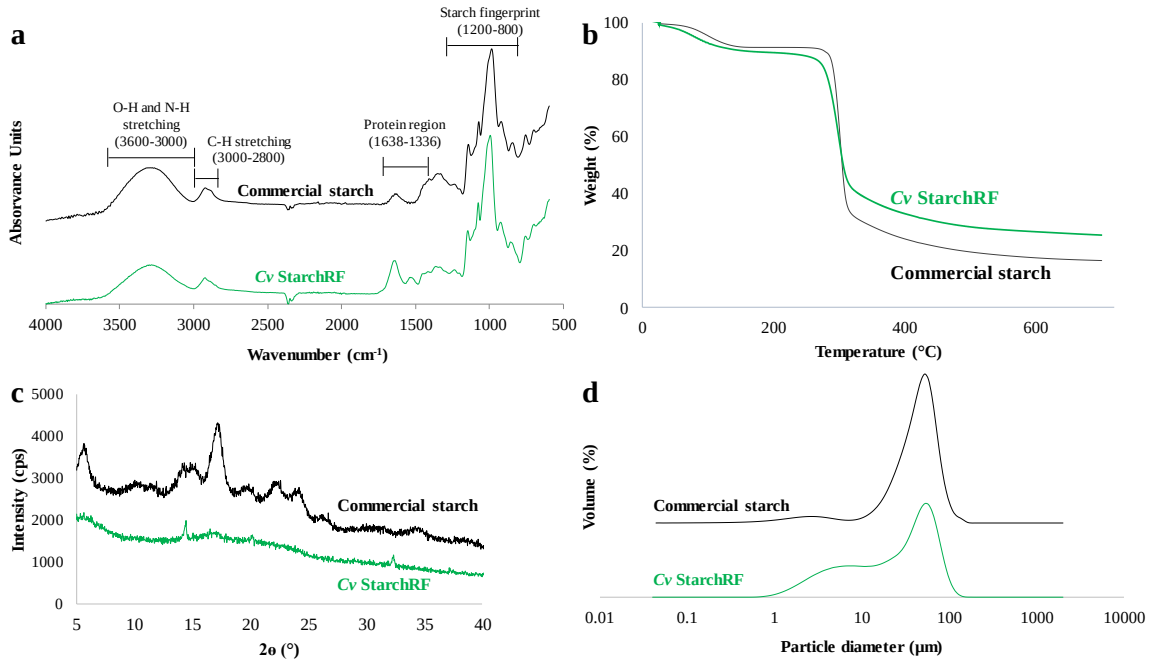

Figure 3.15 – Characterization of *Chlorella vulgaris* starch rich fraction (*Cv* StarchRF, green line) and comparison with potato commercial starch (Commercial starch, black line): a) FTIR spectra, b) Thermogravimetric analysis, c) X-ray diffractograms (40% RH), and d) particle size distribution (logarithmic scale).

The amylose determination allowed to disclose that *C. vulgari*s starch was composed of 30% amylose. The amylose/amylopectin ratio is in agreement with literature, that found 30-40% of amylose in *C. vulgaris* starch [266]. This starch corresponds to a 'normal' amylose starch (between 20-35% of amylose), which is similar to commercial potato (35%) and cereals starch (21-32%) [267]. Amylose is a relatively long and linear polysaccharide, whereas amylopectin is highly branched, with about 5% of 1,4,6-Glc bonds as branching points [268]. Thus, a normal starch with 70% of amylopectin accounts with about 3.5% of branching points in whole molecule. According to the glycosidic linkage analysis (Table 3.5), *C. vulgaris* starch was composed by 3.3% of 1,4,6-Glc, which corresponded to a 4.7% of branching points in amylopectin, confirming the results obtained by enzymatic analysis, allowing to conclude that *C. vulgaris* can be included in the normal starch group.

The X-ray diffraction patterns of *C. vulgaris* StarchRF and commercial starch tested at different relative humidity (RH) percentages (0, 40, and 80%) (Figure 3.16) showed a slight semi-crystalline pattern between 40 and 80% RH for both samples (Figure 3.15c), which was in accordance with literature [269]. Typically, native starches have a semi-crystalline structure, with a crystalline element of about 15-45% [270]. The low degree of crystallinity could be related with some starch degradation due to the extraction methodology, namely the gelatinization occurring during the hot water extraction. Nevertheless, it is possible to observe an A-type pattern, which is in accordance with literature for *C. vulgaris* [271] and *C. kessleri* [272], consisting in shorter branch-chains of amylopectin and with double helices packed in a monoclinic unit cell [273]. A-type pattern is also largely present in cereal starches [267], showing also similarity with *C. vulgaris*. On the contrary, potato commercial starch exhibited a well-defined semi-crystalline B-pattern [269], showing to have a different pattern from *C. vulgaris* starch.

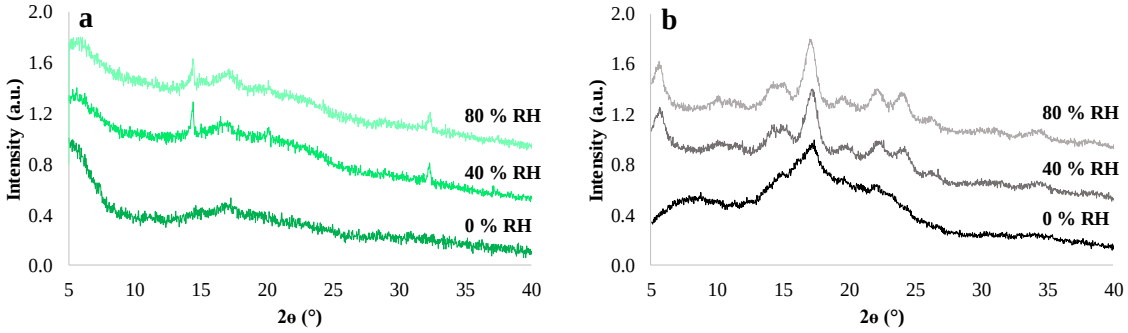

Figure 3.16 – X-ray diffractograms of: a) starch rich fraction (StarchRF) of *Chlorella vulgaris*; b) commercial potato starch; at different relativity humidity (0, 40, and 80%). A.u. arbitrary units.

Particle size distribution of StarchRF and commercial starch was evaluated by light scattering in a range from 0.040 to 2000 µm (Figure 3.15d). Besides the bimodal distribution, *C. vulgaris* StarchRF and commercial starch particles showed different size distributions: 25% of StarchRF had less than 8.6 µm and 90% showed a size lower than 74.1 µm, while 25% of commercial starch was constituted by particles lower than 27.5 µm and 90% of the material had less than 71.1 µm. *C. vulgaris* starch showed a mean size (35 µm) higher than the 0.96-2 µm reported for *C. kessleri* [272,274], possibly due to the presence of amorphous material, as revealed by X-ray diffraction. SEM analysis of StarchRF allowed to observe the presence of some aggregates of polymeric material with a broad range size, reaching a size slightly above 100 µm (Figure 3.17a), which is in accordance with the second peak of the bimodal size distribution (Figure 3.15d).

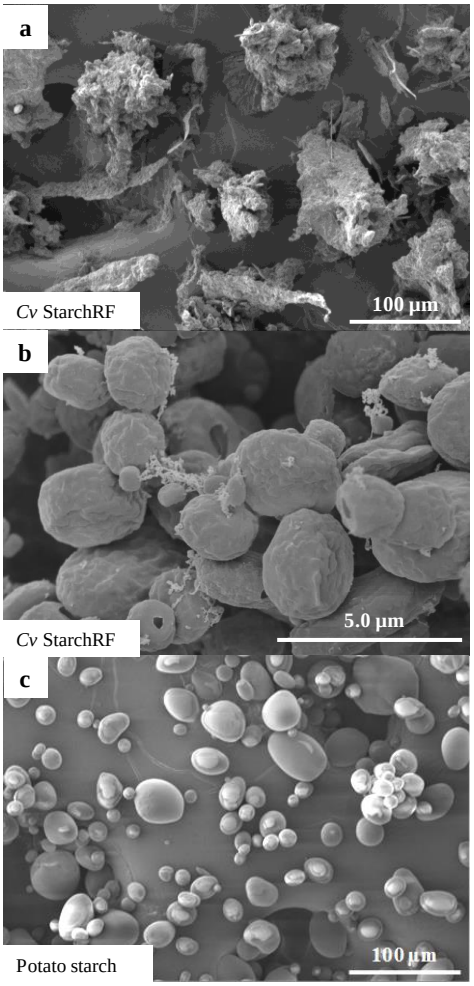

Figure 3.17 – Scanning electronic micrographs of a) Cv StarchRF – *Chlorella vulgaris* starch rich fraction (magnification of 300x); b) Intact granules present in of Cv StarchRF (magnification of 10000x), and c) commercial potato starch granules (magnification of 300x).

During gelatinization the granule burst, the starch crystallites melt and form a polymeric network [267]. However, despite the majority of amorphous polymeric material, it was possible to observe some preserved granules in *C. vulgaris* StarchRF of about 2-3 µm, with a spherical shape (Figure 3.17b), resulting in the semi-crystallinity observed by X-ray diffraction. *Chlorella* granules showed lower size and different morphology when compared with commercial potato starch (Figure 3.17c), revealing ultrastructural differences. Accordingly, the granules size seem to approach those reported for cereals [267].

In vitro digestibility of *C. vulgaris* starch was higher than that of the commercial potato starch (Figure 3.14a), becoming more available for enzymes degradation, possibly due to the pregelatinization performed during the hot water extraction. Nevertheless, the glycemic index of both starches was similar (Figure 3.14b) (GI=70). Therefore, the higher digestibility

of mostly amorphous *C. vulgaris* starch could have some advantages over semi-crystalline starch in nutritional point of view, since represents a quicker source of glucose.

3.2.5 *C. vulgaris* non-starch polysaccharides

During hot water and alkali solution extractions it was possible to detect the presence of galactose, uronic acids and rhamnose (Table 3.4). The fractionation of the hot water extract (HWE) by graded ethanol precipitation allowed to separate the starch derived polysaccharides, precipitated in solutions containing 50% ethanol (HWE50), from the galactose, uronic acids, and rhamnose rich polysaccharides, precipitated mainly with 75% ethanol (HWE75, Table 3.4). In total, hot water was able to extract 34% of the non-starch carbohydrates. The highest relative content of rhamnose, uronic acids and galactose obtained by the alkaline solutions (Table 3.4) showed that the 1 M KOH and 4 M KOH extractions were able to remove 51% of non-starch polysaccharides. The molar percentage of galactose decreased with the increase of the KOH concentration in supernatants, as observed by the content of galactose in 1MSn, 4MSn and FinalSn, which was 20, 15, and 9 %mol, respectively. KOH precipitates (1MPp, and 4MPp) and final insoluble material (FinalResidue) accounted with lower molar percentages of Gal (<3 %mol).

The glycosidic linkage analysis of all fractions (Table 3.5) shows the presence of 1,3-Gal, 1,6-Gal, and 1,3,6-Gal residues. This sugars composition is in accordance with the presence of a β-D-galactan, reported to have 1,3 linkages in the backbone and 1,6 linkages in the side chains [149], as well as with the presence of a β-1,6-Gal extracellular glycoprotein [165], also reported to occur in *C. vulgaris*. The presence of 2- and 3-linked rhamnose may have origin in the glucuronorhamnan also described for *C. vulgaris*, composed by a α-D-Glc*p*A-(1-3)-α-L-Rha*p*-(1-2)-α-L-Rha*p* repetitive trisaccharide [148]. Although uronic acids were quantified in Table 3.4, they were not carboxyl reduced. As a consequence, the uronic acids glycosidic linkages were not possible to be identified. The presence of 1,4-linked glucosamine, mainly in KOH precipitate extracts, can be derived from *N*-acetyl-glucosamine, in accordance with the occurrence in *C. vulgaris* of a chitin-like rigid cell-wall [146].

3.2.6 Extracellular polymeric material (EPM)

The presence of polysaccharides in *C. vulgaris* growth medium was evaluated to identify the polysaccharides that are able to be released from the biomass. *Chlorella vulgaris* was cultivated in closed photobioreactors, where a cellular density of 1.4 g/L has been achieved. The high molecular weight compounds were recovered from the growth medium (extracellular polymeric material - EPM) with a yield of 0.11 g/L, which corresponded to 8% of the cellular density. Nevertheless, under optimal conditions, *C. vulgaris* is able to reach 2.76 g/L of microalgal biomass and 1.46 g/L of exopolymeric substances [275], which is dependent on the cultivation conditions [276].

The EPM predominant sugar residue was galactose (50 %mol), followed by uronic acids (19 %mol), mannose (12 %mol), and rhamnose (9 %mol) (Table 3.4). This fraction also revealed the presence of sulfate esters (2% w/w). The fractionation with ethanol allowed to obtain a fraction that precipitate with 50% ethanol (EPM50), yielding 10% (w/w), composed by 17% (w/w) sugars, mainly uronic acids (32 %mol), galactose (29 %mol), rhamnose (9 %mol), mannose and glucose (8 %mol). The fraction that precipitated with 75% ethanol (EPM75) and the polymers that remained soluble in ethanol (EPMSn) accounted for 37% and 42% (w/w), respectively, containing 44 and 38% (w/w) of sugars, with a similar profile composed by 51-58 %mol of galactose, 20-24 %mol uronic acids, 7-8 %mol mannose, and 7 %mol rhamnose (Table 3.4) with 2% (w/w) of sulfate esters. Previous studies also reported *C. vulgaris* extracellular polysaccharides (EPS) mainly composed by galactose (36-45 %mol), with residues of glucosamine (0-28 %mol), arabinose (2-28 %mol), mannose (7-11 %mol), rhamnose (5-15 %mol), glucose (6-7 %mol), and xylose (0-3 %mol) [169,170]. However, the presence of sulfate esters was never reported.

The glycosidic linkage analysis (Table 3.5) demonstrated that galactose residues were mainly linked by 1,6-Gal (37%) and 1,3-Gal (11%), with some branching points at 1,3,6-Gal (9%). The rhamnose containing polymers were mainly linked by 1,2-Rha and 1,3-Rha (11%) with some 1,2,3-Rha branching residues. Similar glycosidic linkages were already described in *C. vulgaris* EPM, namely a β-1,6-Gal glycoprotein [165], and rhamnose containing polymers mainly linked by 1,3-Rha, with branching points at mainly 1,2,3-Rha [169]. The structural characteristics found in this study revealed that the polysaccharides found in growth medium and those described to be present in the cell wall seem to be identical.

3.2.7 Evaluation of *in vitro* lymphocyte stimulatory activity of extracellular polymeric material (EPM)

The extracellular polymeric material fraction richest in polysaccharides, obtained with 75% EtOH precipitation (EPM75), was used to evaluate its potential to stimulate *in vitro* mouse lymphocytes, in the range of 25-250 µg/mL of polysaccharides content. The extract was not cytotoxic, since the different sample concentrations tested did not affect cell viability (95-97% of viable cells, Figure 3.18). No significant differences were observed on the expression of the early activation marker CD69 on the surface of $CD3^+$ cells treated with EPM75 in comparison with the negative control (medium alone) (Figure 3.19). These results showed that EPM75 does not stimulate T cells under the experimental conditions used.

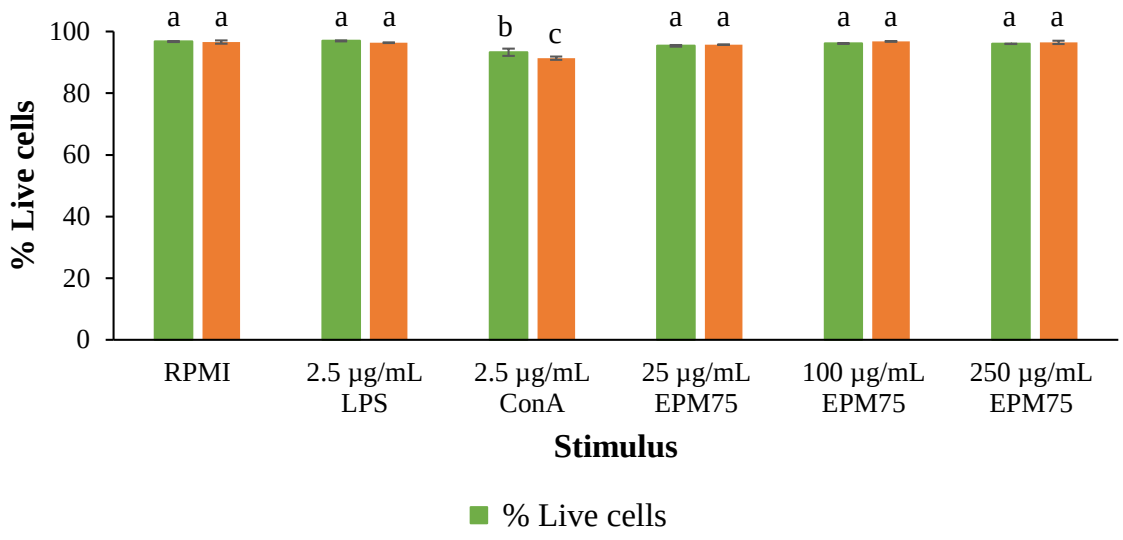

Figure 3.18 – Percentage of propidium iodide negative splenocytes [Live cells (%)] cultured for 6 h with Extracellular Polymeric Material precipitated at 75% ethanol of *C. vulgaris* (EPM75) at polysaccharides concentrations of 25, 100 and 250 µg/mL in the absence and presence of polymyxin B (PB). Culture medium (RPMI), lipopolysaccharides (LPS,) and concanavalin (ConA) were used as controls. Mean values ± SD, *n*=3. The different characters above bar indicate statistical differences ($p<0.05$) between compared groups (One-Way ANOVA, Tukey's multiple comparisons test).

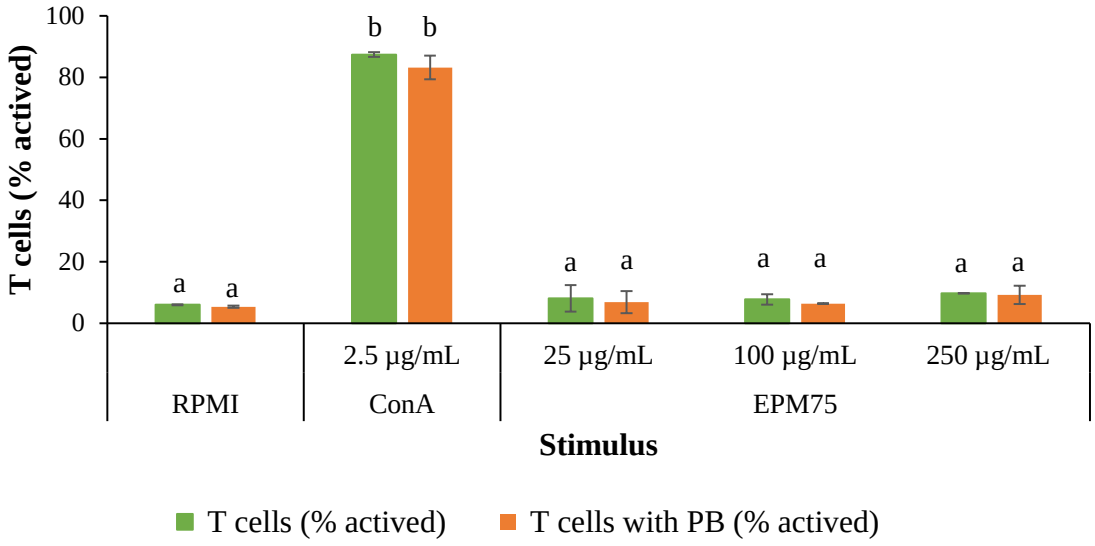

Figure 3.19 – Spleen T lymphocytes activation (%) induced by Extracellular Polymeric Material precipitated at 75% ethanol of *C. vulgaris* (EPM75) at polysaccharides concentrations of 25, 100 and 250 µg/mL in the absence and presence of polymyxin B (PB). Culture medium (RPMI) alone was used as negative control. Concanavalin (ConA) was used as positive control. Mean values ± SD, *n*=3. The different characters above bar indicate statistical differences ($p<0.05$) between compared groups (One-Way ANOVA, Tukey's multiple comparisons test).

Contrastingly, EPM75 induced the activation of $CD19^+$ cells (B cells) in a dose-response manner, in medium containing polymyxin B: 70, 81, and 91%, for 25, 100, and 250 µg/mL, respectively (Figure 3.20). Polymyxin B is a small peptide commonly used to neutralize the effect of contaminant bacterial lipopolysaccharides (LPS), since it binds to LPS inhibiting LPS-induced B cell activation to nearly basal levels [277]. When polymyxin B was added to polysaccharide-stimulated cultures, a decrease was observed only for the 25 µg/mL polysaccharide concentration. Nevertheless, the percentage of CD69-expressing B cells remained significantly higher (70%) than that observed for the negative control (8%). These results showed that the polysaccharides recovered from the *C. vulgaris* cultivation medium rich in galactose have *in vitro* stimulatory activity on B lymphocytes. Indeed, whole *C. vulgaris* cells [278,279], as well as their water extracts [280,281], revealed various *in vitro* and *in vivo* immunostimulatory activities, namely a β1,6-Gal-rich glycoprotein [282] and a polysaccharide composed by 1,6-linked glucose residues with branches at C-3 [172]. Moreover, an acetylated polysaccharide from *C. pyrenoidosa* composed by β1,3 Gal in the backbone substituted in *O*-6 by β-Glc*p* units and by α-Man*p*-1-phosphate and 3-*O*-Me-α-Man*p*-1-phosphate diesters was also reported to produce nitric oxide by peritoneal macrophages (RAW264.7 cell line) [283]. However, the polysaccharides present in EPM75

were different from these reported structures. Nevertheless, several structural characteristics may be involved in the immunostimulatory activity of polysaccharides, namely galactans [186] and sulfated polysaccharides [245,284].

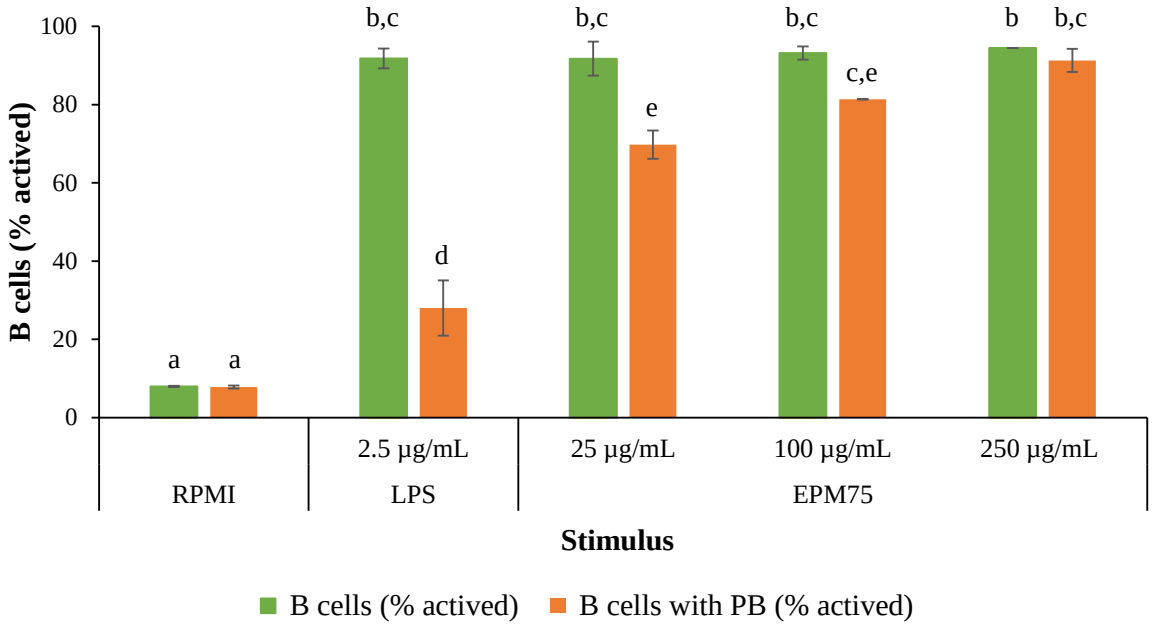

Figure 3.20 – Spleen B lymphocytes activation, as assessed by the % of CD69-expressing cells, induced by extracellular polymeric material precipitated at 75% ethanol of *C. vulgaris* (EPM75) at polysaccharides concentrations of 25, 100 and 250 µg/mL in the absence and presence of polymyxin B (PB). Culture medium (RPMI) alone was used as negative control. Lipopolysaccharides (LPS) was used as positive control. Mean values ± SD, *n*=3. The different characters above bar indicate statistical differences ($p<0.05$) between compared groups (One-Way ANOVA, Tukey's multiple comparisons test).

3.2.8 Concluding remarks

Starch is the most abundant polysaccharide in *C. vulgaris*, although with a low digestibility. Its extraction with hot water and alkali solutions allowed to obtain a pregelatinized starch easily digested and with similar physicochemical characteristics to cereal starches. These results show the feasibility of using *C. vulgaris* as unconventional and sustainable source of starch for a multitude of food industry applications.

Almost all current products of industrial microalgae are derived from their biomass, leaving large amounts of spent cell-free growth medium to explore. The growth medium of *C. vulgaris* represents a source of easily recovered exopolysaccharides, showing to be a more

sustainable and economic feasible source of polysaccharides in relation to the biomass. Moreover, the exopolysaccharides were able to *in vitro* stimulate B lymphocytes, with the additional advantage of not having the unpleasant fishy-like flavor characteristic of the whole *C. vulgaris* biomass that consumers complain about. This opens a great potential for using extracellular polysaccharides as functional food ingredients for humoral immunoactivity enhancement purposes.

3.3 Impact of growth medium salinity on galactoxylan exopolysaccharides of *Porphyridium purpureum*

As verified for *C. vulgaris*, the marine red *Porphyridium purpureum* microalga, currently referred as *Porphyridium cruentum* [52,285], is also able to produce extracellular polysaccharides. Despite the protector effect of the sEPS, previously studies have established that *Porphyridium* species are capable to modify their growth, sEPS production, and/or biomass biochemical composition, in response to environmental variations, such as nutrient availability [47,175,286], light intensity [47,285,287–289], temperature [46,48], pH [46,48], and salinity [46–48,55,290]. However, the influence of the salinity of the culture medium on the excretion of sulfated polysaccharides into the culture medium during cell growth of *P. purpureum*, as well as the influence on its primary structure remained unknown yet. Thus, the aim of the present work was to study the influence of culture salt concentration on the growth rate of the euryhaline *P. purpureum* microalga and on the yield and chemical structure of sEPS production. Moreover, immuno-stimulatory activity of the produced sEPS was evaluated to establish a structure-biological activity relationship and clarify their feasibility for economic purposes, namely in aquaculture supplementation. To evaluate the ability of *P. purpureum* as a large-scale sEPS producer, a scale-up of cultivation to an 800 L-flat panel outdoor photobioreactor was performed.

3.3.1 *P. purpureum* growth pattern under different sodium chloride concentrations

The red microalga *P. purpureum* was cultivated for 24 days at three different salt concentrations: 18, 32, and 50 g/L NaCl, and the growth cell evolution was followed through optical density (Figure 3.21a), which is correlated with *P. purpureum* dry weight and cell density (Figure 2.5a and Figure 2.5b). This microalga was found to withstand the 3 different osmolarity levels, ranging from 18 to 50 g/L NaCl, agreeing with literature, where *P. purpureum* tested at salinity levels varied from 4 to 32 g/L, revealed a salinity tolerance ranging from 8 to 32 g/L [290]. A linear neperian logarithmic evolution of cell density was observed in the first 4 days at the three salinity conditions (Figure 3.21b), corresponding to the exponential phase, allowing to estimate a doubling time of 2 days (Table 3.6). The sample grown at salinity of 50 g/L showed a lower cell density after the first day of culture, when

compared with 18 and 32 g/L salinity cultures. After day 19 of each growth condition, the specific growth rate tended to 0 in all growth cultures, allowing to observe the existence of the stationary phase. Nevertheless, the transition phase (5-18 days), between exponential and stationary phases, showed differences between salinity levels (Figure 3.21b), with the higher and intermediate NaCl levels showing the higher specific growth rate (Table 3.6) and, consequently, the lower doubling time (0.09 and 0.07 $days^{-1}$, corresponding to 8 and 10 days of doubling time, respectively), than the lower salinity level (specific growth rate of 0.04 $days^{-1}$ and 17 days of doubling time). The range where the maximum specific growth rate was achieved (32-50 g/L of NaCl) is in accordance with the literature, where 26 - 47 g/L NaCl presented higher growth (0.55 $days^{-1}$), than extreme salinities of 12 and 58 g/L (0.36 $days^{-1}$) [54].

Maximum growth of an estimated DW content of 0.87 g/L and cell density of 5.7×10^6 cells/mL was achieved for a salinity of 32 g/L, determined from the correlation of the OD in Figure 3.21a with DW (Figure 2.5a) and cell density (Figure 2.5b), respectively. For a culture at 50 g/L and an estimated DW of 0.67 g/L, the cell estimated density was 4.4×10^6 cells/mL, which was higher than the DW and cell density achieved for the salinity of 18 g/L (DW of 0.44 g/L and cell density of 3.0×10^6 cells/mL). Similar behaviour was observed in *P. purpureum*, where the optimal salinity of 41.8 g/L presented the higher growth (4.9×10^6 cells/mL) after 21 days, compared to extreme salinities (tested from 11.7 to 81.8 g/L NaCl) [48]. These data show that possibly an increase of cell density of *P. purpureum* could be obtained by slightly increasing the salinity of 32 g/L, naturally occurring at Ria Formosa.

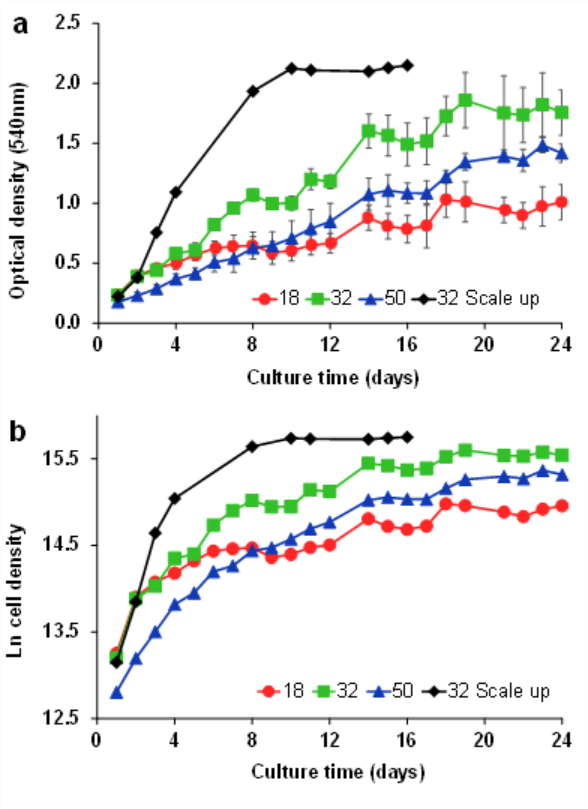

Figure 3.21 – Optical density (a) and ln of cell density (b) of *P. purpureum* grown under different salinities (18, 32, and 50 g/L NaCl) at laboratory (2.5 L reactor) and scaled up (800 L reactor). Mean values ± SD, *n*=3

Table 3.6 – Specific growth rate (μ, days^{-1}), doubling time (g, days) and correlation coefficient of the exponential, transition, and stationary phases of *P. purpureum* grown under different salinities (18, 32, and 50 g/L NaCl) at laboratory (2.5 L reactor) and scaled up (800 L flat panel photobioreactor).

Phase	Salinity	Days	μ (days^{-1})	g (days)	r^2
Exponential	18	1-4	0.30	2.3	0.84
	32	1-4	0.36	1.9	0.92
	50	1-4	0.34	2.1	1.00
	32 scale up	1-4	0.65	1.1	0.98
Transition	18	5-18	0.04	17.1	0.78
	32	5-18	0.07	9.8	0.88
	50	5-18	0.09	7.9	0.95
	32 scale up	-	-	-	-
Stationary	18	19-24	0.00	-	-
	32	19-24	-0.01	-	-
	50	19-24	0.01	-	-
	32 scale up	8-16	0.01	-	-

3.3.2 Impact of salinity on biomass composition of *Porphyridium purpureum*

P. purpureum cells obtained at stationary phase for the different salinities were recovered from the growth medium by centrifugation and dialysis (Figure 2.4f). The composition of carbohydrates, proteins, lipids, and inorganic material of the obtained biomass is presented in Table 3.7.

Carbohydrates were the major constituents of *P. purpureum* biomass, ranging from 31 to 35% of total weight, agreeing with literature [288], being glucose the predominant sugar residue (44-52 %mol), followed by xylose (26-27 %mol), galactose (14-17 %mol) and uronic acids (9-12 %mol). Glucose is possibly part of floridean starch, described as the reserve polysaccharide in red microalgae, which cellular accumulation varies through the growing phase of culture, increasing in the early stage and decreasing subsequently to possibly fulfil the demand of energy necessary for cell division [47]. Regardless the different salinity level in cultures, the amount of carbohydrates present in biomass did not show significant differences, contrarily to what was observed for *P. marinum* that accumulated higher amount of starch at 20 g/L of NaCl, than at 30 or 40 g/L [47].

Table 3.7 – Biochemical composition of biomass of the microalga *P. purpureum* grown under different salinities (18, 32, and 50 g/L NaCl). Mean values ± SD, *n*=3

NaCl (g/L)	Carbohydrates					Sulfates (%w/w)	Protein (%w/w)	Lipids (%w/w)	Inorganic material (%w/w)	Phycobiliprotein (%w/w)
	%mol				Total					
	Xyl	Gal	Glc	UA	(%w/w)					
P. purpureum biomass										
18	27.1	17.3	43.9	11.8	32.1±5.3[a]	1.1±0.2 [a]	16.1±0.8[a]	0.9±0.1[a]	19.8±0.5[a]	-
32	25.5	17.1	47.2	10.2	30.9±3.8[a]	1.2±0.4 [a]	17.6±0.2[a]	1.4±0.4[a]	19.6±0.8[a]	-
50	25.5	14.4	52.3	7.8	35.0±1.2[a]	1.0±0.3 [a]	13.1±0.0[b]	1.1±0.1[a]	24.9±1.2[b]	-
Supernatant of *P. purpureum* biomass dialysis										
18	24.9	28.4	11.5	35.1	6.3±0.3 [a]	-	-	-	-	85.7±8.6 [a]
32	22.0	29.3	12.2	36.5	5.1±0.0 [b]	-	-	-	-	85.4±5.2 [a]
50	19.3	28.0	16.1	36.5	6.0±0.2 [ab]	-	-	-	-	81.9±1.2 [a]

Sample with the same character represent values that are not significantly different (p<0.05) when analyzing each parameter individually (One-Way ANOVA, Tukey's multiple comparisons test). Xyl - xylose; Gal – galactose; Glc – glucose; UA – uronic acids

P. purpureum biomass shown a protein content that varied from 13% w/w in sample grown at 50 g/L to 18% w/w in sample grown at 32 g/L. At 18 g/L the protein content was

16% w/w (Table 3.7), agreeing with literature for *Porphyridium* species [291]. Lipids content was approximately 1% w/w and the major esterified fatty acids was C16:0 (palmitic acid, 69-71%, Table 3.8) in accordance with literature [66,292]. *P. purpureum* grown with 18 and 32 g/L NaCl presented about 20% w/w of inorganic material (Table 3.7), which is in line with the 18% w/w reported for this microalga species [164]. However, when *P. purpureum* is cultivated in 50 g/L NaCl growth medium, the inorganic material represented 25% w/w of dry weight. This inorganic material should be mainly Na^+ , K^+, and Cl^-, involved in the intracellular fluid osmolarity [52].

Table 3.8 – Fatty acid composition as percentage of total fatty acids of *P. purpureum* biomass grown under different salinities (18, 32, and 50 g/L NaCl). Mean values ± SD, *n*=3

	Salinity (g/L NaCl)		
	18	**32**	**50**
C16:0	68.9±0.4	71.0±4.2	70.2±2.1
C18:0	15.0±3.1	15.6±3.0	12.0±0.6
C18:2	8.1±1.0	6.5±3.6	8.6±1.0
C18:3	8.1±2.1	7.0±3.6	9.1±1.7
C20:4	tr	tr	tr
C20:5	tr	tr	tr

The analysis performed to the *P. purpureum* grown at different salinities allowed to infer that the composition did not greatly change with salinities, agreeing with the thermogravimetric analysis (Figure 3.22). This analysis showed a minor peak at 244-250 ºC and a major peak at 270-280 ºC.

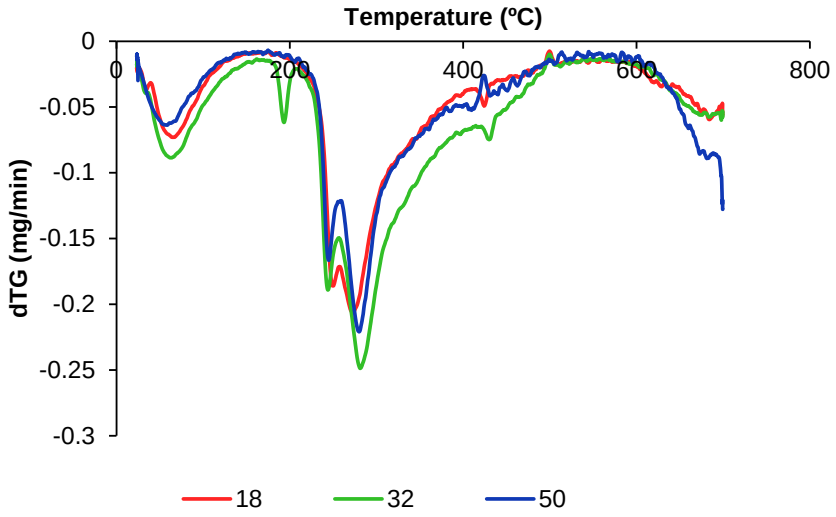

Figure 3.22 – First derivate of thermogravimetric analysis of *P. purpureum* biomass grown under different salinities (18, 32, and 50 g/L NaCl).

Because *P. purpureum* cells were encapsulated in a mucilage that was excreted to the medium during growth and a fraction remains attached to the cells [151], the water that remained inside the dialysis bag was collected and the polymeric soluble material recovered (Figure 2.4d) and analysed. These pink/purple colored material recovered in the supernatant of the dialysis were constituted mainly by phycobiliprotein (82-86% w/w), namely phycoerythrin [293], in accordance with the low amounts of polysaccharides (5-6% w/w). Possibly, during dialysis some *P. purpureum* cells burst due to intracellular osmotic pressure, releasing phycobiliproteins.

3.3.3 Extracellular polysaccharides of *P. purpureum*

The extracellular polysaccharides produced by *P. purpureum* from each culture growth medium was centrifuged and dialysed, and the polymeric material was recovered by freeze drying (Initial sEPS). This extracellular polymeric material was subjected to graded ethanol precipitation (Purified sEPS), allowing to obtain a purified fraction insoluble in ethanol (Figure 2.4f), slightly enriching the polysaccharides content, from 48-54 to 58-61% of total weight, without affecting the monosaccharides profile (Table 3.9), although slightly lowing the contribution of sulfate. The dynamic viscosity also increased from 2.4-2.6 to 3.0-3.3 cP

with the polysaccharide's enrichment. The extracellular polysaccharides were sulfated (8-13%) and mostly composed by xylose (45-49 %mol), galactose (19-22 %mol), uronic acids (16-21 %mol), and glucose (15-17 %mol).

Similar sugar residue ratios and amounts were previously reported as the main constituent in extracellular polysaccharides of *Porphyridium* species [151,294]. The total content of carbohydrates, as well as the sulfate and protein content, did not present differences between the different osmotic level growth media. However, the yield of excreted polymeric material was significantly different, where the growth medium with 32 g/L NaCl achieved the higher polymeric material yield (150 mg/L), when compared with the growth medium with 50 g/L NaCl (78 mg/L) (Table 3.9). The yield of polymeric material produced by 18 and 32 g/L NaCl cultures is in agreement with those obtained for *P. cruentum* (synonym of *P. purpureum*), varying from 0.12 to 0.16 g/L [295]. Salt can cause osmotic stress and have effect on microalgae physiological responses. However, the increase of the salinity did no led to an increase of the sEPS excretion yield, possibly due to an adaptation of the cells to the salinity of the culture media. Similar results were also observed when 0.5 – 1 g/L NaCl was added into the growth media, and a decrease of sEPS produced by the green microalga *Neochloris oleoabundans* was observed [296].

Table 3.9 – Chemical composition of Initial sEPS and Purified sEPS of the microalga *P. purpureum* grown under different salinities (18, 32, and 50 g/L NaCl) at laboratory (2.5 L reactor) and scaled up (800 L flat panel photobioreactor). Mean values ± SD, *n*=3

NaCl (g/L)	Yield	Carbohydrates					Sulfate (%w/w)	Protein (%w/w)	Dynamic viscosity (cP)
		%mol				Total			
		Xyl	Gal	Glc	UA	(%w/w)			
Initial sEPS									
18	116±22 mg/L^{a,b}	44.9	18.8	15.5	20.7	54.0±3.9^{a}	13.0±1.0^{a}	2.8±0.3^{b}	2.38±0.02^{a}
32	150±22 mg/L^{a}	46.0	21.8	16.2	16.0	50.0±3.5^{a}	10.5±0.3^{a}	6.5±1.0^{a}	2.64±0.01^{b}
50	78±1 mg/L^{b}	44.6	21.2	16.3	17.9	47.6±2.8^{a}	11.6±0.4^{a}	5.2±0.7^{a}	2.40±0.02^{a}
32*	240 mg/L^{c}	44.0	28.4	15.9	11.6	50.5±3.4^{a}	9.4±1.6^{a}	-	-
Purified sEPS									
18	77%	48.8	18.9	15.7	16.6	60.8±2.5^{a}	8.7±0.8^{a}	3.5±0.4^{a}	3.15±0.02^{a}
32	88%	45.8	21.6	15.2	17.3	58.8±1.7^{a}	8.9±1.0^{a}	4.5±0.3^{a}	2.96±0.03^{b}
50	80%	44.7	21.0	16.6	17.6	58.1±0.8^{a}	8.4±0.7^{a}	7.5±1.1^{b}	3.31±0.09^{c}

Yield: Polymeric material extraction yield (mg/L) and ethanol precipitation yield (%); 32*- Scale up at salinity 32 g/L NaCl. Sample with the same character represent values that are not significantly different (p<0.05) when analysing each parameter individually (One-Way ANOVA, Tukey's multiple comparisons test). Xyl - xylose; Gal – galactose; Glc – glucose; UA – uronic acids

To disclosure the extracellular sulfated polysaccharide structures, the nature of glycosidic linkages, position of branching points, and sulfate groups of sEPS (Initial) and correspondent purified sEPS (Purified) of the three different growth media salinities (18, 32, and 50 g/L NaCl) were evaluated before (native-N) and after desulfation (desulfated-D). The desulfation allows to distinguish if the substitution of sugar residues corresponds to a branching point or a sulfate ester. When a position is acetylated in the native polymer and remained acetylated in the desulfated polymer, it is indication that this position contains a branching point. On the other hand, when a position is acetylated in the native polymer and became methylated after desulfation, it means that it contained a sulfate ester residue at that position [237]. The GC-MS analysis (Table 3.11) revealed the presence of mainly by t-Xyl, (terminally linked xylose), t-Xyl4S, 3-Xyl, 4-Xyl, t-Glc, 3-Glc6S, t-Gal, and 2,3,4-Gal.

Table 3.10 – Glycosidic linkages analysis (%) of extracellular polysaccharides (initial and purified with graded ethanol) of the microalga *P. purpureum* grown under different salinities (18, 32, and 50 g/L NaCl) before (native-N) and after desulfation (desulfated-D).

Substitution	**Initial 18**		**Initial 32**		**Initial 50**		**Purified 18**		**Purified 32**		**Purified 50**	
	N	**D**	**N**	**D**	**N**	**D**	**N**	**D**	**N**	**D**	**N**	**D**
t-Xyl	11.8	26.5	9.8	26.7	10.0	25.0	10.5	26.3	9.9	27.3	8.7	28.5
3-Xyl	14.6	14.6	12.4	13.8	11.9	13.4	13.7	14.6	13.0	14.8	11.9	13.8
4-Xyl	16.9	13.8	15.0	12.2	15.9	12.5	15.2	13.5	15.9	14.0	16.1	14.8
Total	**43.3**	**54.9**	**37.2**	**52.8**	**37.7**	**50.9**	**39.4**	**54.4**	**38.9**	**56.0**	**36.8**	**57.2**
t-Gal	8.0	5.6	8.4	5.8	7.3	6.0	8.8	5.5	6.3	6.0	6.0	5.5
2-Gal	1.4	1.1	2.3	1.4	1.8	1.3	1.5	0.9	2.0	1.3	1.7	1.0
3-Gal	1.7	1.1	2.9	1.7	2.4	1.8	1.9	1.2	2.3	1.6	2.1	1.3
4-Gal	2.5	1.8	2.8	2.3	2.8	2.5	2.6	1.8	2.5	2.2	2.8	2.3
2,3-Gal	0.7	1.3	1.5	1.6	2.5	1.5	0.8	1.1	1.5	1.2	2.6	1.0
2,4-Gal	1.3	0.9	1.7	0.9	1.4	0.7	1.4	0.7	1.7	0.7	1.5	0.6
3,6-Gal	2.2	0.5	3.5	0.4	2.6	0.4	2.4	0.4	3.0	0.3	2.6	0.0
2,3,4-Gal	14.0	15.3	13.7	15.9	15.0	15.4	14.9	16.4	15.8	14.3	16.0	13.9
Total	**31.8**	**27.5**	**36.8**	**30.0**	**35.8**	**29.4**	**34.3**	**27.9**	**35.1**	**27.7**	**35.3**	**25.7**
t-Glc	7.8	7.7	7.0	7.5	7.4	9.3	8.4	8.3	7.1	7.3	7.6	8.4
3-Glc	3.4	5.8	5.2	6.3	5.3	7.1	3.8	6.0	4.5	5.9	5.4	6.6
3,4-Glc	3.9	2.9	5.6	3.1	6.5	2.8	3.7	2.8	5.9	2.5	6.7	2.2
3,6-Glc	9.9	1.2	8.3	0.3	7.1	0.5	10.3	0.6	8.6	0.6	8.3	0.0
Total	**24.9**	**17.6**	**26.1**	**17.2**	**26.5**	**19.7**	**26.3**	**17.7**	**26.1**	**16.3**	**27.9**	**17.2**

Considering that sEPS obtained from the growth medium with 32 g/L NaCl was chosen as a control, a detailed analysis of the glycosidic linkages and sulfation positions were performed. The sEPS sample obtained after purification from the *P. purpureum* culture grown at 32 g/L NaCl (Purified 32), in native polymers, t-Xyl corresponded to 26% of total analysed Xyl of the sample, and 3-Xyl and 4-Xyl corresponded to 33 and 41%, respectively. After desulfation, an increase of t-Xyl for almost the double (49% in total analysed xylose in the sample) occurred with a concomitant decrease of 3-Xyl and 4-Xyl for 26% and 25%, respectively (Table 3.11). These results showed the presence of terminally linked xylose residues (49%), which almost half were substituted by sulfate at *O*-3 (t-Xyl-3S, 31%) and at *O*-4 (t-Xyl-4S, 69%). Although the presence of sulfated xylose residues has never been described for sEPS of *P. purpureum*, the presence of t-Xyl [159,160], and 3-Xyl [160,297] and 4-Xyl [160,297,298] in the same proportion [297] in the polysaccharide backbone [160] are in accordance with literature.

Table 3.11 – Calculated values of the percentage of each glycosidic linkage in relation to the total analysed sugar residues (Xyl, Gal, and Glc) of the extracellular polysaccharides (initial and purified with graded ethanol) of the microalga *P. purpureum* grown under different salinities (18, 32, and 50 g/L NaCl) before (native-N) and after desulfation (desulfated-D).

Substitution	**Initial 18**		**Initial 32**		**Initial 50**		**Purified 18**		**Purified 32**		**Purified 50**	
	N	**D**	**N**	**D**	**N**	**D**	**N**	**D**	**N**	**D**	**N**	**D**
t-Xyl	27	48	26	51	26	49	27	48	26	49	24	50
3-Xyl	34	27	33	26	32	26	35	27	33	26	33	24
4-Xyl	39	25	40	23	42	25	39	25	41	25	44	26
Total	100	100	100	100	100	100	100	100	100	100	100	100
t-Glc	31	44	27	44	28	47	32	47	27	45	27	49
3-Glc	13	33	20	37	20	36	15	34	17	36	19	39
3,4-Glc	16	17	22	18	25	14	14	16	23	15	24	13
3,6-Glc	40	7	32	2	27	3	39	3	33	3	30	0
Total	100	100	100	100	100	100	100	100	100	100	100	100
t-Gal	25	20	23	19	20	20	26	20	18	22	17	22
2-Gal	4	4	6	5	5	5	4	3	6	5	5	4
3-Gal	5	4	8	6	7	6	6	4	7	6	6	5
4-Gal	8	7	8	8	8	8	8	6	7	8	8	9
2,3-Gal	2	5	4	5	7	5	2	4	4	4	7	4
2,4-Gal	4	3	5	3	4	2	4	2	5	3	4	2
3,6-Gal	7	2	9	1	7	1	7	1	8	1	7	0
2,3,4-Gal	44	56	37	53	42	52	43	59	45	52	45	54
Total	100	100	100	100	100	100	100	100	100	100	100	100

Glucose residues present in sample Purified 32 were constituted by 3,6-Glc (33%), t-Glc (27%) 3,4-Glc (23%), and 3-Glc (17%) in native polymers, while after desulfation it was observed the decrease of the substituted glucose (Table 3.11), meaning that great part of the substituents were sulfate esters that were removed during desulfation procedure. An increase of 3-Glc with the concomitant decrease of 3,6 and 3,4-Glc residues after desulfation allowed to infer that sulfate esters were mainly linked in *O*-6 (81%) or *O*-4 position of glucose (19%) with a backbone of 3-Glc. The increase of t-Glc after desulfation may also suggest the presence of doubly sulfated terminally linked glucose, at position *O*-3 or/and *O*-4 or/and *O*-6, not yet described in the literature.

Regarding to galactose substitution, in native polymer of the sample Purified 32, 2,3,4-Gal was the major residue, corresponding to 45% of total galactose analysed in the sample, followed by t-Gal (18%), 3,6-Gal (8%), 3 and 4-Gal (7%), and 2-Gal (6%) (Table 3.11). Minor amounts of 2,3-Gal and 2,4-Gal were also observed. After desulfation, the 2,3,4-Gal residue did not decrease, allowing to infer a highly substituted polymer, which was not reported in literature, possibly because of the high viscosity of the polymer, pretreatments such as ultrasounds, known to promote debranching [299] have been performed [159]. In desulfated polymers, the galactose profile did not greatly change, when compared with xylose or glucose analyses, indicating only a slightly sulfation. However, 2,4-Gal residues decreased in desulfated polymer, and 4-Gal slightly increased, revealing a sulfation in *O*-2 position (4-Gal-2S). Moreover, 3,6-Gal residues also decreased. Since there was no 6-Gal residue, it can be hypothesized that the sulfate esters were also present in position *O*-6 (3-Gal-6S), agreeing with literature [300]. The desulfated polymer was constituted by the linear residues 2-Gal (5%), 3-Gal (6%), and 4-Gal (8%). The 3-Gal and 4-Gal residues were already described in literature [160,297,298]. It is established in the literature that polysaccharides of various unicellular red algae, including *Porphyridium* species, contain 3-GlcA-3-Gal disaccharide, an aldobiouronic acid, as basic building block [159]. Because the initial and purified sEPS were not carboxyl reduced after methylation, it was not possible to directly determine the uronic acids linkages. Nevertheless, the presence of aldobiouronic acids can be inferred by the analyses performed, since galactose was undervalued in sugar analysis (22%) in relation to methylation analysis (28%), a characteristic of acid hydrolysis resistance of aldobiouronic glycosidic linkages when compared with their methylation forms [301].

The results of methylation analyses, along with the information already stated in literature, allowed to propose a possible structure of *P. purpureum* extracellular polysaccharides (Figure 3.23).

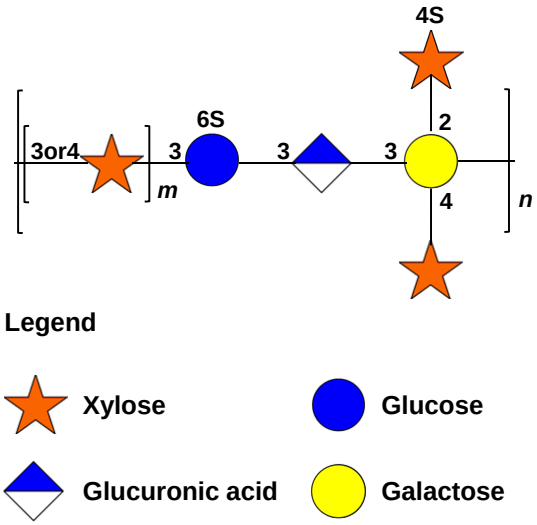

Figure 3.23 – Possible most representative repeating unit of sulfated extracellular polysaccharides produced by *P. purpureum* grown at salinity 32 g/L NaCl, according to The Symbol Nomenclature for Glycans, https://www.ncbi.nlm.nih.gov/glycans/snfg.html.

3.3.4 Impact of salinity on extracellular polysaccharides

To evaluate possible differences in sEPS of *P. purpureum*, namely to identify possible changes in sEPS glycosidic linkage composition promoted by the growth of microalga at different salinities, principal component analyses (PCA) were performed before and after desulfation (Figure 3.24a and Figure 3.24b, respectively). Since a preliminary test revealed no distinguishable differences between initial and purified samples (data not shown) concerning the glycosidic linkages composition of the extracellular polysaccharides obtained from the same growth medium salinity, each salinity was represented with 4 replicates, 2 replicates of the dialysed sEPS (Initial) and other 2 replicates corresponding to the ethanol purified sample (Purified), expressed as Sample 18, Sample 32, and Sample 50.

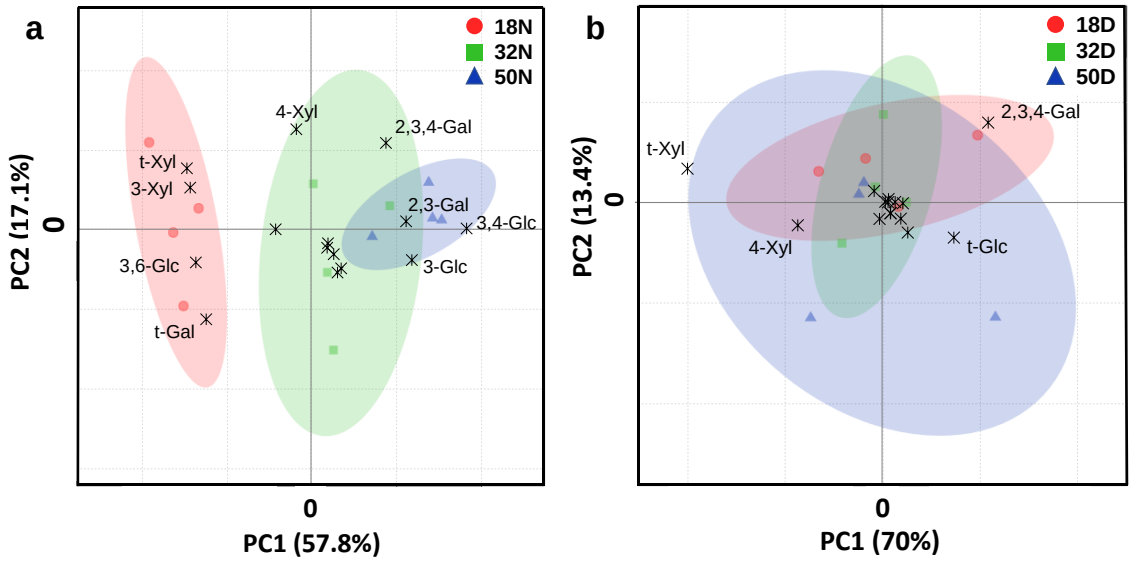

Figure 3.24 – PCA of glycosidic linkages of sEPS (Initial and Purified) produced by *P. purpureum* grown under different salinities: 18, 32, and 50 g/L NaCl presented in Table 2. a) Native P. *purpureum* sEPS; b) Desulfated *P. purpureum* EPS. In each figure the scores and loadings are represented.

The Principal Component 1 (PC1) of glycosidic linkages of sEPS of *P. purpureum* grown under different salinities (Figure 3.24a) explained 58% of the data set variability. Sample 18 was located at PC1 negative, while Sample 32 and Sample 50 were located at PC1 positive, allowing a clear distinction of Sample 18 from samples obtained from the other salinities. Between Sample 32 and Sample 50 no significant differences were disclosed. Regarding to loadings, it was observed that t-Xyl, 3-Xyl, 3,6-Glc, and t-Gal were the main features that contributed for separation of Sample 18, while 4-Xyl, 2,3,4-Gal, 2,3-Gal, 3,4-Gal, and 3-Glc were the main features that contributed for Sample 32 and Sample 50. Figure 3.24b represents the scores and loadings of desulfated EPS, where no significant (p<0.05) differences concerning the glycosidic linkages composition were observed between salinities concerning the glycosidic linkages composition were observed between the EPS obtained from the different growth media salinities, allowing to infer that the differences between the polysaccharides obtained from different osmotic medium cultures could be related with the sulfation pattern. Thus, seeking more information about the variables that could be responsible for the distinction of samples, six PCA were performed for each sugar residue (xylose, glucose, and galactose) before and after desulfation, normalized for the total

of each sugar residue (Figure 3.25, Figure 3.26, and Figure 3.27). Moreover, several boxplots were also performed in each PCA to understand the variability within each variable.

PCA of xylose glycosidic linkages of sEPS (Figure 3.25a) showed a PC1 that explained 78.2% of the variability, allowing to observe a separation between Sample 18 and Sample 50. Boxplots (Figure 3.25b) showed the higher contribution of 3-Xyl in Sample 18, while 4-Xyl was higher in Sample 50. After desulfation, no statistical differences were observed between samples (Figure 3.25c,d), allowing to conclude that the polysaccharides were more sulfated in in *O*-3 position of xylose at lower salinity (Sample 18), whereas higher salinity (Sample 50) promoted the sulfation of xylose in *O*-4 position. Sample 32 showed an intermediate effect, closer to Sample 50.

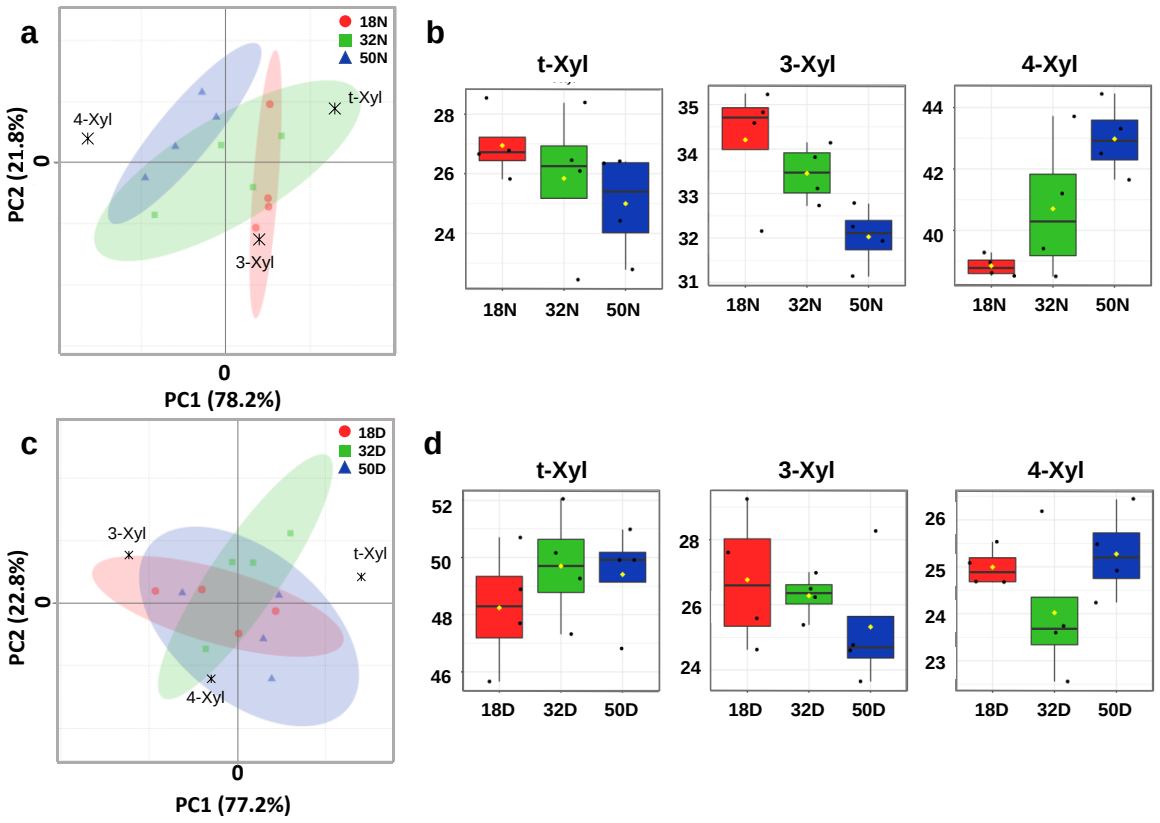

Figure 3.25 – PCA (a, c) and box plots (b, d) of the glycosidic linkages of xylose residues of extracellular polysaccharides of the microalga *P. purpureum* grown under different salinities (18, 32, and 50 g/L NaCl), before (native-N) and after desulfation (desulfated-D).

The PCA of native polysaccharide in relation to glucose glycosidic linkages (Figure 3.26a) has a PC1 that explained 91.9% of variability between salinities. Sample 18 was

separated from Sample 32 and Sample 50, mostly due to the higher contribution of 3,6-Glc, while Sample 32 and 50 presented higher contribution of 3,4-Glc, and 3-Glc (Figure 3.26b). As observed for xylose residues, after desulfation no differences were observed between the three samples (Figure 3.26c), allowing to conclude that the growth at a lower salinity medium (18 g/L NaCl) promoted the sulfation of glucose at *O*-6 position, while higher salinity (Sample 50) promoted more sulfation at *O*-4 position of glucose. Sample 32 showed an intermediate effect, closer to Sample 50, as observed for xylose. Furthermore, the boxplot analysis of samples after desulfation (Figure 3.26d) revealed a higher contribution of 3-Glc and lower contribution of 3,4 and 3,6-Glc for the higher salinity (Sample 50). Thus, beyond the different sulfation pattern, the higher growth medium salinity seems to promote the occurrence of less branched glucose residues.

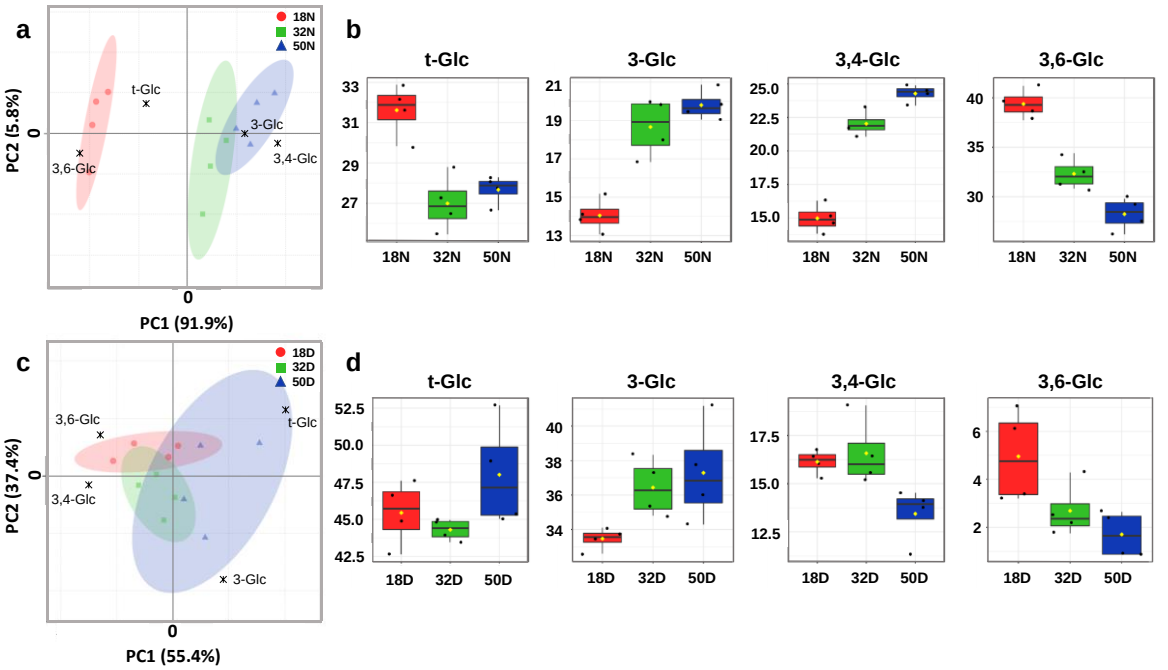

Figure 3.26 – PCA (a, c) and box plots (b, d) of the glycosidic linkages of glucose residues of extracellular polysaccharides of the microalga *P. purpureum* grown under different salinities (18, 32, and 50 g/L NaCl), before (native-N) and after desulfation (desulfated-D).

In relation to galactose glycosidic linkages, PCA of native polymers (Figure 3.27a) presented a PC1 explaining 58.5% of the variability among polysaccharides obtained from the different growth media salinities. The scores and loadings showed that Sample 18 was different from Sample 32 and 50, with higher contribution of t-Gal in Sample 18 and higher

contribution of 2,3-Gal residues in Sample 32 and Sample 50 (Figure 3.27b). The PCA of desulfated polysaccharide showed no statistical differences between each salinity (Figure 3.27c). However, the boxplot analysis allowed to observe that 2-Gal, 3-Gal, and 4-Gal residues had lower contribution in the polysaccharides produced from *P. purpureum* grown at lower salinity (Figure 3.27d), possibly because growth medium salinity could also slightly influence glycosidic linkages composition.

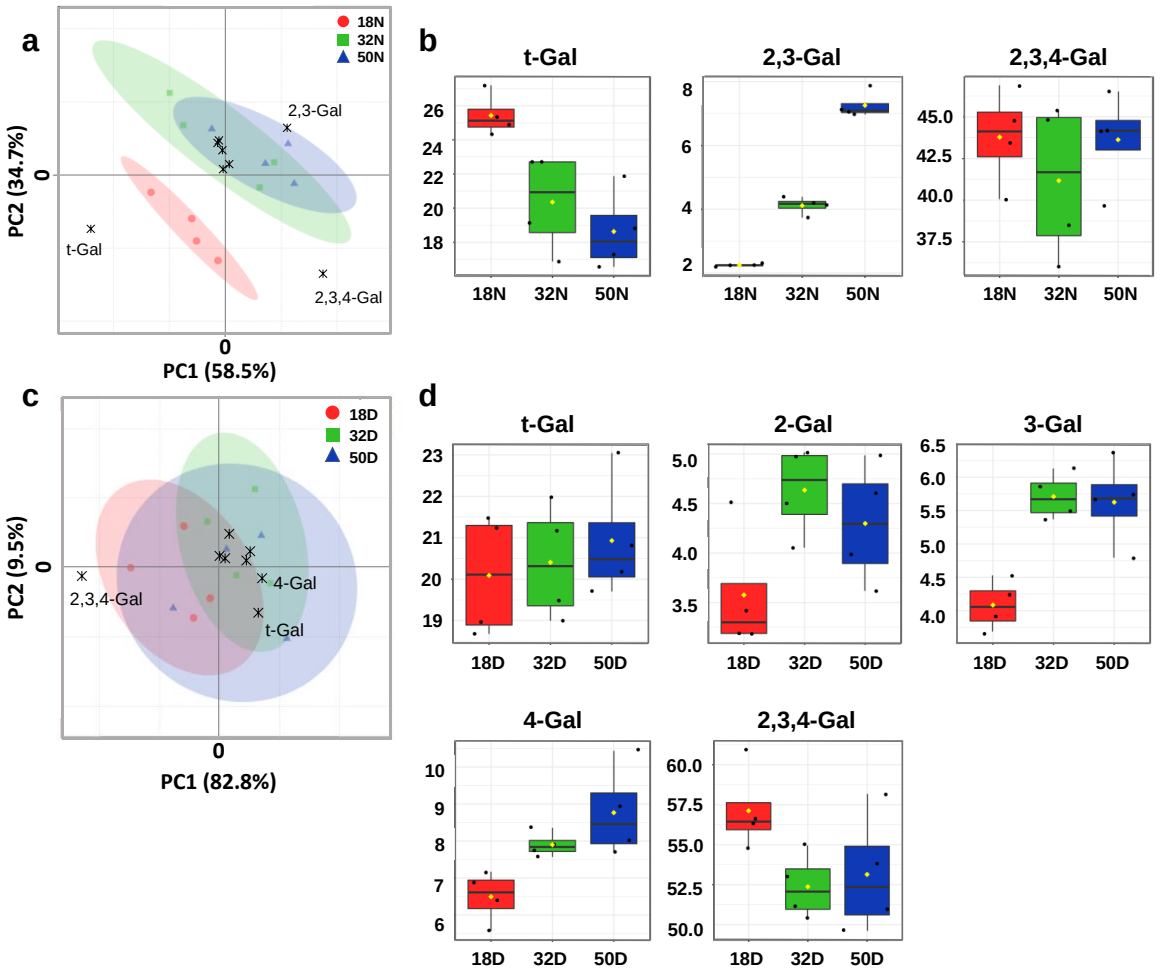

Figure 3.27 – PCA (a, c) and box plots (b, d) of the glycosidic linkages of galactose residues of extracellular polysaccharides of the microalga *P. purpureum* grown under different salinities (18, 32, and 50 g/L NaCl), before (native-N) and after desulfation (desulfated-D).

Thus, *P. purpureum* produces extracellular polysaccharides with a sulfation pattern slightly different in xylose and glucose, according to the growth media, despite the overall similarity in sugars profile and sulfate content. However, those differences were not

substantial enough to change the proposal of the most representative repeating units of sEPS showed in Figure 3.23.

3.3.5 Evaluation of *in vitro* lymphocyte stimulatory activity of purified sEPS

The purified extracellular polysaccharides of *P. purpureum* cultured at 32 g/L of NaCl, as well as the respective desulfated material, were used to evaluate their potential to stimulate *in vitro* murine lymphocytes. Polysaccharide concentrations in the range of 2.5–200 µg/mL were assessed. In addition, the purified material of the lower and higher salinity tested in the present study (18 and 50 g/L of NaCl, respectively), as well as the correspondent desulfated material, were also tested at 200 µg/mL polysaccharide concentration, in order to evaluate the impact of the structural differences of polysaccharides in immunostimulatory activity.

The different tested samples did not induce loss of cell viability when compared to non-stimulated controls, cultured with medium alone, indicating lack of cytotoxicity (Figure 3.28). Expression of the early activation marker CD69 on the surface of $CD3^+$ cells (T cells) treated with the different extracellular polymeric material and the correspondent desulfated samples was not different from that observed in non-treated controls, showing that none of the tested samples stimulated T cells (Figure 3.29). In contrast, $CD19^+$ cells (B cells) were activated in a dose response-manner by purified sEPS produced with a 32 g/L NaCl culture, in a medium containing polymyxin B, 17, 28, 47, 67 and 77% of activated cells, for 2.5, 25, 50, 100, and 200 µg/mL, respectively (Figure 3.30).

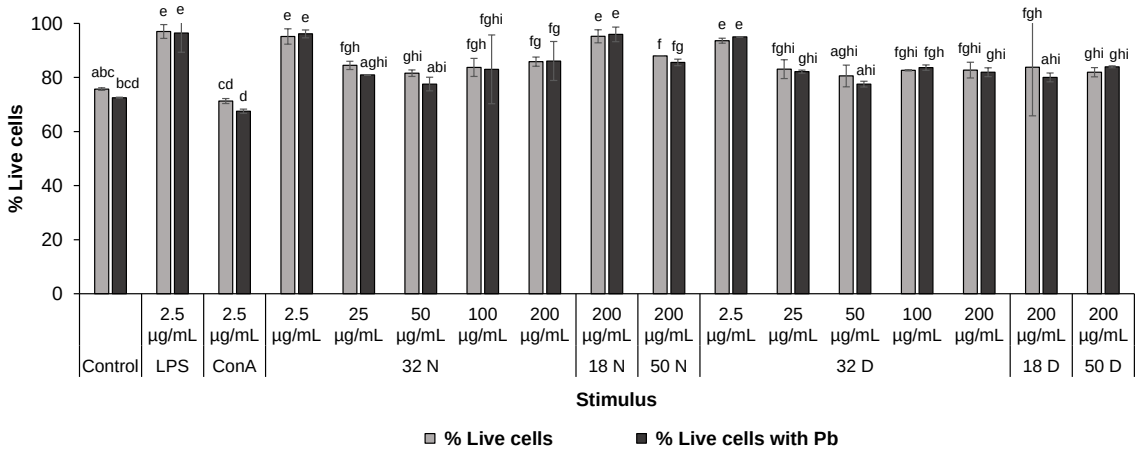

Figure 3.28 – Percentage of propidium iodide negative splenocytes [Live cells (%)] upon cultured for 6 h with purified sEPS (N) and corresponding desulfated EPS (D) at polysaccharides concentrations of 2.5, 25, 100 and 200 µg/mL of *P. purpureum* grown at 32 g/L NaCl concentration, and at polysaccharides concentrations of 200 µg/mL of *P. purpureum* grown at 18 and 50 g/L NaCl concentration in the absence and presence of polymyxin B (PB). Culture medium (RPMI), lipopolysaccharides (LPS,) and concanavalin (ConA) were used as controls. Mean values ± SD, *n*=3. The different characters above bar indicate statistical differences ($p<0.05$) between compared groups (One-Way ANOVA, Tukey's multiple comparisons test).

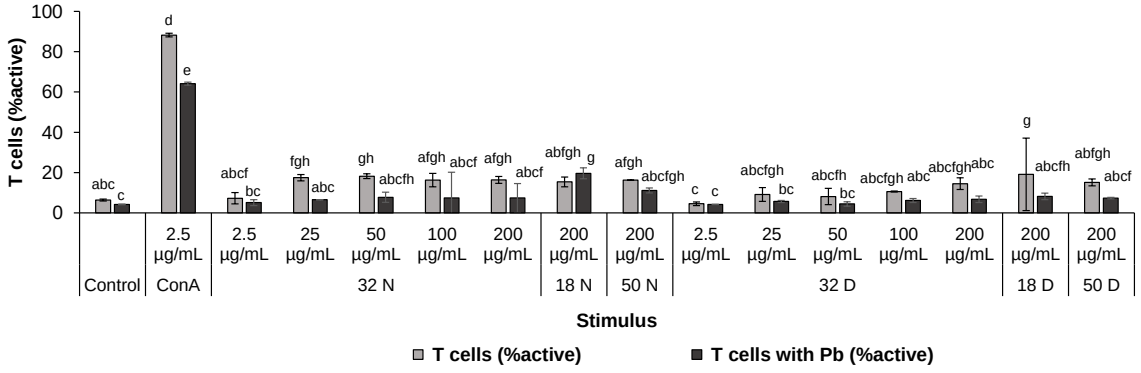

Figure 3.29 – Spleen T lymphocytes activation (%) induced by purified sEPS (N) and correspondent desulfated EPS (D) at polysaccharides concentrations of 2.5, 25, 100 and 200 µg/mL of *P. purpureum* grown at 32 g/L NaCl concentration, and at polysaccharides concentrations of 200 µg/mL of *P. purpureum* grown at 18 and 50 g/L NaCl concentration in the absence and presence of polymyxin B (PB). Culture medium (RPMI) alone was used as negative control. Concanavalin (ConA) was used as positive control. Mean values ± SD, *n*=3. The different characters above bar indicate statistical differences ($p<0.05$) between compared groups (One-Way ANOVA, Tukey's multiple comparisons test).

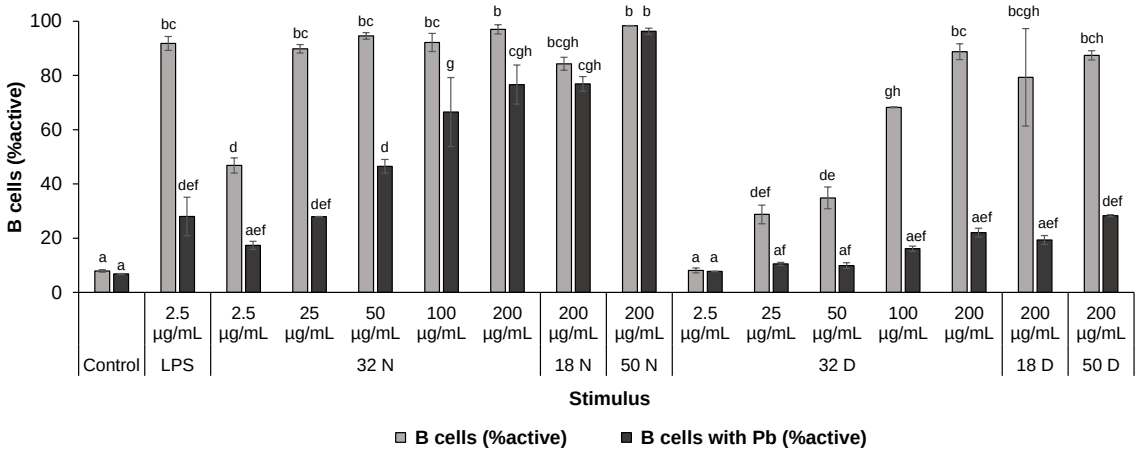

Figure 3.30 – Spleen B lymphocyte activation, as assessed by the % of CD69-expressing cells, induced by purified sEPS (N) and the correspondent desulfated EPS (D) at polysaccharides concentrations of 2.5, 25, 100 and 200 µg/mL of *P. purpureum* grown at 32 g/L NaCl concentration, and at polysaccharides concentrations of 200 µg/mL of *P. purpureum* grown at 18 and 50 g/L NaCl concentration in the absence and presence of polymyxin B (PB). Culture medium (RPMI) alone was used as negative control. Lipopolysaccharides (LPS) were used as positive control. Mean values ± SD, *n*=3. The different characters above bar indicate statistical differences ($p<0.05$) between samples (One-Way ANOVA, Tukey's multiple comparisons test).

A decrease in B cells stimulation was observed when polymyxin B was added to cell cultures, indicating some level of endotoxin contamination. Nonetheless, the percentage of stimulated B cells was significantly higher than in the non-treated controls. The sEPS recovered from 18 and 50 g/L NaCl cultures also induced higher B cell early activation than the control (77 and 96%, respectively), at 200 µg/mL polysaccharide concentration. These results showed that purified sulfated polysaccharides recovered from *P. purpureum* broth cultivated at different salinities have *in vitro* activity on B lymphocytes. Accordingly, previous reports also showed the immunostimulatory properties of *P. purpureum* sEPS, by promoting the proliferation of splenocytes in a dose-dependent manner [183], and inducing the production of pro-inflammatory cytokines and NO by Raw 264.7 cell line macrophages [183,184].

Desulfated extracellular polysaccharides were tested in order to confirm the importance of sulfate groups in immunostimulatory activity. Indeed, the desulfated samples showed significantly lower percentage of B cells stimulation than native samples (Figure 3.30), corroborating the sulfate esters relevance, in accordance with previous reports on sulfated polysaccharides immunostimulatory activity [186,284,302]. Nevertheless, the stimulation slightly increased with the increase of polysaccharides concentration, which could both

indicate the presence of residual sulfates after desulfation [237], or the ability of *P. purpureum* extracellular desulfated polysaccharides to stimulate B cells.

3.3.6 Scale-up

Since *P. purpureum* extracellular polysaccharides presented relevant physico-chemical and immunostimulatory properties for their commercial exploitation, this microalga was cultivated at large scale, allowing to evaluate the large-scale extracellular polysaccharides production viability. Thus, a gradual scale up was applied, where firstly *P. purpureum* was cultivated at 2.5 L scale (Figure 2.4a), and posteriorly a new scale up to 800 L was performed (Figure 2.4b). The scale-up outdoor test was performed at 32 g/L of NaCl, the intermediate salinity previously used, since this culture condition revealed higher *P. purpureum* cell density and higher amount of extracellular polysaccharides, without affecting their sugar profile.

The cells growth evolution at large scale was followed through optical density (Figure 3.21a) for 16 days. The growth rate was higher than that observed in lab scale, where the stationary phase was only reached after 24 days. An exponential phase was observed in the first 4 days (Figure 3.21b), which was similar to the laboratorial evolution. However, cells doubled 2 times faster than the cells cultivated at laboratorial scale, i.e. doubled every day, instead of the 2 days generation time (Table 3.6). These faster cells growth could be possibly related with the better adaptation phase of the inoculum cells due to the gradual scale up, and with the differences in the reactor, since the flat panel photobioreactor had higher contact surface and, consequently, higher amount of light incidence per cells. After exponential phase, a stationary phase was observed (Figure 3.21a), where maximum dry weight and cell density was reached, 1.0 g/L and 6.7 $\times 10^6$ cells/mL, respectively. Thus, contrarily to laboratorial scale, no transition phase was observed. Moreover, dry weight/cell density also performed better in the outdoor flat panel photobioreactor than at laboratorial scale.

In the 800 L outdoor pilot culture system, the polymeric material of growth medium yielded 240 mg/L, 60% higher than laboratorial scale at the same osmotic pressure, which is in line with the higher biomass production. The extracellular polymeric material production yield was within the lower limit of the 240-1490 mg/L range described for *P. purpureum* grown in a 130 L outdoor system for 19 days [303].

The polymeric material was found to be constituted by 50.5% w/w of sugar residues and 9.4% w/w of sulfate esters (Table 3.9). The monosaccharides composition revealed xylose as major residue (44 %mol), followed by galactose (28 %mol), glucose (16 %mol), and uronic acids (12 %mol). These results are similar to those obtained at laboratorial scale and, consequently, it was possibly to conclude that it is feasible to produce sEPS from *P. purpureum* at large scale.

3.3.7 Concluding remarks

This study showed that *P. purpureum* cells were able to grow under a large range of salinity (18-50 g/L NaCl), with a maximum accumulation of 5.7×10^6 cells/mL cells at a laboratorial scale in 19 days culture. These conditions were successfully scaled up for an 800 L culture, with an accumulation of 6.7×10^6 cells in 8 days, with a culture salinity of 32 g/L NaCl. Nevertheless, the effect of salinity under the studied conditions had impact in extracellular polysaccharides excretion yield, higher for 32 g/L NaCl (90 mg/L) than for 50 g/L (46 mg/L). At pilot scale (800 L) this yield was even higher (144 mg/L). Those extracellular polysaccharides confirmed to be sulfated and highly branched glucuronoglucogalactoxylan, whose sulfation pattern slightly changed in xylose and glucose residues with the variation of NaCl concentration in culture medium. The sEPS produced from *P. purpureum* grown at lower salinity tended to be more sulfated in *O*-3 position of xylose and *O*-6 position of glucose, while at higher salinity the sEPS tended to be more sulfated in *O*-4 position of xylose and glucose, with higher linear 2-Gal, 3-Gal, and 4-Gal residues.

The sulfated EPS can be easily recovered and purified from culture medium. Moreover, they are capable to *in vitro* stimulate B lymphocytes. This justifies the use of *P. purpureum* in aquaculture and also allows to purpose the use of their sulfated extracellular polysaccharides in fish aquaculture for humoral immunity enhancement.

CHAPTER 4. Conclusions

This PhD thesis contributed to highlight the potential of microalgae to produce pigments and polysaccharides for food and feed applications. *C. vulgaris* chlorophylls were extracted with a food grade solvent and showed to be more stable in 96% ethanolic solution, protected from light at room temperature or below. Despite the known influence of modified atmosphere and the alkaline environment on the chlorophyll's preservation, the argon rich atmosphere and the addition of NaOH were not necessary to preserve the green color of the ethanolic extract under the studied conditions. The *C. vulgaris* extract was successful in greening cooked cold rice to be used in sushi, revealing their potential as a natural food colorant. This work open perspectives to explore more combination of variables in the green color conservation, such as the development of chlorophyll derivatives containing Cu as central ion in the macrocycle that are also approved food colorings (E141).

Beyond *C. vulgaris* being a great source of chlorophylls, this microalga also showed their feasibility as unconventional source of starch, that can be co-extracted with the pigments, increasing its interest in the commercial point of view. Moreover, *C. vulgaris* excreted a galactan to the growth medium, with similar structural characteristics to its cell wall related polysaccharides, that were able to *in vitro* stimulate B lymphocytes. The microalga *P. purpureum* also showed the ability to release polysaccharides to the growth medium, namely, sulfated galactoxylans, whose structure slightly changed with the salt concentration of the culture medium: at 18 g/L the sEPS tended to be more sulfated in *O*-3 position of xylose and *O*-6 position of glucose, while at 50 g/L the sEPS tended to be more sulfated in *O*-4 position of xylose and glucose. At 32 g/L NaCl, the salinity naturally occurring at Ria Formosa, the salinity has an intermediate effect on the sEPS, closer to the effect of 50 g/L. At this intermediate salinity, *P. purpureum* were able to produce higher amounts of sEPS at a pilot scale (800 L). Moreover, the sulfated galactoxylans have also revealed immunostimulatory effect in B cells *in vitro*, which activity is strongly related in the presence of sulfate esters in their structure. The exploitation of EPS produced by these two microalgae showed a sustainable and economic feasible source of polysaccharides with immunostimulatory activity. They were easily recovered from growth medium and purified by centrifugation and ethanol precipitation, respectively, increasing their commercial viability for functional food and feed applications.

In a world with limited resources, such as clean water or arable land, and increasing anthropogenic pressure on the environment, microalgae such as *Chlorella vulgaris* and

Porphyridium purpureum possess the assets to make them suitable as an efficient carbon-neutral bioresource of food, feed, or multiple molecules that can be co-exploited in the various sectors of food and biotechnology industry. Moreover, the use of microalgae meets the consumers demands for natural healthy foods and supplements with a sustainable production, becoming a “fashioned nutraceutical” and a “future food”.

CHAPTER 5. References

1. V Aishvarya, J Jena, N Pradhan, PK Panda, LB Sukla, Microalgae: Cultivation and Application, In: Sukla LB, Pradhan N, Panda S, Mishra BK, editors. Environmental Microbial Biotechnology Cham: Springer International Publishing; 2015. Page 289–311.
2. G Zuccaro, A Yousuf, A Pollio, J-P Steyer, Microalgae cultivation systems, Microalgae cultivation for biofuels production (2020) 11–29.
3. WG Morais Junior, M Gorgich, PS Corrêa, AA Martins, TM Mata, NS Caetano, Microalgae for biotechnological applications: Cultivation, harvesting and biomass processing, Aquaculture 528(2020) 735562.
4. FX Malcata, IS Pinto, AC Guedes, Marine Macro-and Microalgae: An Overview, CRC Press; 2018.
5. S Hemaiswarya, R Raja, R Ravikumar, IS Carvalho, Microalgae taxonomy and breeding, Biofuel crops: production, physiology and genetics 44(2013) .
6. MC Pina-Pérez, W Brück, T Brück, M Beyrer, Microalgae as healthy ingredients for functional foods, Elsevier; 2019. Page 103-137.
7. MA Borowitzka, Chapter 3 - Biology of Microalgae, In: Levine IA, Fleurence JBT-M in H and DP, editors. Academic Press; 2018. Page 23–72.
8. MDG and GM Guiry, AlgaeBase, National University of Ireland, Galway. 2017. http://www.algaebase.org.
9. W Levasseur, P Perré, V Pozzobon, A review of high value-added molecules production by microalgae in light of the classification, Biotechnology Advances (2020) 107545.
10. C Safi, B Zebib, O Merah, P-Y Pontalier, C Vaca-Garcia, Morphology, composition, production, processing and applications of *Chlorella vulgaris*: A review, Renewable and Sustainable Energy Reviews 35(2014) 265–278.
11. MF de J Raposo, RMSC de Morais, AMM Bernardo de Morais, Bioactivity and applications of sulphated polysaccharides from marine microalgae, Marine drugs 11 (1) (2013) 233–252.
12. RAI Abou-Shanab, M-K Ji, H-C Kim, K-J Paeng, B-H Jeon, Microalgal species growing on piggery wastewater as a valuable candidate for nutrient removal and biodiesel production, Journal of environmental management 115(2013) 257–264.
13. Q Hu, M Sommerfeld, E Jarvis, M Ghirardi, M Posewitz, M Seibert, A Darzins, Microalgal triacylglycerols as feedstocks for biofuel production: perspectives and advances, The plant journal 54 (4) (2008) 621–639.
14. J-P Cadoret, M Garnier, B Saint-Jean, Chapter Eight - Microalgae, Functional Genomics and Biotechnology, In: Piganeau GBT-A in BR, editor. Genomic Insights into the Biology of Algae Academic Press; 2012. Page 285–341.
15. JJ Milledge, Commercial application of microalgae other than as biofuels: a brief review,

Reviews in Environmental Science and Bio/Technology 10 (1) (2011) 31–41.

16. J Sánchez, MD Curt, N Robert, J Fernández, Chapter Two - Biomass Resources, In: Lago C, Caldés N, Lechón YBT-TR of B in the B, editors. Academic Press; 2019. Page 25–111.
17. P Spolaore, C Joannis-Cassan, E Duran, A Isambert, Commercial applications of microalgae, Journal of Bioscience and Bioengineering 101 (2) (2006) 87–96.
18. V Kotrbáček, J Doubek, J Doucha, The chlorococcalean alga *Chlorella* in animal nutrition: a review, Journal of Applied Phycology 27 (6) (2015) 2173–2180.
19. RE Blankenship, DM Tiede, J Barber, GW Brudvig, G Fleming, M Ghirardi, MR Gunner, W Junge, DM Kramer, A Melis, TA Moore, CC Moser, DG Nocera, AJ Nozik, DR Ort, WW Parson, RC Prince, RT Sayre, Comparing Photosynthetic and Photovoltaic Efficiencies and Recognizing the Potential for Improvement, Science 332 (6031) (2011) 805 LP – 809.
20. G Markou, I Angelidaki, D Georgakakis, Microalgal carbohydrates: an overview of the factors influencing carbohydrates production, and of main bioconversion technologies for production of biofuels, Applied microbiology and biotechnology 96 (3) (2012) 631–645.
21. T Cai, SY Park, Y Li, Nutrient recovery from wastewater streams by microalgae: Status and prospects, Renewable and Sustainable Energy Reviews 19(2013) 360–369.
22. MT Ale, M Pinelo, AS Meyer, Assessing Effects and interactions among key variables affecting the growth of mixotrophic microalgae: pH, inoculum volume, and growth medium composition, Preparative Biochemistry and Biotechnology 44 (3) (2014) 242–256.
23. JCM Pires, Mass production of microalgae, In: Handbook of marine microalgae Elsevier; 2015. Page 55–68.
24. V Bhola, F Swalaha, RR Kumar, M Singh, F Bux, Overview of the potential of microalgae for CO_2 sequestration, International Journal of Environmental Science and Technology 11 (7) (2014) 2103–2118.
25. JA Raven, PG Falkowski, Oceanic sinks for atmospheric CO_2, Plant, Cell & Environment 22 (6) (1999) 741–755.
26. AK Vuppaladadiyam, P Prinsen, A Raheem, R Luque, M Zhao, Microalgae cultivation and metabolites production: a comprehensive review, Biofuels, Bioproducts and Biorefining 12 (2) (2018) 304–324.
27. J Singh, RC Saxena, An introduction to microalgae: diversity and significance, In: Handbook of marine microalgae Elsevier; 2015. Page 11–24.
28. J Hu, D Nagarajan, Q Zhang, J-S Chang, D-J Lee, Heterotrophic cultivation of microalgae for pigment production: A review, Biotechnology Advances 36 (1) (2018) 54–67.
29. J Zhan, J Rong, Q Wang, Mixotrophic cultivation, a preferable microalgae cultivation mode for biomass/bioenergy production, and bioremediation, advances and prospect, International

Journal of Hydrogen Energy 42 (12) (2017) 8505–8517.

30. L Brennan, P Owende, Biofuels from microalgae—a review of technologies for production, processing, and extractions of biofuels and co-products, Renewable and sustainable energy reviews 14 (2) (2010) 557–577.
31. R Anyanwu, C Rodriguez, A Durrant, A-G Olabi, Microalgae cultivation technologies, In: Reference Module in Materials Science and Materials Engineering Elsevier BV; 2018.
32. AS Carlsson, JB Van Beilen, R Möller, D Clayton, Micro-and macro-algae: utility for industrial applications, University of York (2007) .
33. MA Borowitzka, Commercial production of microalgae: ponds, tanks, tubes and fermenters, Journal of Biotechnology 70 (1) (1999) 313–321.
34. ME Montingelli, S Tedesco, AG Olabi, Biogas production from algal biomass: A review, Renewable and Sustainable Energy Reviews 43(2015) 961–972.
35. T Matsunaga, H Takeyama, H Miyashita, H Yokouchi, Marine microalgae, In: Marine Biotechnology I Springer; 2005. Page 165–188.
36. MA Chia, AT Lombardi, MGG Melão, Growth and biochemical composition of *Chlorella vulgaris* in different growth media, Anais da Academia Brasileira de Ciências 85(2013) 1427–1438.
37. SP Singh, P Singh, Effect of temperature and light on the growth of algae species: A review, Renewable and Sustainable Energy Reviews 50(2015) 431–444.
38. A Vonshak, Laboratory techniques for the cultivation of microalgae, Handbook of microalgal mass culture (1986) 117–145.
39. JU Grobbelaar, Handbook of microalgal culture: biotechnology and applied phycology, Israel: Wiley-Blackwell (2004) .
40. MI Khan, JH Shin, JD Kim, The promising future of microalgae: current status, challenges, and optimization of a sustainable and renewable industry for biofuels, feed, and other products, Microbial Cell Factories 17 (1) (2018) 36.
41. NO Zhila, GS Kalacheva, TG Volova, Effect of salinity on the biochemical composition of the alga *Botryococcus braunii* Kütz IPPAS H-252, Journal of Applied Phycology 23 (1) (2011) 47–52.
42. I Elenkov, K Stefanov, S Dimitrova-Konaklieva, S Popov, Effect of salinity on lipid composition of *Cladophora vagabunda*, Phytochemistry 42 (1) (1996) 39–44.
43. G Kan, C Shi, X Wang, Q Xie, M Wang, X Wang, J Miao, Acclimatory responses to high-salt stress in *Chlamydomonas* (Chlorophyta, Chlorophyceae) from Antarctica, Acta Oceanologica Sinica 31 (1) (2012) 116–124.
44. AR Rao, C Dayananda, R Sarada, TR Shamala, GA Ravishankar, Effect of salinity on growth

of green alga *Botryococcus braunii* and its constituents, Bioresource Technology 98 (3) (2007) 560–564.

45. S Venkata Mohan, MP Devi, Salinity stress induced lipid synthesis to harness biodiesel during dual mode cultivation of mixotrophic microalgae, Bioresource Technology 165(2014) 288–294.
46. ETY Lee, MJ Bazin, Environmental factors influencing photosynthetic efficiency of the micro red alga *Porphyridium cruentum* (Agardh) Nägeli in light-limited cultures, New phytologist 118 (4) (1991) 513–519.
47. H Ben Hlima, M Dammak, N Karkouch, F Hentati, C Laroche, P Michaud, I Fendri, S Abdelkafi, Optimal cultivation towards enhanced biomass and floridean starch production by *Porphyridium marinum*, International journal of biological macromolecules 129(2019) 152–161.
48. AM Nuutila, A-M Aura, M Kiesvaara, V Kauppinen, The effect of salinity, nitrate concentration, pH and temperature on eicosapentaenoic acid (EPA) production by the red unicellular alga *Porphyridium purpureum*, Journal of biotechnology 55 (1) (1997) 55–63.
49. Z Cohen, A Vonshak, A Richmond, Effect of environmental conditions on fatty acid composition of the red alga *Porphyridium cruentum*: Correlation to growth rate., Journal of Phycology 24 (3) (1988) 328–332.
50. U Karsten, Seaweed acclimation to salinity and desiccation stress, In: Seaweed biology Springer; 2012. Page 87–107.
51. A Richmond, Q Hu, Handbook of microalgal culture: applied phycology and biotechnology, John Wiley & Sons; 2013.
52. R Gilles, A Pequeux, Effect of salinity on the free amino acids pool of the red alga *Porphyridium purpureum* (= *P. cruentum*), Comparative Biochemistry and Physiology Part A: Physiology 57 (1) (1977) 183–185.
53. S Ohta, T Chang, O Aozasa, N Ikegami, H Miyata, Alterations in fatty acid composition of marine red alga *Porphyridium purpureum* by environmental factors, Botanica marina 36 (2) (1993) 103–108.
54. Y-K Lee, H-M Tan, C-S Low, Effect of salinity of medium on cellular fatty acid composition of marine alga *Porphyridium cruentum* (Rhodophyceae), Journal of Applied Phycology 1 (1) (1989) 19–23.
55. S Kathiresan, R Sarada, S Bhattacharya, GA Ravishankar, Culture media optimization for growth and phycoerythrin production from *Porphyridium purpureum*, Biotechnology and bioengineering 96 (3) (2007) 456–463.
56. X Lu, F Nan, J Feng, J Lv, Q Liu, X Liu, S Xie, Effects of Different Environmental Factors

on the Growth and Bioactive Substance Accumulation of *Porphyridium purpureum*, International Journal of Environmental Research and Public Health 17 (7) (2020) 2221.

57. O Pignolet, S Jubeau, C Vaca-Garcia, P Michaud, Highly valuable microalgae: biochemical and topological aspects, Journal of industrial microbiology & biotechnology 40 (8) (2013) 781–796.
58. MA Borowitzka, High-value products from microalgae—their development and commercialisation, Journal of Applied Phycology 25 (3) (2013) 743–756.
59. C Wan, B Chen, X Zhao, F Bai, Current Advances in Biotechnology of Marine Microalgae, Encyclopedia of Marine Biotechnology 3(2020) 1809–1825.
60. SPM Ventura, BP Nobre, F Ertekin, M Hayes, M Garciá-Vaquero, F Vieira, M Koc, L Gouveia, MR Aires-Barros, AMF Palavra, Extraction of value-added compounds from microalgae, In: Microalgae-Based Biofuels and Bioproducts Elsevier; 2017. Page 461–483.
61. AP Abreu, B Fernandes, AA Vicente, J Teixeira, G Dragone, Mixotrophic cultivation of *Chlorella vulgaris* using industrial dairy waste as organic carbon source, Bioresource technology 118(2012) 61–66.
62. I Hamed, The evolution and versatility of microalgal biotechnology: a review, Comprehensive Reviews in Food Science and Food Safety 15 (6) (2016) 1104–1123.
63. A Sahu, I Pancha, D Jain, C Paliwal, T Ghosh, S Patidar, S Bhattacharya, S Mishra, Fatty acids as biomarkers of microalgae, Phytochemistry 89(2013) 53–58.
64. SP Cuellar-Bermudez, I Aguilar-Hernandez, DL Cardenas-Chavez, N Ornelas-Soto, MA Romero-Ogawa, R Parra-Saldivar, Extraction and purification of high-value metabolites from microalgae: essential lipids, astaxanthin and phycobiliproteins, Microbial biotechnology 8 (2) (2015) 190–209.
65. M Piorreck, K-H Baasch, P Pohl, Biomass production, total protein, chlorophylls, lipids and fatty acids of freshwater green and blue-green algae under different nitrogen regimes, Phytochemistry 23 (2) (1984) 207–216.
66. M Asgharpour, B Rodgers, JA Hestekin, Eicosapentaenoic acid from *Porphyridium cruentum*: Increasing growth and productivity of microalgae for pharmaceutical products, Energies 8 (9) (2015) 10487–10503.
67. E Ryckebosch, C Bruneel, K Muylaert, I Foubert, Microalgae as an alternative source of omega-3 long chain polyunsaturated fatty acids, Lipid Technology 24 (6) (2012) 128–130.
68. AP DeFilippis, MJ Blaha, TA Jacobson, Omega-3 Fatty Acids for Cardiovascular Disease Prevention, Current Treatment Options in Cardiovascular Medicine 12 (4) (2010) 365–380.
69. RL Mendes, HL Fernandes, J Coelho, EC Reis, JMS Cabral, JM Novais, AF Palavra, Supercritical CO_2 extraction of carotenoids and other lipids from *Chlorella vulgaris*, Food

Chemistry 53 (1) (1995) 99–103.

70. H Hu, H-F Wang, L-L Ma, X-F Shen, RJ Zeng, Effects of nitrogen and phosphorous stress on the formation of high value LC-PUFAs in *Porphyridium cruentum*, Applied microbiology and biotechnology 102 (13) (2018) 5763–5773.
71. ÂP Matos, R Feller, EHS Moecke, JV de Oliveira, AF Junior, RB Derner, ES Sant'Anna, Chemical characterization of six microalgae with potential utility for food application, Journal of the American Oil Chemists' Society 93 (7) (2016) 963–972.
72. EW Becker, Micro-algae as a source of protein, Biotechnology advances 25 (2) (2007) 207–210.
73. C Safi, M Charton, O Pignolet, F Silvestre, C Vaca-Garcia, P-Y Pontalier, Influence of microalgae cell wall characteristics on protein extractability and determination of nitrogen-to-protein conversion factors, Journal of applied phycology 25 (2) (2013) 523–529.
74. Z Zhang, P Gao, L Guo, Y Wang, Z She, M Gao, Y Zhao, C Jin, G Wang, Elucidating temperature on mixotrophic cultivation of a *Chlorella vulgaris* strain: Different carbon source application and enzyme activity revelation, Bioresource Technology 314(2020) 123721.
75. C Safi, M Charton, O Pignolet, P-Y Pontalier, C Vaca-Garcia, Evaluation of the protein quality of *Porphyridium cruentum*, Journal of applied phycology 25 (2) (2013) 497–501.
76. FAO/WHO/UNU, Energy and protein requirements. Report of the Joint FAO/WHO/UNU Expert Consultation. Technical Report Series No. 724. FAO, WHO and the United Nations University, Geneva, Switzerland., 1985.
77. CECC Ejike, SA Collins, N Balasuriya, AK Swanson, B Mason, CC Udenigwe, Prospects of microalgae proteins in producing peptide-based functional foods for promoting cardiovascular health, Trends in Food Science & Technology 59(2017) 30–36.
78. S Khanra, M Mondal, G Halder, ON Tiwari, K Gayen, TK Bhowmick, Downstream processing of microalgae for pigments, protein and carbohydrate in industrial application: A review, Food and Bioproducts Processing 110(2018) 60–84.
79. HJ Morris, A Almarales, O Carrillo, RC Bermúdez, Utilisation of *Chlorella vulgaris* cell biomass for the production of enzymatic protein hydrolysates, Bioresource technology 99 (16) (2008) 7723–7729.
80. Joint F., Energy and protein requirements: report of a Joint FA, (1985) .
81. E Christaki, E Bonos, P Florou-Paneri, Innovative microalgae pigments as functional ingredients in nutrition, In: Handbook of marine microalgae Elsevier; 2015. Page 233–243.
82. AL Morocho-Jácome, N Ruscinc, RM Martinez, JCM de Carvalho, TS de Almeida, C Rosado, JG Costa, MVR Velasco, AR Baby, (Bio) Technological aspects of microalgae pigments for cosmetics, Applied Microbiology and Biotechnology (2020) 1–10.

83. JL García, M de Vicente, B Galán, Microalgae, old sustainable food and fashion nutraceuticals, Microbial Biotechnology 10 (5) (2017) 1017–1024.
84. F Pagels, D Salvaterra, HM Amaro, AC Guedes, Chapter 18 - Pigments from microalgae, In: Jacob-Lopes E, Maroneze MM, Queiroz MI, Zepka LQBT-H of M-BP and P, editors. Academic Press; 2020. Page 465–492.
85. R Pangestuti, S-K Kim, Biological activities and health benefit effects of natural pigments derived from marine algae, Journal of functional foods 3 (4) (2011) 255–266.
86. JC da Silva, AT Lombardi, Chlorophylls in Microalgae: Occurrence, Distribution, and Biosynthesis, In: Pigments from Microalgae Handbook Springer; 2020. Page 1–18.
87. E Jacob-Lopes, MI Queiroz, LQ Zepka, Pigments from Microalgae Handbook, Springer; 2020.
88. CS Grant, JW Louda, Microalgal pigment ratios in relation to light intensity: implications for chemotaxonomy, Aquatic Biology 11 (2) (2010) 127–138.
89. V Hynstova, D Sterbova, B Klejdus, J Hedbavny, D Huska, V Adam, Separation, identification and quantification of carotenoids and chlorophylls in dietary supplements containing *Chlorella vulgaris* and *Spirulina platensis* using High Performance Thin Layer Chromatography, Journal of Pharmaceutical and Biomedical Analysis 148(2018) 108–118.
90. S-C Shen, H-Y Hsu, C-N Huang, JS-B Wu, Color loss in ethanolic solutions of chlorophyll a, Journal of agricultural and food chemistry 58 (13) (2010) 8056–8060.
91. W Kong, N Liu, J Zhang, Q Yang, S Hua, H Song, C Xia, Optimization of ultrasound-assisted extraction parameters of chlorophyll from *Chlorella vulgaris* residue after lipid separation using response surface methodology, Journal of food science and technology 51 (9) (2014) 2006–2013.
92. SC Silva, ICFR Ferreira, MM Dias, MF Barreiro, Microalgae-Derived Pigments: A 10-Year Bibliometric Review and Industry and Market Trend Analysis, Molecules 25 (15) (2020) 3406.
93. H Begum, FMD Yusoff, S Banerjee, H Khatoon, M Shariff, Availability and utilization of pigments from microalgae, Critical reviews in food science and nutrition 56 (13) (2016) 2209–2222.
94. N Koca, F Karadeniz, HS Burdurlu, Effect of pH on chlorophyll degradation and colour loss in blanched green peas, Food Chemistry 100 (2) (2007) 609–615.
95. AA Ryan, MO Senge, How green is green chemistry? Chlorophylls as a bioresource from biorefineries and their commercial potential in medicine and photovoltaics, Photochemical & Photobiological Sciences 14 (4) (2015) 638–660.
96. TJ Mangos, RG Berger, Determination of major chlorophyll degradation products, Zeitschrift

für Lebensmitteluntersuchung und -Forschung A 204 (5) (1997) 345–350.

97. Y Zheng, J Shi, Z Pan, Y Cheng, Y Zhang, N Li, Effect of heat treatment, pH, sugar concentration, and metal ion addition on green color retention in homogenized puree of Thompson seedless grape, LWT-Food Science and Technology 55 (2) (2014) 595–603.
98. P Nisha, RS Singhal, AB Pandit, A study on the degradation kinetics of visual green colour in spinach (*Spinacea oleracea L.*) and the effect of salt therein, Journal of food engineering 64 (1) (2004) 135–142.
99. MG Bellomo, B Fallico, G Muratore, Stability of pigments and oil in pistachio kernels during storage, International journal of food science & technology 44 (12) (2009) 2358–2364.
100. FM Clydesdale, FJ Francis, Chlorophyll changes in thermally processed spinach as influenced by enzyme conversion and pH adjustment, Food Technology 22 (6) (1968) 135-+.
101. MF Salama, HA Moharram, Relationship between colour improvement and metallo-chlorophyll complexes during blanching of peas and broccoli, Alexandria Journal for Food Science and Technology 4 (1) (2007) .
102. SG Rudra, BC Sarkar, US Shivhare, Thermal degradation kinetics of chlorophyll in pureed coriander leaves, Food and Bioprocess Technology 1 (1) (2008) 91–99.
103. PW Araujo, RG Brereton, Stability studies of chlorophyll a using different storage systems, In: Analytical Proceedings including Analytical Communications The Royal Society of Chemistry; 1995. Page 415–417.
104. CD 95/45/EC., Laying down specific purity criteria concerning colours for use in foodstuffs, Official Journal of the European Community 226(1995) 19.
105. K Solymosi, B Mysliwa-Kurdziel, Chlorophylls and their derivatives used in food industry and medicine, Mini reviews in medicinal chemistry 17 (13) (2017) 1194–1222.
106. S Jurić, M Jurić, Ż Król-Kilińska, K Vlahoviček-Kahlina, M Vinceković, V Dragović-Uzelac, F Donsì, Sources, stability, encapsulation and application of natural pigments in foods, Food Reviews International (2020) 1–56.
107. MG Ferruzzi, J Blakeslee, Digestion, absorption, and cancer preventative activity of dietary chlorophyll derivatives, Nutrition Research 27 (1) (2007) 1–12.
108. KJM Mulders, PP Lamers, DE Martens, RH Wijffels, Phototrophic pigment production with microalgae: biological constraints and opportunities, Journal of phycology 50 (2) (2014) 229–242.
109. J Seyfabadi, Z Ramezanpour, ZA Khoeyi, Protein, fatty acid, and pigment content of *Chlorella vulgaris* under different light regimes, Journal of applied phycology 23 (4) (2011) 721–726.
110. K Miazek, S Ledakowicz, Chlorophyll extraction from leaves, needles and microalgae: A

kinetic approach, International Journal of Agricultural and Biological Engineering 6 (2) (2013) 107–115.

111. S Kulkarni, Z Nikolov, Process for selective extraction of pigments and functional proteins from *Chlorella vulgaris*, Algal research 35(2018) 185–193.
112. H Safafar, P Uldall Nørregaard, A Ljubic, P Møller, S Løvstad Holdt, C Jacobsen, Enhancement of protein and pigment content in two *Chlorella* species cultivated on industrial process water, Journal of Marine Science and Engineering 4 (4) (2016) 84.
113. C Safi, S Camy, C Frances, MM Varela, EC Badia, P-Y Pontalier, C Vaca-Garcia, Extraction of lipids and pigments of *Chlorella vulgaris* by supercritical carbon dioxide: influence of bead milling on extraction performance, Journal of applied phycology 26 (4) (2014) 1711–1718.
114. L Schüler, E Greque de Morais, M Trovão, A Machado, B Carvalho, M Carneiro, I Maia, M Soares, P Duarte, A Barros, H Pereira, J Silva, J Varela, Isolation and Characterization of Novel *Chlorella Vulgaris* Mutants With Low Chlorophyll and Improved Protein Contents for Food Applications, Frontiers in bioengineering and biotechnology 8(2020) 469.
115. M Gong, A Bassi, Investigation of Chlorella vulgaris UTEX 265 cultivation under light and low temperature stressed conditions for lutein production in flasks and the coiled tree photo-bioreactor (CTPBR), Applied biochemistry and biotechnology 183 (2) (2017) 652–671.
116. KH Cha, HJ Lee, SY Koo, D-G Song, D-U Lee, C-H Pan, Optimization of pressurized liquid extraction of carotenoids and chlorophylls from *Chlorella vulgaris*, Journal of agricultural and food chemistry 58 (2) (2010) 793–797.
117. J Kim, M Kim, S Lee, E Jin, Development of a *Chlorella vulgaris* mutant by chemical mutagenesis as a producer for natural violaxanthin, Algal Research 46(2020) 101790.
118. L Gouveia, G Choubert, N Pereira, J Santinha, J Empis, E Gomes, Pigmentation of gilthead seabream, Sparus aurata (L. 1875), using *Chlorella vulgaris* (Chlorophyta, Volvocales) microalga, Aquaculture Research 33 (12) (2002) 987–993.
119. JA Del Campo, M García-González, MG Guerrero, Outdoor cultivation of microalgae for carotenoid production: current state and perspectives, Applied microbiology and biotechnology 74 (6) (2007) 1163–1174.
120. H Safafar, J Van Wagenen, P Møller, C Jacobsen, Carotenoids, phenolic compounds and tocopherols contribute to the antioxidative properties of some microalgae species grown on industrial wastewater, Marine drugs 13 (12) (2015) 7339–7356.
121. S Takaichi, Carotenoids in Phototrophic Microalgae: Distributions and Biosynthesis, Pigments from Microalgae Handbook (2020) 19–41.
122. A Juneja, RM Ceballos, GS Murthy, Effects of environmental factors and nutrient availability on the biochemical composition of algae for biofuels production: a review, Energies 6 (9)

(2013) 4607–4638.

123. MF de Jesus Raposo, RMSC de Morais, AMMB de Morais, Health applications of bioactive compounds from marine microalgae, Life sciences 93 (15) (2013) 479–486.
124. AC Guedes, HM Amaro, FX Malcata, Microalgae as sources of carotenoids, Marine drugs 9 (4) (2011) 625–644.
125. E Christaki, E Bonos, I Giannenas, P Florou-Paneri, Functional properties of carotenoids originating from algae, Journal of the Science of Food and Agriculture 93 (1) (2013) 5–11.
126. F Pagels, AC Guedes, HM Amaro, A Kijjoa, V Vasconcelos, Phycobiliproteins from cyanobacteria: Chemistry and biotechnological applications, Biotechnology advances 37 (3) (2019) 422–443.
127. VK Kannaujiya, PR Singh, D Kumar, RP Sinha, Phycobiliproteins in Microalgae: Occurrence, Distribution, and Biosynthesis, In: Pigments from Microalgae Handbook Springer; 2020. Page 43–68.
128. SM Arad, A Yaron, Natural pigments from red microalgae for use in foods and cosmetics, Trends in Food Science & Technology 3(1992) 92–97.
129. Z Yaakob, E Ali, A Zainal, M Mohamad, MS Takriff, An overview: biomolecules from microalgae for animal feed and aquaculture, Journal of Biological Research-Thessaloniki 21 (1) (2014) 6.
130. TMM Bernaerts, L Gheysen, I Foubert, ME Hendrickx, AM Van Loey, The potential of microalgae and their biopolymers as structuring ingredients in food: a review, Biotechnology advances 37 (8) (2019) 107419.
131. R De Philippis, C Sili, M Vincenzini, Glycogen and poly-β-hydroxybutyrate synthesis in *Spirulina maxima*, Microbiology 138 (8) (1992) 1623–1628.
132. SM Myklestad, Production, chemical structure, metabolism, and biological function of the (1→ 3)-linked, β3-D-glucans in diatoms, Biological oceanography 6 (3–4) (1989) 313–326.
133. E Suzuki, M Onoda, C Colleoni, S Ball, N Fujita, Y Nakamura, Physicochemical variation of cyanobacterial starch, the insoluble α-glucans in cyanobacteria, Plant and cell physiology 54 (4) (2013) 465–473.
134. A Buléon, P Colonna, V Planchot, S Ball, Starch granules: structure and biosynthesis, International journal of biological macromolecules 23 (2) (1998) 85–112.
135. Y Nakamura, J Takahashi, A Sakurai, Y Inaba, E Suzuki, S Nihei, S Fujiwara, M Tsuzuki, H Miyashita, H Ikemoto, Some cyanobacteria synthesize semi-amylopectin type α-polyglucans instead of glycogen, Plant and cell physiology 46 (3) (2005) 539–545.
136. D Dauvillée, P Deschamps, J-P Ral, C Plancke, J-L Putaux, J Devassine, A Durand-Terrasson, A Devin, SG Ball, Genetic dissection of floridean starch synthesis in the cytosol of the model

dinoflagellate *Crypthecodinium cohnii*, Proceedings of the National Academy of Sciences 106 (50) (2009) 21126–21130.

137. S Kottuparambil, RL Thankamony, S Agusti, *Euglena* as a potential natural source of value-added metabolites. A review, Algal Research 37(2019) 154–159.
138. F Wang, B Gao, C Dai, M Su, C Zhang, Comprehensive utilization of the filamentous oleaginous microalga *Tribonema utriculosum* for the production of lipids and chrysolaminarin in a biorefinery concept, Algal Research 50(2020) 101973.
139. E Suzuki, R Suzuki, Variation of storage polysaccharides in phototrophic microorganisms, Journal of applied glycoscience 60 (1) (2013) 21–27.
140. RG Sheath, JA Hellebust, T Sawa, Floridean starch metabolism of *Porphyridium purpureum* (Rhodophyta) I. Changes during ageing of batch culture, Phycologia 18 (2) (1979) 149–163.
141. HG Gerken, B Donohoe, EP Knoshaug, Enzymatic cell wall degradation of *Chlorella vulgaris* and other microalgae for biofuels production, Planta (2013) .
142. AM Abo-Shady, YA Mohamed, T Lasheen, Chemical composition of the cell wall in some green algae species, Biologia Plantarum 35 (4) (1993) 629–632.
143. MF de Jesus Raposo, AMB de Morais, RMSC de Morais, Marine polysaccharides from algae with potential biomedical applications, Marine drugs 13 (5) (2015) 2967–3028.
144. JW de Leeuw, GJM Versteegh, PF van Bergen, Biomacromolecules of algae and plants and their fossil analogues, Plant Ecology 182 (1) (2006) 209–233.
145. H Takeda, Sugar composition of the cell wall and the taxonomy of *Chlorella* (Chlorophyceae), Journal of Phycology 27 (2) (1991) 224–232.
146. E Kapaun, W Reisser, A chitin-like glycan in the cell wall of a *Chlorella* sp. (Chlorococcales, Chlorophyceae), 25(1995) 577–582.
147. H Takeda, Chemical composition of cell walls as a taxonomical marker, Journal of plant research 106 (3) (1993) 195–200.
148. K Ogawa, Y Ikeda, S Kondo, A new trisaccharide, α-d-glucopyranuronosyl-(1→ 3)-α-l-rhamnopyranosyl-(1→ 2)-α-l-rhamnopyranose from *Chlorella vulgaris*, Carbohydrate research 321 (1) (1999) 128–131.
149. K Ogawa, M Arai, H Naganawa, Y Ikeda, S Kondo, A New β-D-Galactan Having 3-*O*-Methyl-D-galactose from *Chlorella vulgaris*, Journal of Applied Glycoscience 48 (4) (2001) 325–330.
150. S Pieper, I Unterieser, F Mann, P Mischnick, A new arabinomannan from the cell wall of the chlorococcal algae *Chlorella vulgaris*, Carbohydrate Research (2012) .
151. SM Arad, O Levy-Ontman, Red microalgal cell-wall polysaccharides: biotechnological aspects, Current opinion in biotechnology 21 (3) (2010) 358–364.

152. RP Shrestha, Y Weinstein, D Bar-Zvi, SM Arad, A Glycoprotein noncovalently associated with cell-wall polysaccharide of the red microalga *Porphyridium* sp.(Rhodophyta), Journal of phycology 40 (3) (2004) 568–580.
153. R Balti, R Le Balc'h, N Brodu, M Gilbert, B Le Gouic, S Le Gall, C Sinquin, A Massé, Concentration and purification of *Porphyridium cruentum* exopolysaccharides by membrane filtration at various cross-flow velocities, Process Biochemistry 74(2018) 175–184.
154. C Delattre, G Pierre, C Laroche, P Michaud, Production, extraction and characterization of microalgal and cyanobacterial exopolysaccharides, Biotechnology Advances 34 (7) (2016) 1159–1179.
155. L Trabelsi, H Ben Ouada, F Zili, N Mazhoud, J Ammar, Evaluation of *Arthrospira platensis* extracellular polymeric substances production in photoautotrophic, heterotrophic and mixotrophic conditions, Folia microbiologica 58 (1) (2013) 39–45.
156. S-Y Li, Y Shabtai, S Arad, Production and composition of the sulphated cell wall polysaccharide of *Porphyridium* (Rhodophyta) as affected by CO_2 concentration, Phycologia 39 (4) (2000) 332–336.
157. S-I Han, MS Jeon, YM Heo, S Kim, Y-E Choi, Effect of *Pseudoalteromonas* sp. MEBiC 03485 on biomass production and sulfated polysaccharide biosynthesis in *Porphyridium cruentum* UTEX 161, Bioresource Technology 302(2020) 122791.
158. A Mishra, B Jha, Isolation and characterization of extracellular polymeric substances from micro-algae *Dunaliella salina* under salt stress, Bioresource technology 100 (13) (2009) 3382–3386.
159. S Geresh, SM Arad, O Levy-Ontman, W Zhang, Y Tekoah, R Glaser, Isolation and characterization of poly-and oligosaccharides from the red microalga *Porphyridium* sp., Carbohydrate research 344 (3) (2009) 343–349.
160. V Gloaguen, G Ruiz, H Morvan, A Mouradi-Givernaud, E Maes, P Krausz, G Strecker, The extracellular polysaccharide of *Porphyridium* sp.: an NMR study of lithium-resistant oligosaccharidic fragments, Carbohydrate Research 339 (1) (2004) 97–103.
161. AK Patel, C Laroche, A Marcati, AV Ursu, S Jubeau, L Marchal, E Petit, G Djelveh, P Michaud, Separation and fractionation of exopolysaccharides from *Porphyridium cruentum*, Bioresource technology 145(2013) 345–350.
162. I Dvir, R Chayoth, U Sod-Moriah, S Shany, A Nyska, AH Stark, Z Madar, SM Arad, Soluble polysaccharide and biomass of red microalga *Porphyridium* sp. alter intestinal morphology and reduce serum cholesterol in rats, British journal of Nutrition 84 (04) (2000) 469–476.
163. S Geresh, O Dubinsky, SM Arad, D Christiaen, R Glaser, Structure of 3-*O*-(α-D-glucopyranosyluronic acid)-L-galactopyranose, an aldobiouronic acid isolated from the

polysaccharides of various unicellular red algae, Carbohydrate research 208(1990) 301–305.

164. TMM Bernaerts, L Gheysen, C Kyomugasho, Z Jamsazzadeh Kermani, S Vandionant, I Foubert, ME Hendrickx, AM Van Loey, Comparison of microalgal biomasses as functional food ingredients: Focus on the composition of cell wall related polysaccharides, Algal Research (2018) .
165. K Noda, N Ohno, K Tanaka, N Kamiya, M Okuda, T Yadomae, K Nomoto, Y Shoyama, A water-soluble antitumor glycoprotein from *Chlorella vulgaris*, Planta medica 62 (05) (1996) 423–426.
166. P Capek, M Matulová, M Šutovská, J Barboríková, M Molitorisová, I Kazimierová, *Chlorella vulgaris* α-L-arabino-α-L-rhamno-α,β-D-galactan structure and mechanisms of its anti-inflammatory and anti-remodelling effects, International Journal of Biological Macromolecules 162(2020) 188–198.
167. MS Matsui, N Muizzuddin, S Arad, K Marenus, Sulfated polysaccharides from red microalgae have antiinflammatory properties *in vitro* and *in vivo*, Applied biochemistry and biotechnology 104 (1) (2003) 13–22.
168. H Li, F Ding, L Xiao, R Shi, H Wang, W Han, Z Huang, Food-Derived Antioxidant Polysaccharides and Their Pharmacological Potential in Neurodegenerative Diseases, Nutrients 9 (7) (2017) 778.
169. J Barboríková, M Šutovská, I Kazimierová, M Jošková, S Fraňová, J Kopecký, P Capek, Extracellular polysaccharide produced by *Chlorella vulgaris* – Chemical characterization and anti-asthmatic profile, International Journal of Biological Macromolecules 135(2019) 1–11.
170. J Zhang, L Liu, F Chen, Production and characterization of exopolysaccharides from *Chlorella zofingiensis* and *Chlorella vulgaris* with anti-colorectal cancer activity, International Journal of Biological Macromolecules 134(2019) 976–983.
171. M Yu, M Chen, J Gui, S Huang, Y Liu, H Shentu, J He, Z Fang, W Wang, Y Zhang, Preparation of *Chlorella vulgaris* polysaccharides and their antioxidant activity *in vitro* and *in vivo*, International journal of biological macromolecules 137(2019) 139–150.
172. M Tabarsa, I-S Shin, JH Lee, U Surayot, W Park, S You, An immune-enhancing water-soluble α-glucan from *Chlorella vulgaris* and structural characteristics, Food Sci Biotechnol 24 (6) (2015) 1933–1941.
173. S Mirzaie, M Tabarsa, M Safavi, Effects of extracted polysaccharides from a *Chlorella vulgaris* biomass on expression of interferon-γ and interleukin-2 in chicken peripheral blood mononuclear cells, Journal of Applied Phycology (2020) .
174. J Huang, L Liu, Y Yu, W Lin, B Chen, M Li, X Rao, Reduction in the Blood Glucose Level of Exopolysaccharide of *Porphyridium cruentum* in Alloxan-induced Diabetic Mice, Journal

of Fujian Normal University (Natural Science Edition) 3(2006) .

175. MF de Jesus Raposo, AMMB de Morais, RMSC de Morais, Influence of sulphate on the composition and antibacterial and antiviral properties of the exopolysaccharide from *Porphyridium cruentum*, Life sciences 101 (1) (2014) 56–63.

176. J Fábregas, D Garcıa, M Fernandez-Alonso, AI Rocha, P Gomez-Puertas, JM Escribano, A Otero, JM Coll, *In vitro* inhibition of the replication of haemorrhagic septicaemia virus (VHSV) and African swine fever virus (ASFV) by extracts from marine microalgae, Antiviral research 44 (1) (1999) 67–73.

177. M Huheihel, V Ishanu, J Tal, SM Arad, Activity of *Porphyridium* sp. polysaccharide against herpes simplex viruses *in vitro* and *in vivo*, Journal of Biochemical and Biophysical methods 50 (2) (2002) 189–200.

178. A Radonić, S Thulke, J Achenbach, A Kurth, A Vreemann, T König, C Walter, K Possinger, A Nitsche, Anionic polysaccharides from phototrophic microorganisms exhibit antiviral activities to *Vaccinia* virus, (2011) .

179. J Huang, B Chen, W You, Studies on separation of extracellular polysaccharide from *Porphyridium cruentum* and its anti-HBV activity *in vitro*, Chinese Journal of Marine Drugs (05) (2001) .

180. L Sun, C Wang, Q Shi, C Ma, Preparation of different molecular weight polysaccharides from *Porphyridium cruentum* and their antioxidant activities, International Journal of Biological Macromolecules 45 (1) (2009) 42–47.

181. E Gardeva, R Toshkova, K Minkova, L Gigova, Cancer protective action of polysaccharide, derived from red microalga *Porphyridium cruentum*—a biological background, Biotechnology & Biotechnological Equipment 23 (sup1) (2009) 783–787.

182. E Gardeva, R Toshkova, L Yossifova, K Minkova, L Gigova, Cytotoxic and apoptogenic potential of red microalgal polysaccharides, Biotechnology & Biotechnological Equipment 26 (4) (2012) 3167–3172.

183. L Sun, L Wang, Y Zhou, Immunomodulation and antitumor activities of different-molecular-weight polysaccharides from *Porphyridium cruentum*, Carbohydrate Polymers 87 (2) (2012) 1206–1210.

184. RT Abdala-Díaz, M Chabrillón, A Cabello-Pasini, B López-Soler, FL Figueroa, Effect of *Porphyridium cruentum* polysaccharides on the activity of murine macrophage cell line RAW 264.7, Ciencias Marinas 36 (4) (2010) 345–353.

185. R Toshkova, E Gardeva, K Minkova, T Panova, E Zvetkova, Immunopotential and Mitogenic Properties of Marine Microalgal Polysaccharides Extracted from *Porphyridium Cruentum* and *Dixoniella Grisea* (Rhodophyta), comptes rendus de l'Academie bulgare des Sciences 62

(5) (2009) .

186. SS Ferreira, CP Passos, P Madureira, M Vilanova, MA Coimbra, Structure–function relationships of immunostimulatory polysaccharides: A review, Carbohydrate polymers 132(2015) 378–396.
187. AO Tzianabos, Polysaccharide immunomodulators as therapeutic agents: structural aspects and biologic function, Clinical microbiology reviews 13 (4) (2000) 523–533.
188. F Konishi, K Tanaka, S Kumamoto, T Hasegawa, M Okuda, I Yano, Y Yoshikai, K Nomoto, Enhanced resistance against *Escherichia coli* infection by subcutaneous administration of the hot-water extract of *Chlorella vulgaris* in cyclophosphamide-treated mice, Cancer Immunology, Immunotherapy 32 (1) (1990) 1–7.
189. K Tanaka, T Koga, F Konishi, M Nakamura, M Mitsuyama, K Himeno, K Nomoto, Augmentation of host defense by a unicellular green alga, *Chlorella vulgaris*, to *Escherichia coli* infection., Infection and immunity 53 (2) (1986) 267–271.
190. T Hasegawa, M Okuda, K Nomoto, Y Yoshikai, Augmentation of the Resistance Against *Listeria Monocytogenes* by Oral Administration of A Hot Water Extract of *Chlorella Vulgaris* in Mice, Immunopharmacology and immunotoxicology 16 (2) (1994) 191–202.
191. K Ibusuki, Y Minamishima, Effect of *Chlorella vulgaris* extracts on murine cytomegalovirus infections., Natural immunity and cell growth regulation 9 (2) (1989) 121–128.
192. C Qingman, L Wenxue, Z Wenhao, Y Chunying, Effects of *Chlorella vulgaris* on Immuno-Related Factors and their Expression in Penaeus vannamei, (2019) .
193. J Qi, SM Kim, Effects of the molecular weight and protein and sulfate content of *Chlorella ellipsoidea* polysaccharides on their immunomodulatory activity, International Journal of Biological Macromolecules 107(2018) 70–77.
194. F Chen, G Huang, Preparation and immunological activity of polysaccharides and their derivatives, International Journal of Biological Macromolecules 112(2018) 211–216.
195. W Zhao, H-H Fang, B-Y Gao, C-M Dai, Z-Z Liu, C-W Zhang, J Niu, Dietary *Tribonema* sp. supplementation increased growth performance, antioxidant capacity, immunity and improved hepatic health in golden pompano (*Trachinotus ovatus*), Aquaculture 529(2020) 735667.
196. M Brown, R Robert, Preparation and assessment of microalgal concentrates as feeds for larval and juvenile Pacific oyster (*Crassostrea gigas*), Aquaculture 207 (3) (2002) 289–309.
197. WF Carneiro, TFD Castro, TM Orlando, F Meurer, DA de Jesus Paula, B do CR Virote, AR da CB Vianna, LDS Murgas, Replacing fish meal by *Chlorella* sp. meal: Effects on zebrafish growth, reproductive performance, biochemical parameters and digestive enzymes, Aquaculture (2020) 735612.

198. A Aslam, T Fazal, Q uz Zaman, A Shan, F Rehman, J Iqbal, N Rashid, MSU Rehman, Biorefinery of Microalgae for Nonfuel Products, In: Microalgae Cultivation for Biofuels Production Elsevier; 2020. Page 197–209.
199. J Paniagua-Michel, Chapter 16 - Microalgal Nutraceuticals, In: Kim S-KBT-H of MM, editor. Boston: Academic Press; 2015. Page 255–267.
200. G Dineshbabu, G Goswami, R Kumar, A Sinha, D Das, Microalgae–nutritious, sustainable aqua-and animal feed source, Journal of functional foods 62(2019) 103545.
201. V Patil, T Källqvist, E Olsen, G Vogt, HR Gislerød, Fatty acid composition of 12 microalgae for possible use in aquaculture feed, Aquaculture International 15 (1) (2007) 1–9.
202. S Hemaiswarya, R Raja, RR Kumar, V Ganesan, C Anbazhagan, Microalgae: a sustainable feed source for aquaculture, World Journal of Microbiology and Biotechnology 27 (8) (2011) 1737–1746.
203. MT Ahmad, M Shariff, F Md. Yusoff, YM Goh, S Banerjee, Applications of microalga *Chlorella vulgaris* in aquaculture, Reviews in Aquaculture 12 (1) (2020) 328–346.
204. Y Torres-Tiji, FJ Fields, SP Mayfield, Microalgae as a future food source, Biotechnology Advances 41(2020) 107536.
205. FDA, U.S. Food and Drug Administration, 2020. Web page https://www.fda.gov/.
206. EFSA, European Food Safety Authority, 2021. Web page https://www.efsa.europa.eu/en
207. NF and FA (NDA) EFSA Panel on Nutrition, D Turck, J Castenmiller, S De Henauw, KI Hirsch-Ernst, J Kearney, A Maciuk, I Mangelsdorf, HJ McArdle, A Naska, Safety of Schizochytrium sp. oil as a novel food pursuant to Regulation (EU) 2015/2283 (a), EFSA Journal 18 (10) (2020) e06242.
208. NF and FA (NDA) EFSA Panel on Nutrition, D Turck, J Castenmiller, S de Henauw, KI Hirsch-Ernst, J Kearney, A Maciuk, I Mangelsdorf, HJ McArdle, A Naska, Safety of astaxanthin for its use as a novel food in food supplements, EFSA Journal 18 (2) (2020) e05993.
209. C Enzing, M Ploeg, M Barbosa, L Sijtsma, Microalgae-based products for the food and feed sector: an outlook for Europe, JRC Scientific and policy reports (2014) 19–37.
210. M Fradique, AP Batista, MC Nunes, L Gouveia, NM Bandarra, A Raymundo, Incorporation of *Chlorella vulgari*s and *Spirulina maxim*a biomass in pasta products. Part 1: Preparation and evaluation, Journal of the Science of Food and Agriculture 90 (10) (2010) 1656–1664.
211. H Beheshtipour, AM Mortazavian, R Mohammadi, S Sohrabvandi, K Khosravi-Darani, Supplementation of *Spirulina platensi*s and *Chlorella vulgaris* algae into probiotic fermented milks, Comprehensive Reviews in Food Science and Food Safety 12 (2) (2013) 144–154.
212. MP Caporgno, A Mathys, Trends in Microalgae Incorporation Into Innovative Food Products

With Potential Health Benefits, Frontiers in Nutrition (2018) .

213. A Barros, H Pereira, J Campos, A Marques, J Varela, J Silva, Heterotrophy as a tool to overcome the long and costly autotrophic scale-up process for large scale production of microalgae, Scientific reports 9 (1) (2019) 1–7.
214. AR Wellburn, The spectral determination of chlorophylls a and b, as well as total carotenoids, using various solvents with spectrophotometers of different resolution, Journal of plant physiology 144 (3) (1994) 307–313.
215. HKBT-M in E Lichtenthaler, [34] Chlorophylls and carotenoids: Pigments of photosynthetic biomembranes, In: Plant Cell Membranes Academic Press; 1987. Page 350–382.
216. HK Lichtenthaler, C Buschmann, Chlorophylls and carotenoids: Measurement and characterization by UV-VIS spectroscopy, Current protocols in food analytical chemistry 1 (1) (2001) F4-3.
217. VMR Martins, J Simões, I Ferreira, MT Cruz, MR Domingues, MA Coimbra, *In vitro* macrophage nitric oxide production by *Pterospartum tridentatum* (L.) Willk. inflorescence polysaccharides, Carbohydrate Polymers 157(2017) 176–184.
218. C Nunes, JA Saraiva, MA Coimbra, Effect of candying on cell wall polysaccharides of plums (*Prunus domestica L.*) and influence of cell wall enzymes, Food Chemistry 111 (3) (2008) 538–548.
219. M Ucko, E Cohen, H Gordin, SM Arad, Relationship between the unicellular red alga *Porphyridium* sp. and its predator, the dinoflagellate *Gymnodinium* sp, Applied and environmental microbiology 55 (11) (1989) 2990–2994.
220. MJ Griffiths, C Garcin, RP van Hille, STL Harrison, Interference by pigment in the estimation of microalgal biomass concentration by optical density, Journal of Microbiological Methods 85 (2) (2011) 119–123.
221. S Liu, How cells grow, In: Bioprocess Engineering: Kinetics, Sustainability, and Reactor Design Third edit. Elsevier B.V.; 2020. Page 549.
222. SO Lourenço, E Barbarino, PL Lavín, UM Lanfer Marquez, E Aidar, Distribution of intracellular nitrogen in marine microalgae: calculation of new nitrogen-to-protein conversion factors, European Journal of Phycology 39 (1) (2004) 17–32.
223. RI Krohn, The colorimetric detection and quantitation of total protein, Current Protocols in Toxicology 23 (1) (2005) A-3I.
224. SMA Kawsar, Y Fujii, R Matsumoto, H Yasumitsu, Y Ozeki, Protein R-phycoerythrin from marine red alga *Amphiroa anceps*: extraction, purification and characterization, Phytologia Balcanica 17 (3) (2011) 347–354.
225. LA Marzilli, TR Golden, RJ Cotter, AS Woods, Peptide Sequence Information Derived by

Pronase Digestion and Ammonium Sulfate In-Source Decay Matrix-Assisted Laser, Journal of American Aociety for Mass Spectrometry 11 (00) (2000) 1000–1008.

226. M Ribeiro, FM Nunes, S Guedes, P Domingues, AM Silva, JM Carrillo, M Rodriguez-Quijano, G Branlard, G Igrejas, Efficient chemo-enzymatic gluten detoxification: reducing toxic epitopes for celiac patients improving functional properties, Scientific Reports 5(2015) 18041.
227. Y Qiu, M Su, Y Liu, M Chen, J Gu, J Zhang, W Jia, Application of ethyl chloroformate derivatization for gas chromatography-mass spectrometry based metabonomic profiling, Analytica Chimica Acta 583 (2) (2007) 277–283.
228. H Wu, X Miao, Biodiesel quality and biochemical changes of microalgae *Chlorella pyrenoidosa* and *Scenedesmus obliquus* in response to nitrate levels, Bioresource technology 170(2014) 421–427.
229. S Aued-Pimentel, JHG Lago, MH Chaves, EE Kumagai, Evaluation of a methylation procedure to determine cyclopropenoids fatty acids from *Sterculia striata* St. Hil. Et Nauds seed oil, Journal of Chromatography A 1054 (1) (2004) 235–239.
230. CP Passos, RM Silva, FA Da Silva, MA Coimbra, CM Silva, Supercritical fluid extraction of grape seed (*Vitis vinifera* L.) oil. Effect of the operating conditions upon oil composition and antioxidant capacity, Chemical Engineering Journal 160 (2) (2010) 634–640.
231. KS Dodgson, RG Price, A note on the determination of the ester sulphate content of sulphated polysaccharides, Biochemical Journal 84 (1) (1962) 106.
232. KS Dodgson, Determination of inorganic sulphate in studies on the enzymic and non-enzymic hydrolysis of carbohydrate and other sulphate esters, Biochemical Journal 78 (2) (1961) 312.
233. MA Coimbra, KW Waldron, RR Selvendran, Isolation and characterisation of cell wall polymers from olive pulp (*Olea europaea* L.), Carbohydrate Research 252(1994) 245–262.
234. RR Selvendran, JF March, SG Ring, Determination of aldoses and uronic acid content of vegetable fiber, Analytical biochemistry 96 (2) (1979) 282–292.
235. GR Lopes, AS Ferreira, M Pinto, CP Passos, E Coelho, C Rodrigues, C Figueira, SM Rocha, FM Nunes, MA Coimbra, Carbohydrate content, dietary fibre and melanoidins: Composition of espresso from single-dose coffee capsules, Food Research International 89(2016) 989–996.
236. I Ciucanu, F Kerek, A simple and rapid method for the permethylation of carbohydrates, Carbohydrate research 131 (2) (1984) 209–217.
237. C Oliveira, AS Ferreira, R Novoa-Carballal, C Nunes, I Pashkuleva, NM Neves, MA Coimbra, RL Reis, A Martins, TH Silva, The key role of sulfation and branching on fucoidan antitumor activity, Macromolecular bioscience 17 (5) (2017) 1600340.
238. M Martin-Pastor, AS Ferreira, X Moppert, C Nunes, MA Coimbra, RL Reis, J Guezennec, R

Novoa-Carballal, Structure, rheology, and copper-complexation of a hyaluronan-like exopolysaccharide from *Vibrio*, Carbohydrate Polymers (2019) 114999.

239. IJ Miller, JW Blunt, Desulfation of algal galactans, Carbohydrate research 309 (1) (1998) 39–43.
240. B Fernandes, G Dragone, AP Abreu, P Geada, J Teixeira, A Vicente, Starch determination in *Chlorella vulgaris*—a comparison between acid and enzymatic methods, Journal of applied phycology 24 (5) (2012) 1203–1208.
241. DJ Jenkins, TM Wolever, RH Taylor, H Barker, H Fielden, JM Baldwin, AC Bowling, HC Newman, AL Jenkins, D V Goff, Glycemic index of foods: a physiological basis for carbohydrate exchange., The American journal of clinical nutrition 34 (3) (1981) 362–366.
242. I Goñi, A Garcia-Alonso, F Saura-Calixto, A starch hydrolysis procedure to estimate glycemic index, Nutrition Research 17 (3) (1997) 427–437.
243. ER De Marco, ME Steffolani, CS Martínez, AE León, Effects of *spirulina* biomass on the technological and nutritional quality of bread wheat pasta, LWT-Food Science and Technology 58 (1) (2014) 102–108.
244. OI Standard, ISO 6647-2:2007 - Rice - Determination of amylose content - Part 2: Routine method, (2007) .
245. CO Pandeirada, É Maricato, SS Ferreira, VG Correia, BA Pinheiro, D V. Evtuguin, AS Palma, A Correia, M Vilanova, MA Coimbra, C Nunes, Structural analysis and potential immunostimulatory activity of *Nannochloropsis oculata* polysaccharides, Carbohydrate Polymers 222(2019) 114962.
246. MC Santos, C Nunes, AS Ferreira, M Jourdes, P-L Teissedre, A Rodrigues, O Amado, JA Saraiva, MA Coimbra, Comparison of high pressure treatment with conventional red wine aging processes: impact on phenolic composition, Food research international 116(2019) 223–231.
247. LW Wood, Optimization of ultrasound-assisted extraction parameters of chlorophyll from *Chlorella vulgaris* residue after lipid separation using response surface methodology, Canadian Journal of Fisheries and Aquatic Sciences 42 (1) (1985) 38–43.
248. Z Zhu, Q Wu, X Di, S Li, FJ Barba, M Koubaa, S Roohinejad, X Xiong, J He, Multistage recovery process of seaweed pigments: Investigation of ultrasound assisted extraction and ultra-filtration performances, Food and Bioproducts Processing 104(2017) 40–47.
249. HK Lichtenthaler, C Buschmann, Extraction of phtosynthetic tissues: chlorophylls and carotenoids, Current protocols in food analytical chemistry 1 (1) (2001) F4-2.
250. S Sathya, Separation of algal pigments by thin layer chromatography (TLC) and high performance liquid chromatography (HPLC), World Journal of Pharmaceutical Research

6(2017) 1275–1284.

251. G Pumilia, MJ Cichon, JL Cooperstone, D Giuffrida, G Dugo, SJ Schwartz, Changes in chlorophylls, chlorophyll degradation products and lutein in pistachio kernels (*Pistacia vera* L.) during roasting, Food Research International 65(2014) 193–198.
252. GR Lopes, CP Passos, C Rodrigues, JA Teixeira, MA Coimbra, Modulation of infusion processes to obtain coffee-derived food ingredients with distinct composition, European Food Research and Technology 245 (10) (2019) 2133–2146.
253. S Aronoff, G Mackinney, The photo-oxidation of chlorophyll, Journal of the American Chemical Society 65 (5) (1943) 956–958.
254. LMM Tijskens, E Schijvens, ESA Biekman, Modelling the change in colour of broccoli and green beans during blanching, Innovative Food Science & Emerging Technologies 2 (4) (2001) 303–313.
255. MI Mínguez-Mosquera, B Gandul-Rojas, High-performance liquid chromatographic study of alkaline treatment of chlorophyll, Journal of Chromatography A 690 (2) (1995) 161–176.
256. M Ulbrich, B Schwurack, E Flöter, Alkaline dissolution of native potato starch − impact of the preparation conditions on the solution properties determined by means of SEC-MALS, Starch - Stärke 69 (5–6) (2017) 1600256.
257. CA Weemaes, V Ooms, AM Van Loey, ME Hendrickx, green chilli puree, Journal of Agricultural and Food Chemistry 47 (6) (1999) 2404–2409.
258. J Ahmed, A Kaur, U Shivhare, Color degradation kinetics of spinach, mustard leaves, and mixed puree, Journal of Food Science 67 (3) (2002) 1088–1091.
259. J Ahmed, US Shivhare, GS V Raghavan, Rheological characteristics and kinetics of colour degradation of green chilli puree, Journal of food engineering 44 (4) (2000) 239–244.
260. M Plaza, M Herrero, A Cifuentes, E Ibáñez, Innovative natural functional ingredients from microalgae, Journal of Agricultural and Food Chemistry 57 (16) (2009) 7159–7170.
261. PW Behrens, SE Bingham, SD Hoeksema, DL Cohoon, JC Cox, Studies on the incorporation of CO_2 into starch by *Chlorella vulgaris*, Journal of Applied Phycology 1 (2) (1989) 123–130.
262. E Lau, YY Soong, W Zhou, J Henry, Can bread processing conditions alter glycaemic response?, Food chemistry 173(2015) 250–256.
263. M Černá, AS Barros, A Nunes, SM Rocha, I Delgadillo, J Čopíková, MA Coimbra, Use of FT-IR spectroscopy as a tool for the analysis of polysaccharide food additives, Carbohydrate Polymers 51 (4) (2003) 383–389.
264. FJ Warren, MJ Gidley, BM Flanagan, Infrared spectroscopy as a tool to characterise starch ordered structure—a joint FTIR–ATR, NMR, XRD and DSC study, Carbohydrate Polymers 139(2016) 35–42.

265. MJ Bof, A Jiménez, DE Locaso, MA García, A Chiralt, Grapefruit Seed Extract and Lemon Essential Oil as Active Agents in Corn Starch–Chitosan Blend Films, Food and Bioprocess Technology 9 (12) (2016) 2033–2045.
266. JM Bailey, AC Neish, Starch synthesis in *Chlorella vulgaris*, Canadian journal of biochemistry and physiology 32 (4) (1954) 452–464.
267. H-D Belitz, W Grosh, P Schieberle, Food Chemistry. 4th ed., Springer Berlin Heidelberg; 2009. 315–327 p.
268. RF Tester, J Karkalas, X Qi, Starch—composition, fine structure and architecture, Journal of cereal science 39 (2) (2004) 151–165.
269. S Nara, A Mori, T Komiya, Study on Relative Crystallinity of Moist Potato Starch, Starch - Stärke 30 (4) (1978) 111–114.
270. L Chuang, N Panyoyai, R Shanks, S Kasapis, Structure and phase behaviour of microcrystalline cellulose in mixture with condensed systems of potato starch, International Journal of Food Science & Technology (2016) .
271. T Kobayashi, I Tanabe, A Obayashi, On the properties of the starch granules from unicellular green algae, Agricultural and Biological Chemistry 38 (5) (1974) 941–946.
272. A Izumo, S Fujiwara, Y Oyama, A Satoh, N Fujita, Y Nakamura, M Tsuzuki, Physicochemical properties of starch in *Chlorella* change depending on the CO_2 concentration during growth: Comparison of structure and properties of pyrenoid and stroma starch, Plant Science (2007) .
273. Y Ai, J Jane, Gelatinization and rheological properties of starch, Starch-Stärke 67 (3–4) (2015) 213–224.
274. O u. m. Tanadul, JS Vandergheynst, DM Beckles, ALT Powell, JM Labavitch, The impact of elevated CO_2 concentration on the quality of algal starch as a potential biofuel feedstock, Biotechnology and Bioengineering (2014) .
275. B Cheirsilp, YI Mandik, P Prasertsan, Evaluation of optimal conditions for cultivation of marine *Chlorella* sp. as potential sources of lipids, exopolymeric substances and pigments, Aquaculture International 24 (1) (2016) 313–326.
276. L Liu, G Pohnert, D Wei, Extracellular metabolites from industrial microalgae and their biotechnological potential, Marine Drugs 14 (10) (2016) 1–19.
277. IA Schepetkin, MT Quinn, Botanical polysaccharides: Macrophage immunomodulation and therapeutic potential, International Immunopharmacology 6 (3) (2006) 317–333.
278. D Cheng, Z Wan, X Zhang, J Li, H Li, C Wang, Dietary *Chlorella vulgaris* Ameliorates Altered Immunomodulatory Functions in Cyclophosphamide-Induced Immunosuppressive Mice, Vol. 9, Nutrients . 2017.

279. HK Kang, HM Salim, N Akter, DW Kim, JH Kim, HT Bang, MJ Kim, JC Na, J Hwangbo, HC Choi, OS Suh, Effect of various forms of dietary *Chlorella* supplementation on growth performance, immune characteristics, and intestinal microflora population of broiler chickens, The Journal of Applied Poultry Research 22 (1) (2013) 100–108.
280. T Hasegawa, Y Kimura, K Hiromatsu, N Kobayashi, A Yamada, M Makino, M Okuda, T Sano, K Nomoto, Y Yoshikai, Effect of hot water extract of *Chlorella vulgaris* on cytokine expression patterns in mice with murine acquired immunodeficiency syndrome after infection with Listeria monocytogenes, Immunopharmacology 35 (3) (1997) 273–282.
281. MLS Queiroz, APO Rodrigues, C Bincoletto, CAV Figueirêdo, S Malacrida, Protective effects of *Chlorella vulgaris* in lead-exposed mice infected with Listeria monocytogenes, International Immunopharmacology 3 (6) (2003) 889–900.
282. K Tanaka, A Yamada, K Noda, T Hasegawa, M Okuda, Y Shoyama, K Nomoto, A novel glycoprotein obtained from *Chlorella vulgaris* strain CK22 shows antimetastatic immunopotentiation, Cancer Immunology, Immunotherapy 45 (6) (1998) 313–320.
283. ER Suárez, JA Kralovec, TB Grindley, Isolation of phosphorylated polysaccharides from algae: the immunostimulatory principle of *Chlorella pyrenoidosa*, Carbohydrate research 345 (9) (2010) 1190–1204.
284. C Nunes, A Rocha, P Quitério, SS Ferreira, A Correia, M Vilanova, MA Coimbra, Salt pan brine water as a sustainable source of sulphated polysaccharides with immunostimulatory activity, International Journal of Biological Macromolecules 133(2019) 235–242.
285. Z Csőgör, B Kiessling, I Perner, P Fleck, C Posten, Growth and product formation of *Porphyridium purpureum*, Journal of Applied Phycology 13 (4) (2001) 317–324.
286. A Razaghi, A Godhe, E Albers, Effects of nitrogen on growth and carbohydrate formation in *Porphyridium cruentum*, Open Life Sciences 9 (2) (2014) 156–162.
287. T You, SM Barnett, Effect of light quality on production of extracellular polysaccharides and growth rate of *Porphyridium cruentum*, Biochemical Engineering Journal 19 (3) (2004) 251–258.
288. MMR Fuentes, GGA Fernández, JAS Pérez, JLG Guerrero, Biomass nutrient profiles of the microalga *Porphyridium cruentum*, Food Chemistry 70 (3) (2000) 345–353.
289. S Velea, L Ilie, L Filipescu, Optimization of *Porphyridium purpureum* culture growth using two variables experimental design: light and sodium bicarbonate, UPB Sci Bull Series B 73 (4) (2011) 81–94.
290. NA Aizdaicher, I V Stonik, A V Boroda, The development of *Porphyridium purpureum* (Bory de Saint-Vincent) Drew et Ross, 1965 (Rhodophyta) from Amursky Bay, Sea of Japan, in a laboratory culture, Russian Journal of Marine Biology 40 (4) (2014) 279–285.

291. MFG Assunção, JMTB Varejão, LMA Santos, Nutritional characterization of the microalga *Ruttnera lamellosa* compared to *Porphyridium purpureum*, Algal Research 26(2017) 8–14.
292. R Vazhappilly, F Chen, Eicosapentaenoic acid and docosahexaenoic acid production potential of microalgae and their heterotrophic growth, Journal of the American Oil Chemists' Society 75 (3) (1998) 393–397.
293. P Ardiles, P Cerezal-Mezquita, F Salinas-Fuentes, D Órdenes, G Renato, MC Ruiz-Domínguez, Biochemical Composition and Phycoerythrin Extraction from Red Microalgae: A Comparative Study Using Green Extraction Technologies, Processes 8 (12) (2020) 1628.
294. TMM Bernaerts, C Kyomugasho, N Van Looveren, L Gheysen, I Foubert, ME Hendrickx, AM Van Loey, Molecular and rheological characterization of different cell wall fractions of *Porphyridium cruentum*, Carbohydrate polymers 195(2018) 542–550.
295. RF Jones, Extracellular mucilage of the red alga *Porphyridium cruentum*, Journal of Cellular and Comparative Physiology 60 (1) (1962) 61–64.
296. Y Li, C Wang, H Liu, J Su, CQ Lan, M Zhong, X Hu, Production, isolation and bioactive estimation of extracellular polysaccharides of green microalga *Neochloris oleoabundans*, Algal Research 48(2020) 101883.
297. E Percival, RAJ Foyle, The extracellular polysaccharides of *Porphyridium cruentum* and *Porphyridium aerugineum*, Carbohydrate Research 72(1979) 165–176.
298. DG Medcalf, JR Scott, JH Brannon, GA Hemerick, RL Cunningham, JH Chessen, J Shah, Some structural features and viscometric properties of the extracellular polysaccharide from *Porphyridium cruentum*, Carbohydrate Research 44 (1) (1975) 87–96.
299. SF Reis, E Coelho, MA Coimbra, N Abu-Ghannam, Improved efficiency of brewer's spent grain arabinoxylans by ultrasound-assisted extraction, Ultrasonics Sonochemistry 24(2015) 155–164.
300. N Lupescu, SM Arad, S Geresh, MA Bernstein, R Glaser, Structure of some sulfated sugars isolated after acid hydrolysis of the extracellular polysaccharide of *Porphyridium* sp., a unicellular red alga, Carbohydrate research 210(1991) 349–352.
301. JA Ferreira, MRM Domingues, A Reis, C Figueiredo, MA Monteiro, MA Coimbra, Aldobiouronic acid domains in *Helicobacter pylori*, Carbohydrate research 346 (5) (2011) 638–643.
302. AS Ferreira, SS Ferreira, A Correia, M Vilanova, TH Silva, MA Coimbra, C Nunes, Reserve, structural and extracellular polysaccharides of *Chlorella vulgaris*: A holistic approach, Algal Research 45(2020) 101757.
303. A Vonshak, Z Cohen, A Richmond, The feasibility of mass cultivation of *Porphyridium*, Biomass 8 (1) (1985) 13–25.

Annexes

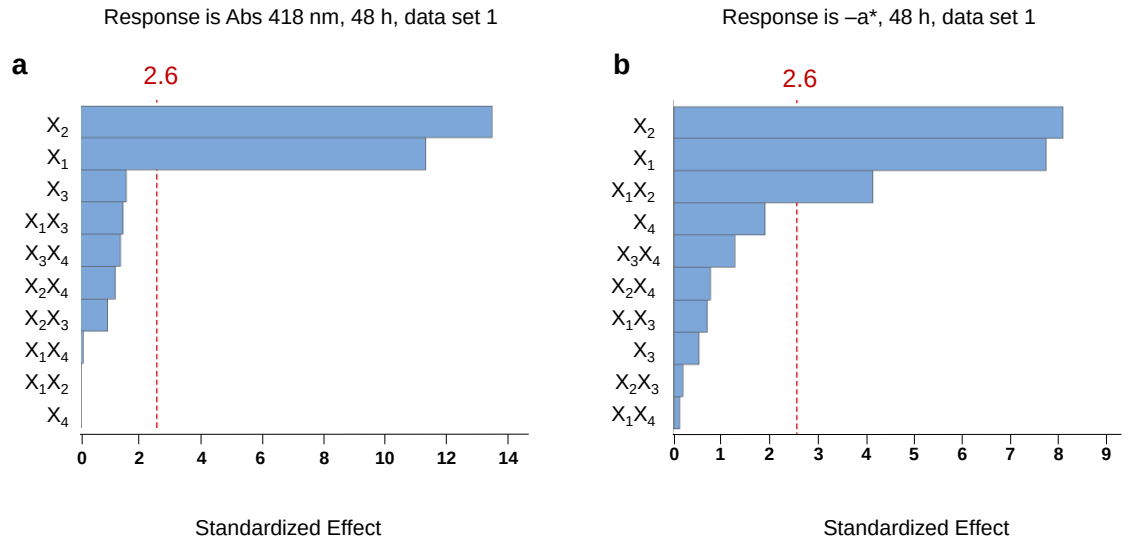

X_1- Temperature **X_2**- Light; **X_3**- Modified atmosphere; **X_4**- Alkaline

Figure A 1 – Pareto charts of the standardized effects for the data set 1: a) response is Abs (418 nm), 48 h (p<0.05); b) response is -a*, 48 h (p<0.05).

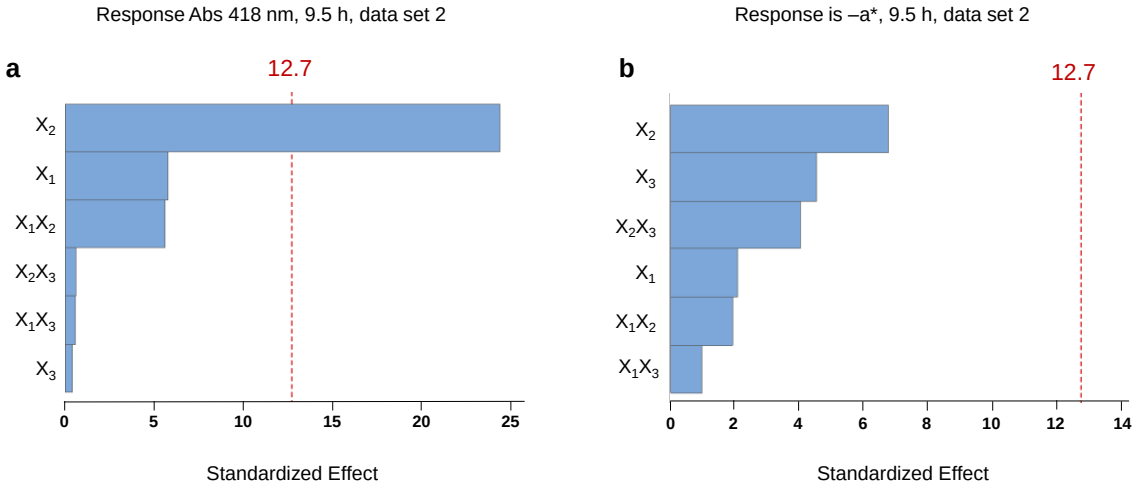

X_1- Temperature **X_2**- Light; **X_3**- Alkaline

Figure A 2 – Pareto charts of the standardized effects for the data set 2: a) response is Abs (418 nm), 9.5 h (p<0.05); b) response is -a*, 9.5 h (p<0.05).

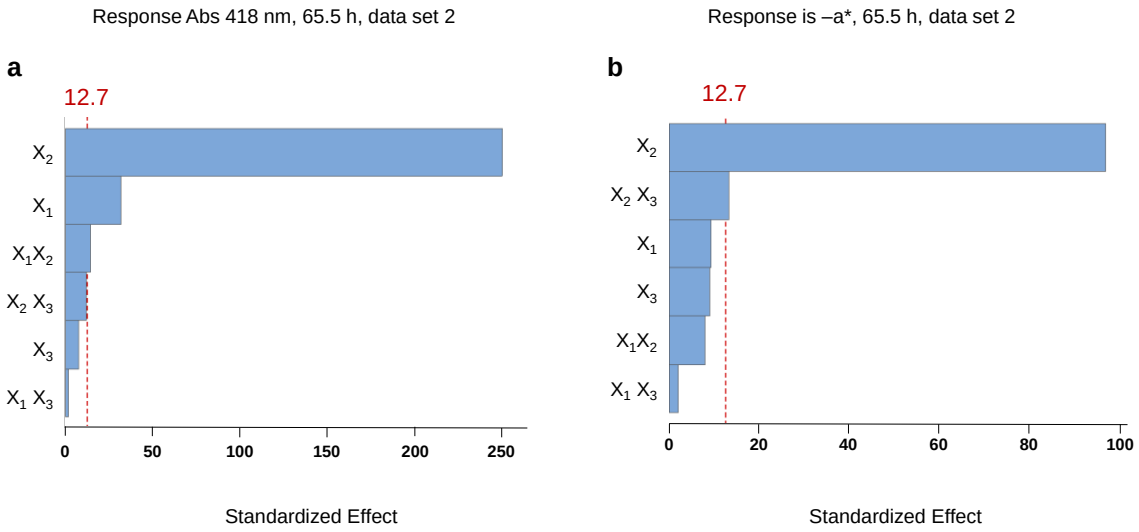

X_1- Temperature **X_2**- Light; **X_3**- Alkaline

Figure A 3 – Pareto charts of the standardized effects for the data set 2: a) response is Abs (418 nm), 65.5 h (p<0.05); b) response is -a*, 65.5 h (p<0.05).